

material and the soil cement column with too high strength can not be moved together after excavation of the treatment slope.

Therefore, the average value of the design strength of soil cement columns constructed in Japan, that is  $2.9 \text{ kg f/cm}^2$ , is selected as the design strength of soil cement columns in this project as shown in FIGURE-4.1.13.

Fig. 4.1.14 shows the past record of improved ratio by the Soil Cement Column in Japan.

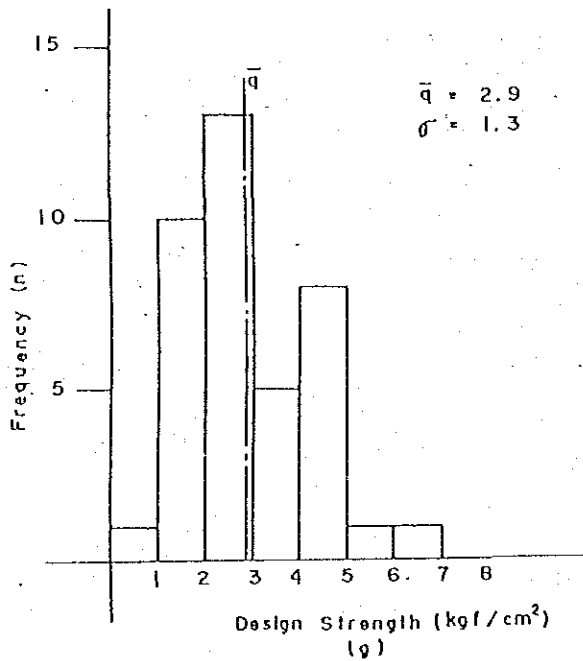


Fig.4.1.13 Past Record of Design Strength in Japan

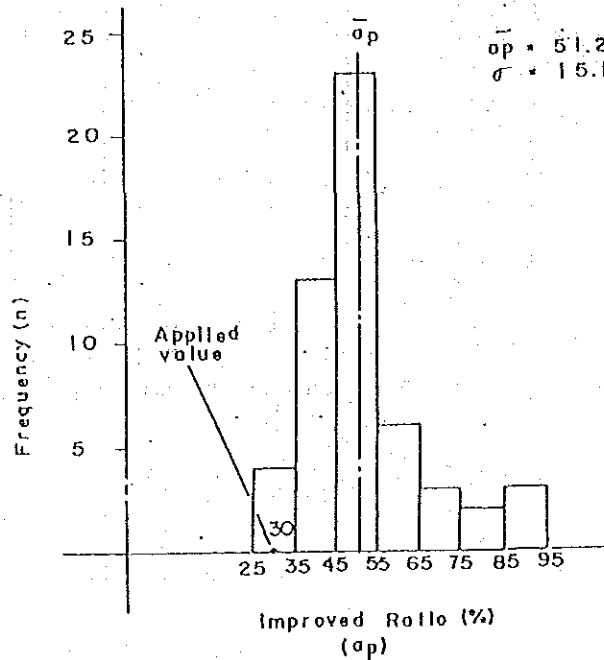


Fig.4.1.14 Past Record of Improved Ratio in Japan

The value of the volume ratio of soil cement columns to original clay material in the improved zone is set at 30% taking into account the economic viewpoint of the construction cost for the treatment slope structure and the construction results regarding to the soil cement column method in Japan.

The design values of the shear strength in the original clay material existing in the treatment slope are calculated by using the undrained shear strength obtained from the field vane tests performed at the point neighbouring with boring No. 1 by taking into account the calculated values of the strength decrease on the same determination method of the non-treatment slope.

The value of 1.2 is determined as the safety factor for the effect of disturbance of the original clay foundation due to soil cement columns in this project.

The design values of the shear strength in the improvement zone by soil cement columns are shown in Table 4.1.7 and Fig. 4.1.15.

Table 4.1.7 Design Parameters and Mobilized Mobilized Shear Strength in Improved Zone by Soil Cement Columns

The mobilized shear strength in the improved zone are calculated by the following equation ;

$$\tau = \frac{1}{n} \{C_p \cdot Ass + (1 - Ass) \cdot Su^*\}$$

EL	Layer	$\mu_A$	$\mu_B$	Su	Su*	Ass	n	Cp	$\tau$	Strength decrease zone	Improved zone by soil cement columns
-1.0	9	-	-	-	-	-	-	-			
-3.0	8	-	-	-	-	-	-	-			
-5.0	7	0.750	0.476	0.960	0.342	0.3	1.2	29.0	7.45		
-7.0	6	0.769	0.648	1.240	0.618	0.3	1.2	29.0	7.61		
-9.0	5	0.769	0.769	1.670	0.988	0.3	1.2	29.0	7.83		
-11.0	4	0.712	0.761	1.950	1.057	0.3	1.2	29.0	7.87		
-13.0	3	0.712	1.000	2.380	1.695	0.3	1.2	29.0	8.24		
-15.0	2	0.712	1.000	2.990	2.012	0.3	1.2	29.0	8.99		
-17.0	1	0.712	1.000	4.650	3.130	0.3	1.2	29.0	9.96		

Original clay
Soil cement columns

Remarks,

- $\mu_A$  : Bjerrum's correction factor
- $\mu_B$  :  $(=OCR^{-\alpha}, \alpha=0.3)$  Coefficient of strength decrease
- Su : Shear strength from F.V. test data
- Su\* :  $(=\mu_A/\mu_B \cdot Su)$  Shear strength for design
- Ass : Improved volume ratio
- n : Safety factor
- Cp : Shear strength of soil cement columns

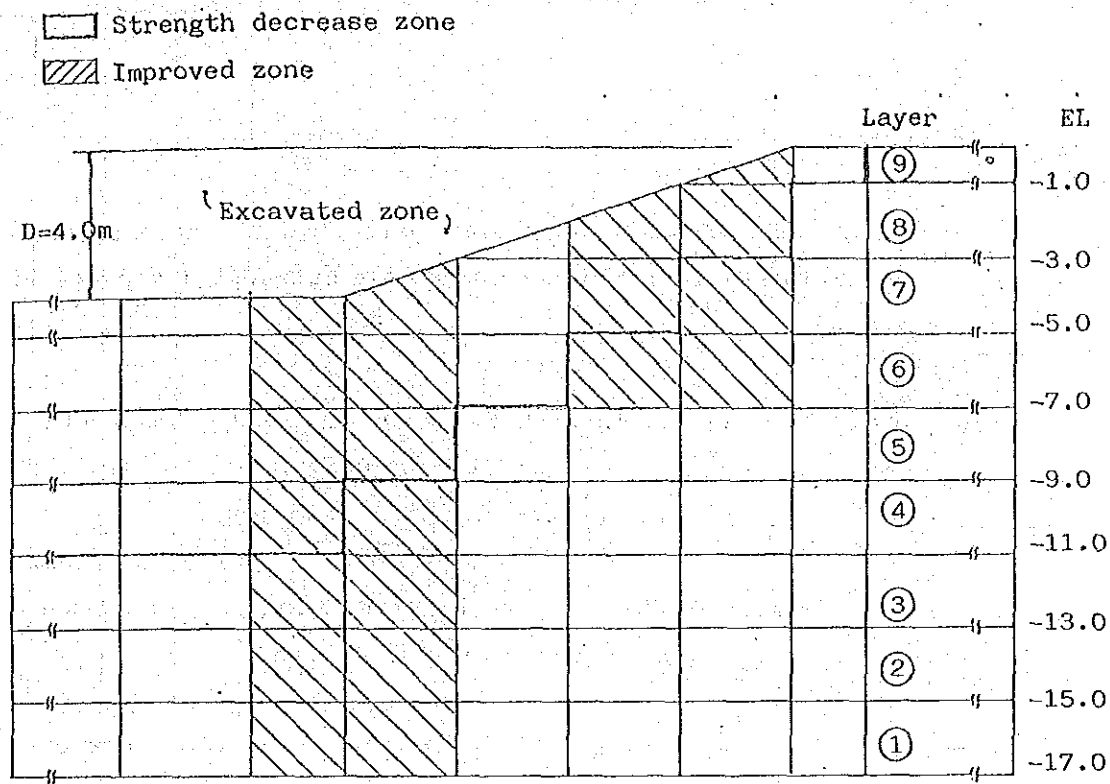


Fig.4.1.15 Strength Decrease Zone and Improved Zone by Soil Cement Columns

#### 4). Determination of Stability Analysis Model

##### i) Non-Treatment Slopes

From the geotechnical investigations performed at the Project Site, the original foundation consists of horizontal deposits of Bangkok clay.

Therefore, the mesh models with the several divided horizontal layers are applied to the stability analysis model for the non-treatment slopes in the testing canal facility.

An example of mesh models for the non-treatment slopes in the testing canal facility is shown in Fig. 4.1.16.

Also, the strength decrease zone caused by excavation work can be assumed as shown in Fig. 4.1.16.

##### ii) Improved Slopes by Sand Compaction Piles or Gravel Compaction Piles

The length of sand or gravel compaction piles shall be determined as 5.0m taking into account the shear strength in the original clay material and the results of the stability analysis model for non-treatment slopes.

The mesh models with the several divided horizontal layers are applied to the stability analysis model for the improved slopes in the testing canal facility as the same manner with the non-treatment slopes.

Fig. 4.1.17 shows the mesh model applied to the stability analysis for the Improved Slopes.

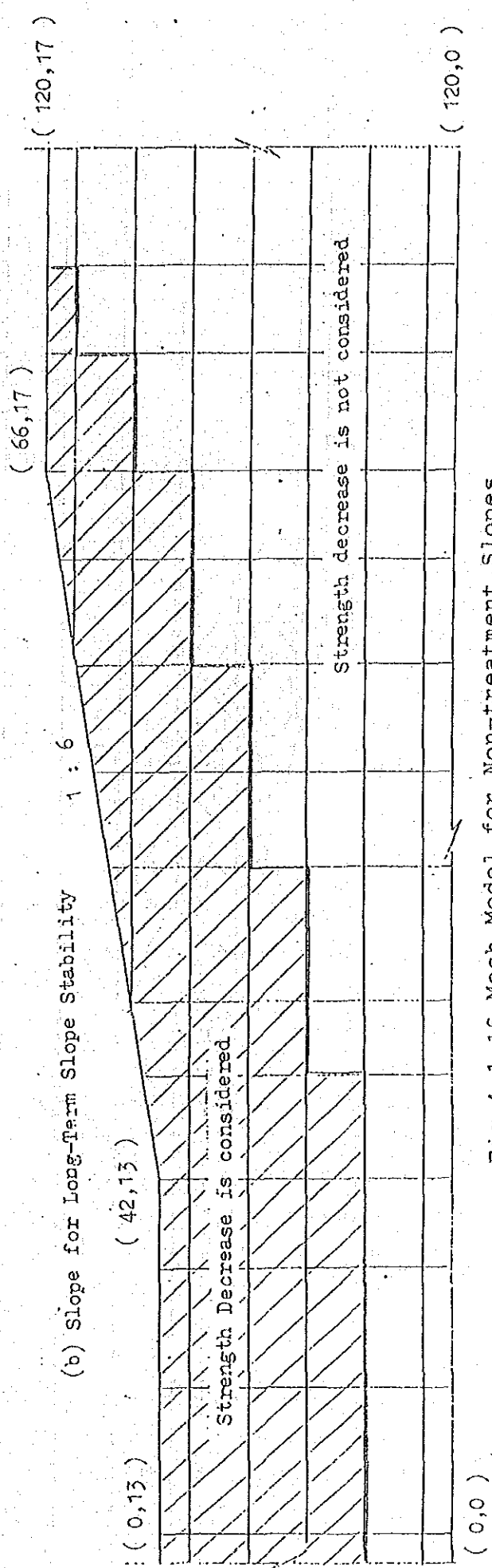
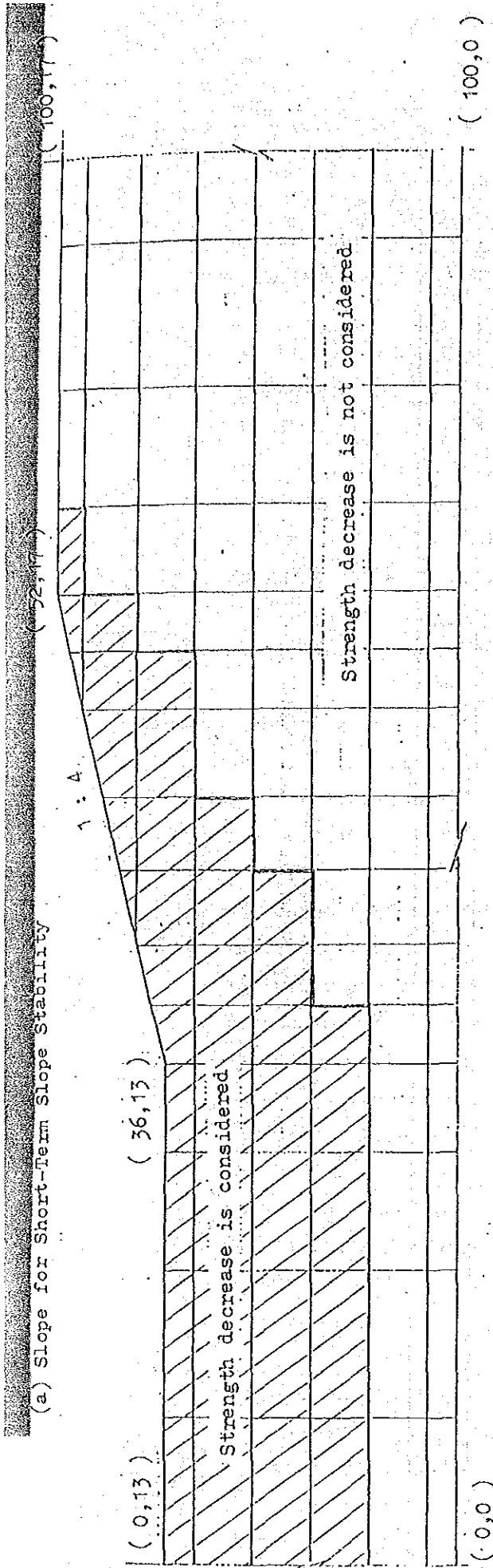


Fig.4.1.16 Mesh Model for Non-treatment Slopes

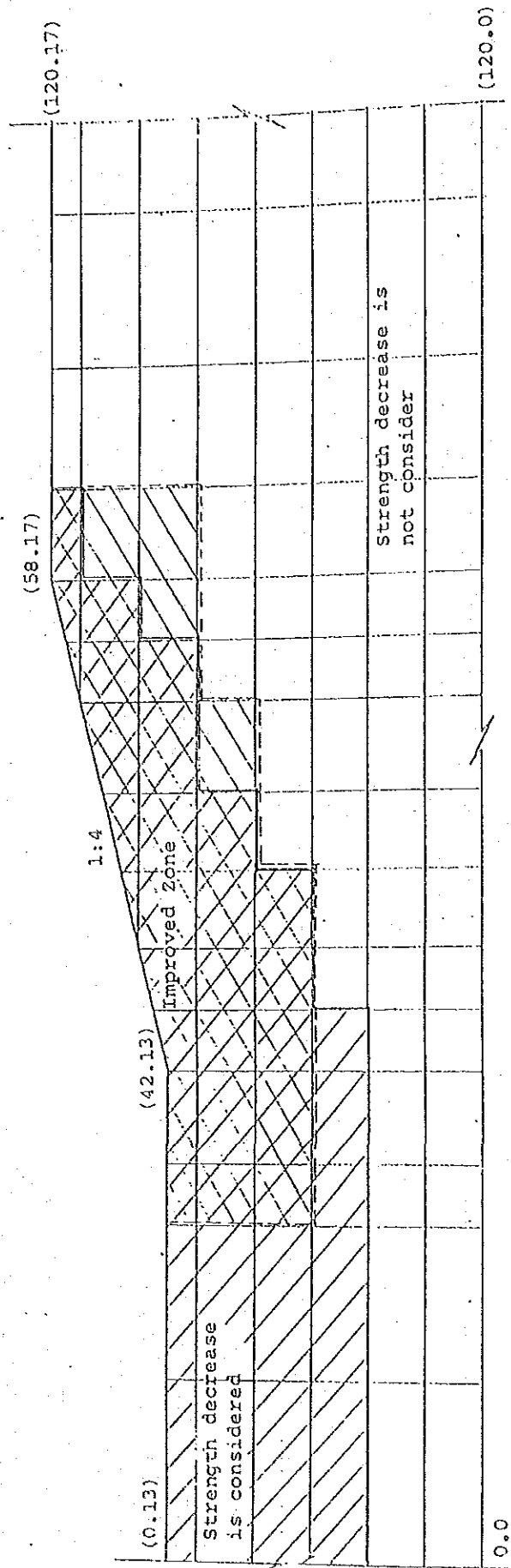


Fig. 4.1.17 Mesh Model for Improved Slope by Sand/Gravel Compaction Piles

### iii) Improved Slope by Soil Cement Columns

Prior to the preliminary analysis, the testing analysis was carried out in order to study the stability of the testing canal slope facing to the National Road Route No. 3.

As the results, in the case of application of sand or gravel compaction piles, the unacceptable values lower than 1.0 were obtained for the safety factors to the deep circular slips including the National Road in the testing canal slope structure.

Therefore, the application of the soil cement columns confirming the large design strength values was accepted for the testing canal slope structure on the National Road side.

From the economic viewpoint of the structure, the improved zone by soil cement columns shall be divided into two portions, that is, the improved zone I and the improved zone II as shown in Fig. 4.1.18.

The purpose of the improved zone (I) treated at the front of the excavated slope structure is to protect the excavated slope against slope failure occurring in the deep portion of the foundation of the excavated slope structure. On the other hand, the purpose of the improved zone (II) treated at the slope portion of the excavated slope structure is to protect the excavated slope against slope failure occurring in the shallow and medium portions of the foundation of the excavated slope structure. The depth of the Zone (I) to be improved by soil cement columns constructed at the front of the excavated slope structure shall reach the stiff clay zone (EL.-17.0) in the Project area.

The average depth of the Zone (II) to be improved by soil cement columns constructed at the slope portion of the excavated slope structure shall be about 5.5 m from the ground surface of the excavated slope taking into account the effects by the circular slips.



The following table shows the average depth of each zone to be improved:

Improved Zone	Average Depth of Soil Cement Column
Improved Zone I	13.5 Meters
Improved Zone II	5.5 Meters

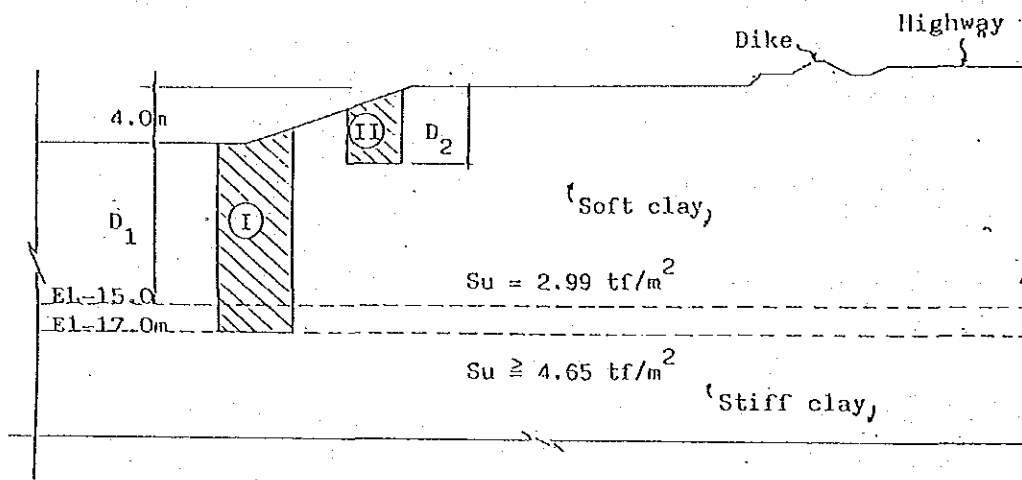


Fig.4.1.18 Improved Zone by Soil Cement Columns

The ratio value of depth to width of the zone to be improved by the soil cement columns shall be greater than 0.5 from the practice and experience gained from those constructed in Japan. Also, the diameter of the soil cement columns shall be selected as one (1.0) meter based on experience and practice of soil cement columns constructed in Japan. Since the volume ratio of soil cement columns to the original clay material is 30%, the value of 1.75m as the distance between each soil cement column is obtained under the condition of the right triangular arrangement (Refer to the Chapter 4-4). Therefore, the Sizes of

the improved zones, Zone I (four lines arrangement) and Zone II (three lines arrangement), are determined as follows:

Improved Zone	Average Depth of Soil Cement Column Zone (D)	Width of Soil Cement Column Zone (W)	W/D
Improved Zone I	13.5 m	5.5 m	41%
Improved Zone II	5.5 m	4.0 m	73%

The soil cement column material and the original clay material including the improved zones by soil cement columns is also expressed by the mesh models with several divided horizontal layers applied to the stability analysis model for the treatment slope structure by soil cement columns in the testing canal facility.

The mesh models for the treatment slope structure by soil cement columns in the testing canal facility are shown in Fig. 4.1.19.

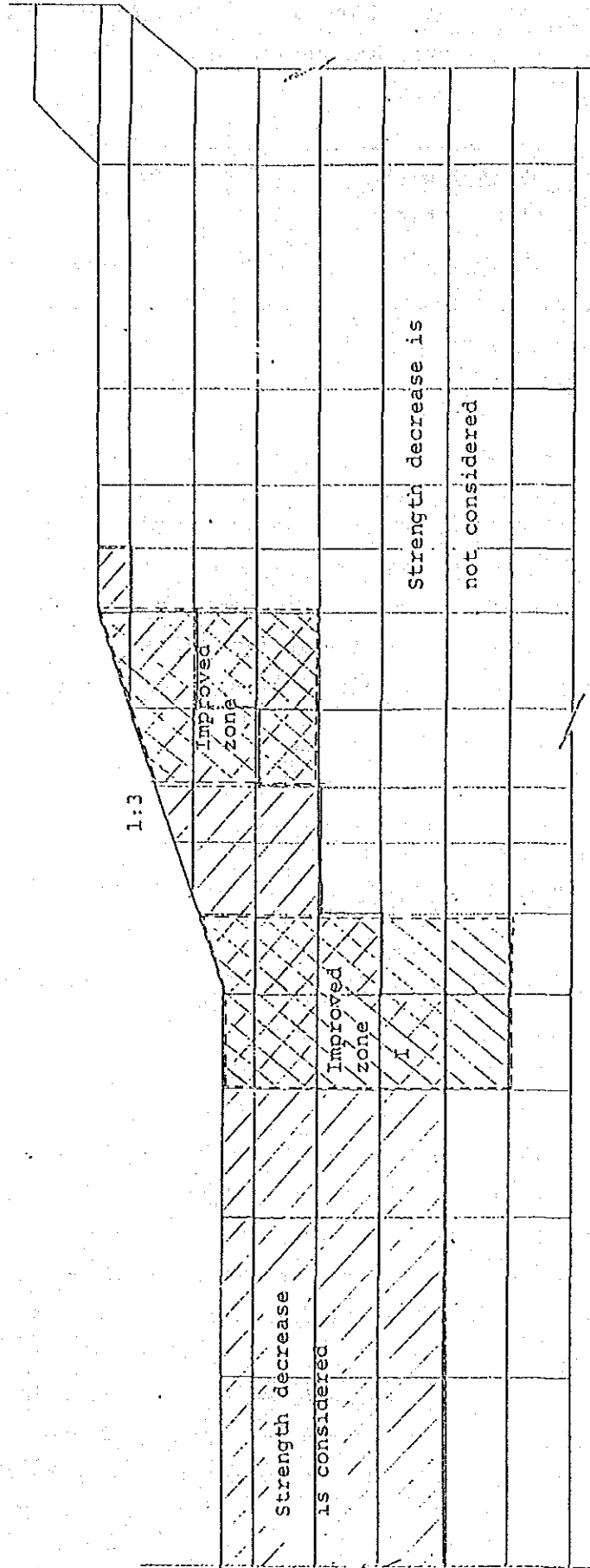


Fig. 4.1.19 Mesh Model for Improvement Slope by Soil Cement Columns

5) Assumption of Groundwater Level and Water Level inside Testing Canal Facility

i) Groundwater Level

The groundwater level for the calculation condition in the slope stability analysis is assumed to be the same elevation as the surface of the excavated testing canal facility shown in Fig. 4.1.20 from the viewpoint of the safety side of slope stability analysis for the Testing Canal Facility.

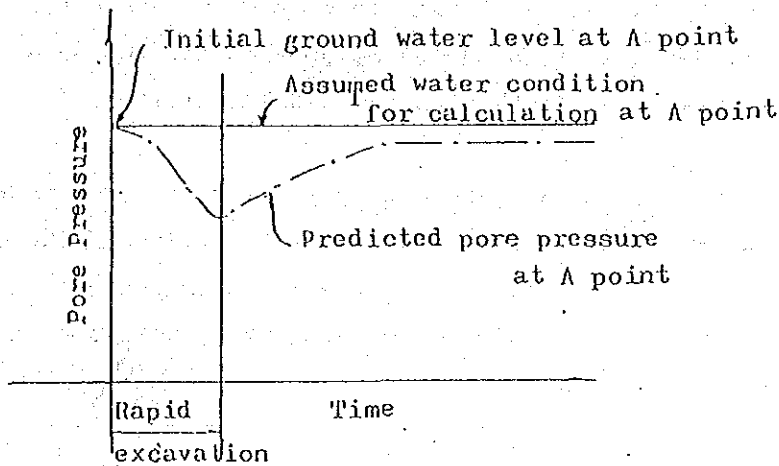


Fig.4.1.20 Ground Water Level for Calculation Condition

ii) Water Level inside Testing Canal Facility

The water level inside the testing canal facility for the calculation condition of slope stability analysis is assumed to be the same elevation as the bottom surface of the excavated slope structures in the testing canal facility shown in Fig. 4.1.21.

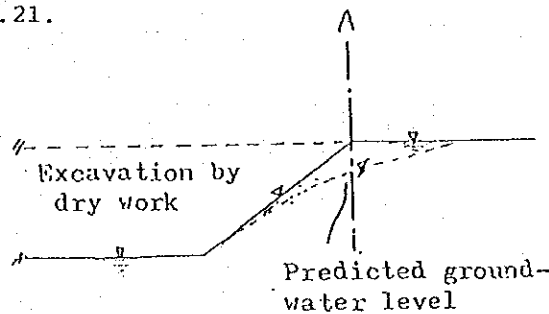


Fig.4.1.21 Water Level inside Testing Testing Canal Facility

6) Evaluation of Results Obtained from Circular Slip Method

i) Non-Treatment Slope Structures

The results of the preliminary analysis on the non-treatment structures are shown in Table 4.1.8 and FIGURE-4.1.22. From the comparison between the results of the preliminary analysis and the past experiences on slope failure caused by canal excavation works in the soft soil foundation, it was judged that the analysis taken into account the strength decrease in original soft soil foundation by excavation work and the anisotropy of strength can be applied for the determination of slope gradients of the testing canal facility.

Therefore, the slope gradient for the non-treatment slope structure shall be decided based on the results of the analysis obtained by taking into account the strength decrease in the original soft soil foundation by excavation work and the anisotropy of strength.

It is said that the canal structures having the depths exceeding 4.0 m will have the slope failure judging from the past experiences.

Therefore, the depth of the excavation work for the testing canal facility shall be decided to be 4.0 m.

Also, the slope gradients for the non-treatment slope for short term stability and the non-treatment slope for long term stability shall be decided to be 1:4 and 1:6 respectively.

Remarks :

- △
}
 Strength decrease due to excavation and anisotropy of shear strength are considered
- }
 Strength decrease due to excavation is considered

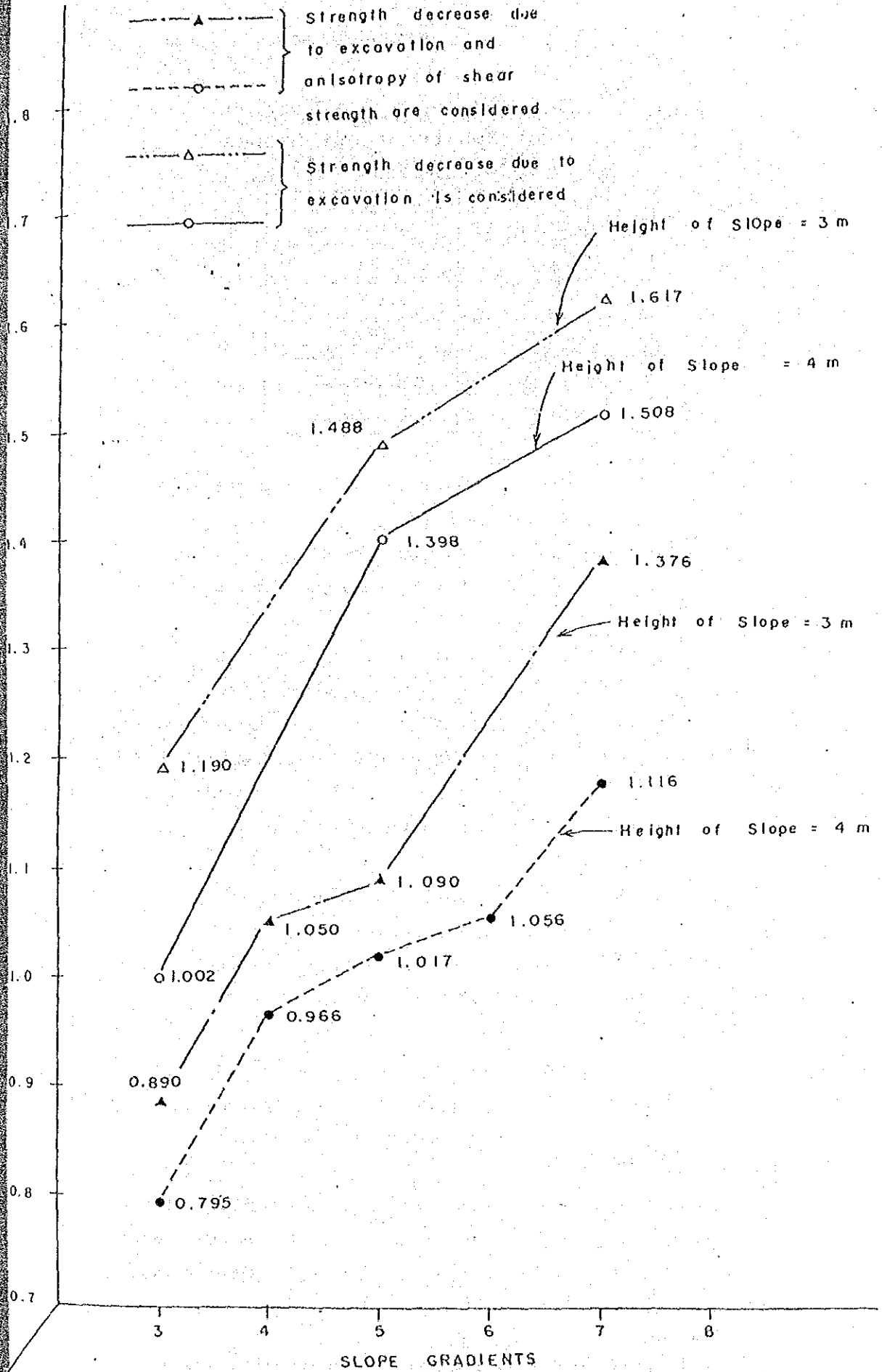
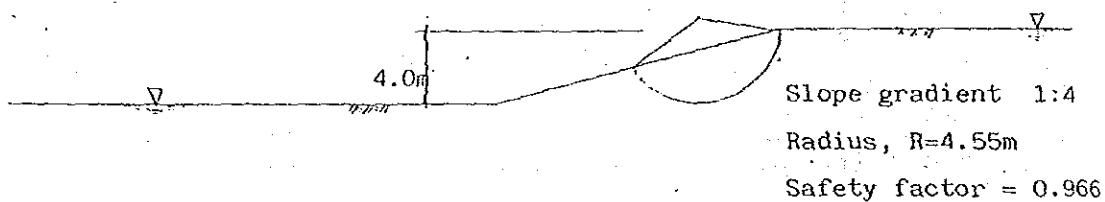


Fig.4.1.22 Relation between Safety Factors and Slope Gradient in Non-treatment Slopes

Table 4.1.8 Minimum Safety Factors of Non-treatment Slopes (In case Height=4m)

Slope Gradient	Minimum Safety Factor
1 ; 3	0.795
1 : 4	0.966
1 : 5	1.017
1 : 6	1.056
1 : 7	1.116

1.) Short Term Stability



2.) Long Term Stability

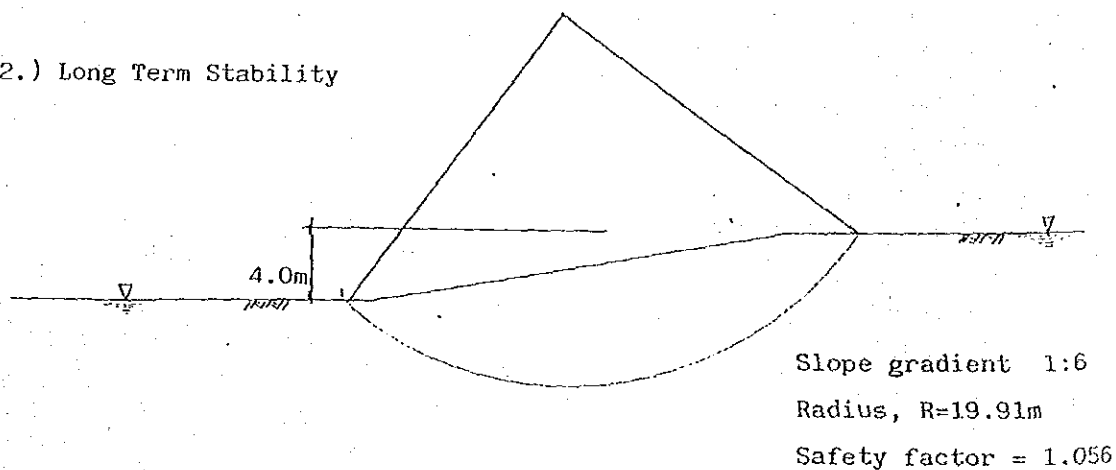


Fig 4.1.22 Minimum Safety Factors of Non-treatment Slopes

ii) Improved Slope Structures

a) Improved Slope by Soil Cement Columns

As already mentioned, the foundation improvement by the soil cement column method is carried out in order to obtain the stability of the testing canal slope facing to the National Road Route No. 3.

The slope gradient shall be decided to be 1:3 which is a little steeper than the slope gradient for the non-treatment slope for short term stability.

The results obtained from the stability analysis on each basis, that is, the deep slip surface, the medium slip surface and the shallow slip surface, are shown in Fig. 4.1.23 and Table 4.1.9.

From the above studies, it is judged that the improved slope by soil cement columns becomes safe against the failures of the testing canal facility and the existing facilities such as the National Road.

b) Improved Slope by Sand or Gravel Compaction Piles

The improvement effectiveness by sand or gravel compaction piles is influenced by the conditions such as the disturbance of the foundation around the piles and the strength of pile itself.

Since the design parameters were assumed in the preliminary design, they have uncertain factors to evaluate the improvement effectiveness.

Therefore, the slope gradient of 1:4 having the same slope gradient as the non-treatment slope for short-term stability shall be employed, and then, the improvement



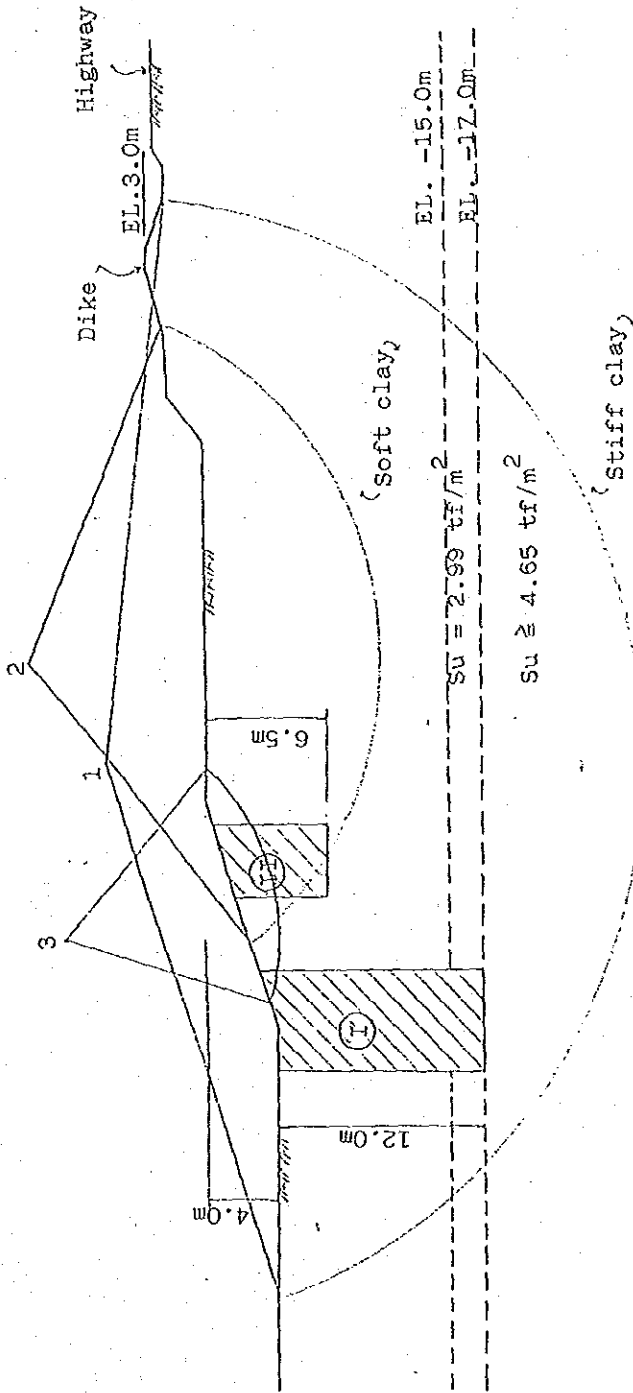


Fig. 4.1.23 Critical Slip Circles in Improved Slope by Soil Cement Columns

Table 4.1.9 Minimum Safety Factors for Improved Slope by Soil Cement Columns

Location of slip circles	Minimum safety factor	Slip circles		Remarks
		Radius (m)	Center	
1. Deep slip circle	1.277	31.25	53.75, 21.25	
2. Medium slip circle	1.579	20.00	60.00, 25.00	
3. Shallow slip circle	6.416	12.30	45.00, 25.00	

effectiveness shall be judged by monitoring the behaviour of the improved slope.

Furthermore, the design parameters and the diameters of piles shall be confirmed by performing the experimental construction before the construction for the improved slope structure, and such data shall be revised, if necessary.

Fig. 4.1.24 and Table 4.1.10 show the results of the stability analysis for the improved slope structures by sand compaction piles.

The stability analysis for the improved slope structures by gravel compaction piles was omitted, because it is surmised that the internal friction angle in the improved slope structures by gravel compaction piles will be greater than that of sand compaction piles.

Internal friction angle  
of sand compaction pile ;  $\phi = 30$   
Strength increase ratio  
of clay ;  $\Delta C/\Delta P = 20\%$   
Improved volume ratio ;  $A_{ss} = 0.1$   
Improved zone ;

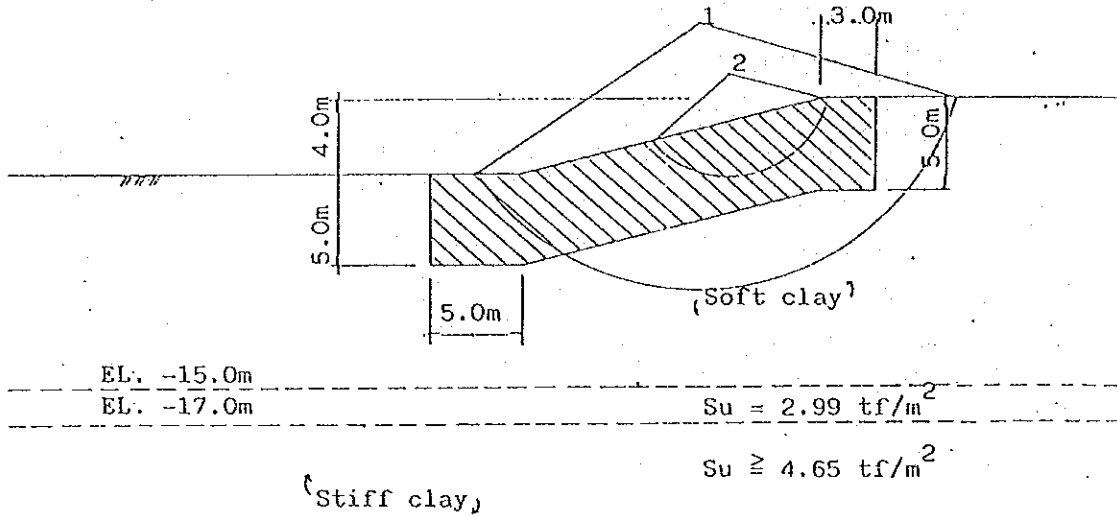


Fig. 4.1.24 Critical Slip Circles in  
Improved Slope by Sand  
Compaction Piles

Table 4.1.10 Minimum Safety Factors for  
Improved Slope by Sand  
Compaction Piles

Location of slip circle	Minimum safety factor	Radius of circle
1. Medium slip circle	1.280	13.95m
2. Shallow slip circle	1.279	5.35m

Table 4.1.11 Summary of Results of Slope Stability Analysis

Type of slope and condition	4.0 m							5.0 m						
	Height of slope		Slope Gradient		1:3	1:4	1:5	1:6	1:7	1:3	1:4	1:5	1:6	1:7
Non-treatment slope structure	Strength decrease due to excavation		1:3		1.002	—	1.398	—	1.508	1.190	—	1.488	—	1.617
	Strength decrease and Bjerrum's factor		1:3		0.795	0.966	1.017	1.056	1.116	0.890	1.050	1.090	—	1.376
Improved slope structure	Sand compaction piles		1:3		—	0.997	—	—	—	—	—	—	—	—
	Gravel connection piles		1:3		—	1.279	—	—	—	—	—	—	—	—
	Soil cement columns		1:3		1.277	—	—	—	—	—	—	—	—	—

7) Layout of the Testing Canal Facility

The slopes of the testing canal facility are allocated as shown in Fig. 4.1.25 taking into account the calculation results by preliminary analysis and comparative study of the construction cost, and also the present condition of the project site.

The foundation improvement method of either sand compaction pile method or gravel compaction method shall be decided based on the results of the experimental construction and the economical viewpoint.

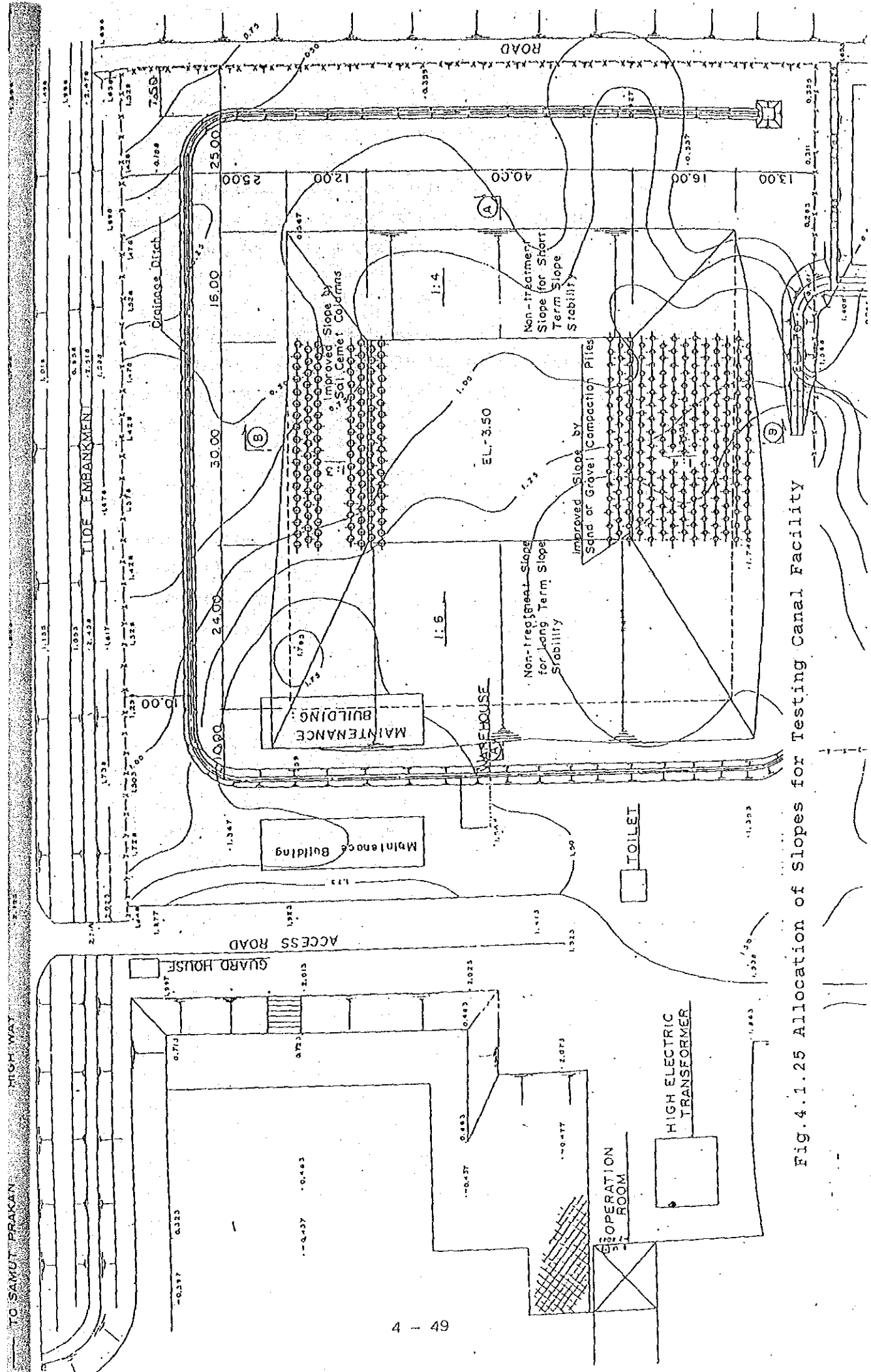


Fig.4.1.25 Allocation of Slopes for Testing Canal Facility

#### 4-2 Slope Stability Analysis by Circular Slip Surface Method

As mentioned in chapter 4-1, the calculation of slope stability by circular slip surface method in the preliminary analysis was performed based on the data obtained from the Boring No. 1 and from the result of the field vane test (FV-1).

The calculation of slope stability in this time is performed based on the design parameters obtained from all of the results of geotechnical investigations, namely, boring No. 1 ~ No. 5 and FV-1 ~ FV-5, in order to examine the slope gradients designed in the preliminary analysis.

##### 1) Calculation of design parameters

As to design parameters, physical properties of each layer, namely, plasticity index PI and undrained shear strength  $S_u$  by field vane tests following the results of chapter 3-3 are obtained in the method mentioned as follows, and then the design parameter  $S_u^*$  is determined.

Regarding undrained shear strength, the values obtained from the field vane tests are applied as well as mentioned in chapter 4-1, and about  $c'$  and  $\phi$  obtained from Ko-note triaxial compression tests, the result can not be compared directly with the former results, therefore, study on the comparison of those values is omitted this time also.

Determination method of design parameters is mentioned in the following.

At first, representing value of plasticity index of each depth corresponding to ground layer model is determined as shown in Fig. 4.2.2.

Regression equation was not considered because it seemed not always to express ground properties, therefore, an average value of plasticity index PI is used.

Secondary, correction coefficient  $\mu_A$  for undrained shear strength which was obtained from the field vane tests was determined by Bjerrum's correction coefficient curve based on the obtained value of PI as shown in Table 4.2.1.

Compared with the undrained shear strength determined in chapter 4-1, these values are judged to have not so many differences except for the undrained shear strength in the surface layer,  $1.2 \text{ tf/m}^2$  which is a little smaller than the value determined in chapter 4-1.

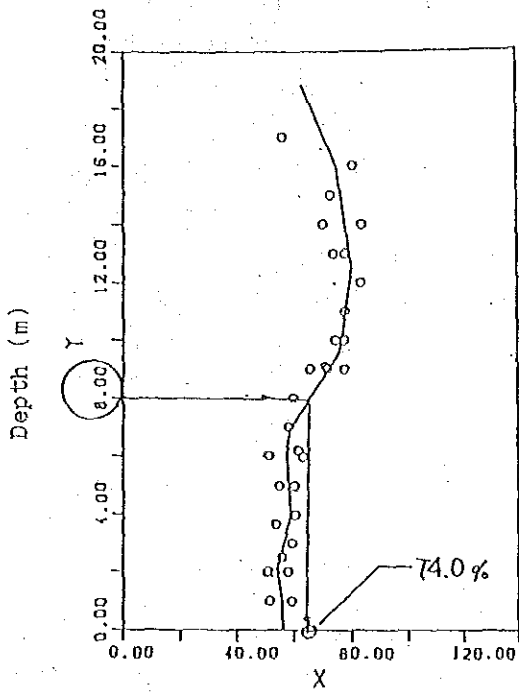
The rate of strength decrease  $\mu_B$  was obtained by the same method mentioned in chapter 4-1, and then the design undrained shear strength  $Su^*$  ( $= \mu_A \cdot \mu_B \cdot Su$ ) was calculated.

## 2) Determination of mesh model

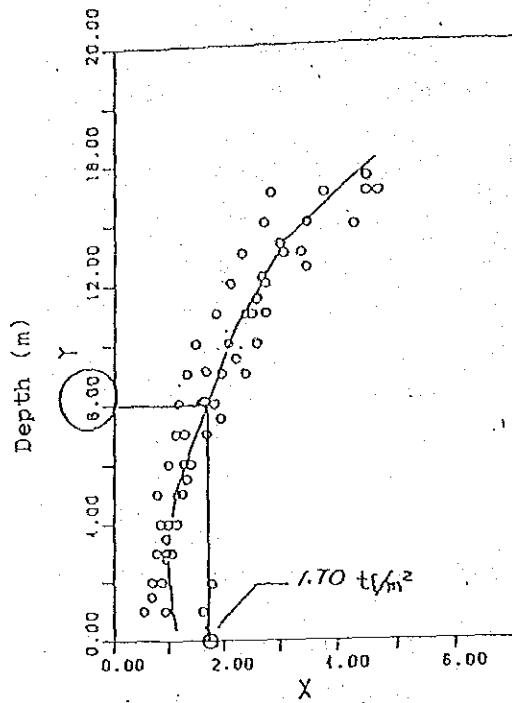
The same section in chapter 4-1 is applied to the mesh model. Layer composition, plasticity index, Bjerrum's correction coefficient  $\mu_A$ , design undrained shear strength  $Su^*$ , volume ratio of improvement materials to original clay  $A_{ss}$ , etc. are as shown in Fig. 4.2.3 ~ Fig. 4.2.8.

On the conditions mentioned above, the slope stability analysis by circular slip method are performed for short term stability of non-treatment slope, long term stability of non-treatment slope, improved slope by sand compaction pile method and improved slope by soil cement column method.





Plasticity index, P.I (%)



Undrained shear strength by F.V,  $S_u$  ( $tf/m^2$ )

$P.I = 74.0$

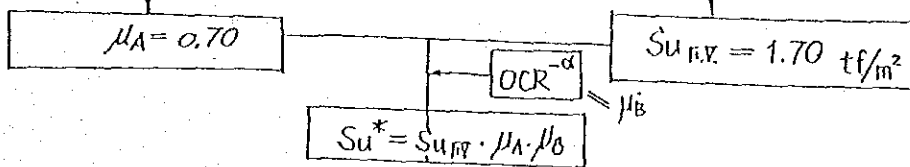
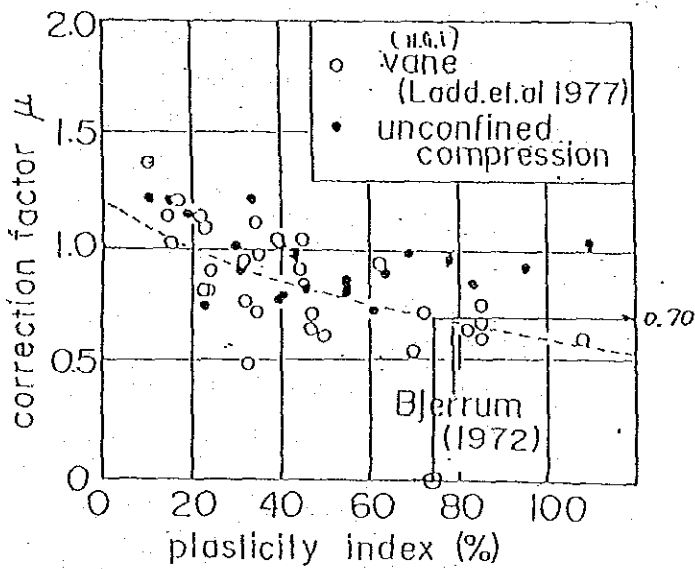


Fig. 4.2.1 Flowchart of Determination of Undrained Shear Strength

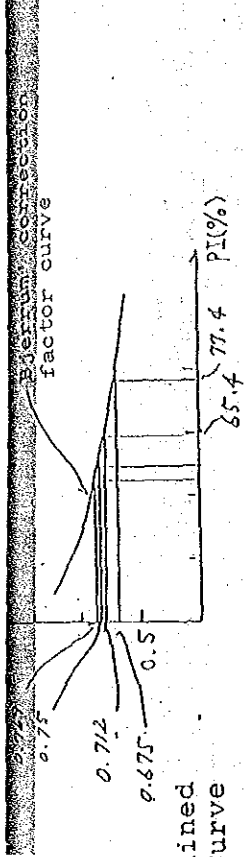


Table 4.2.1

Strength Decrease Ratio Obtained from Beerrum's Correction Curve

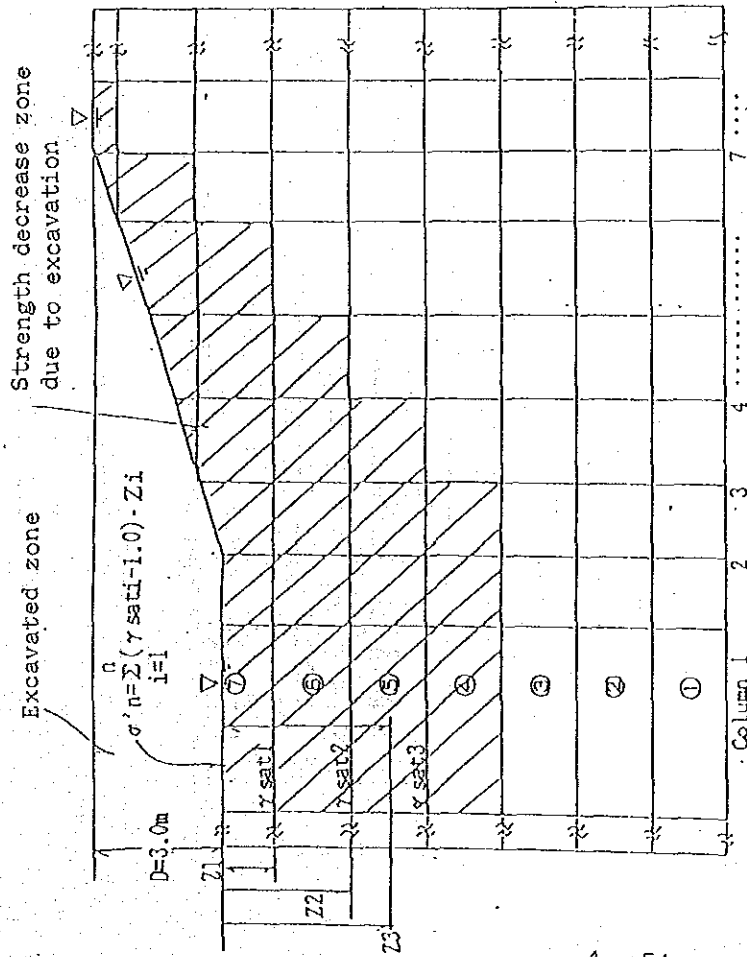
El. (m)	PI	$\mu A$	Remark
0.0	55	0.83	
-1.0	55	0.83	
-3.0	58.8	0.738	
-5.0	59.8	0.728	
-7.0	64.4	0.71	
-9.0	73.5	0.7	
-11.0	79.2	0.681	
-13.0	77.2	0.699	
-15.0	73.4	0.701	
-17.0			

PI : Plasticity index  
 $\mu A$  : Bjerrum's correction factor

El. (m)	Layer	$\sigma'_{zm}$	$\gamma_t$	$S_u$
-4.0	Layer ⑨	2.5	1.47	1.2
-5.0	Layer ⑧	2.5	1.47	1.14
-7.0	Layer ⑦	2	1.47	1.04
-9.0	Layer ⑥	4	1.47	1.27
-11.0	Layer ⑤	4.5	1.44	1.68
-13.0	Layer ④	7	1.4	2.08
-15.0	Layer ③	7.2	1.41	2.62
-17.0	Layer ②	9	1.43	3.35
-17.0	Layer ①	14	1.54	4.5

$\sigma'_{zm}$  : Preconsolidation pressure ( $tf/m^2$ )  
 $S_u$  : Undrained shear strength ( $tf/m^2$ )  
 $\gamma_t$  : Wet density ( $t/m^3$ )

Fig. 4.2.2 Deposit Layer Components



EL. (m)	ELV#	$\sigma'_{vm}$	$\sigma'_n$	OCR	$\alpha$	$\mu_A$	$\mu_B$	SU	SU*
0.0	—	2.3	—	—	—	—	—	—	—
-1.0	—	2.5	—	—	—	—	—	—	—
-3.0	—	2.8	0.235	11.915	0.3	0.83	0.475	1.04	0.411
-5.0	7	4	0.94	4.253	0.3	0.738	0.648	1.27	0.607
-7.0	6	4.5	1.88	2.399	0.3	0.71	0.769	1.53	0.917
-9.0	5	7	2.82	2.482	0.3	0.7	0.761	2.08	1.108
-11.0	4	7.2	—	—	—	0.581	—	2.52	1.784
-13.0	3	9	—	—	—	0.593	—	3.35	2.374
-15.0	2	14	—	—	—	0.701	—	4.5	3.153
-17.0	1	—	—	—	—	—	—	—	—

Remarks :  $\sigma'_{vm}$  : Preconsolidation pressure (tf/m<sup>2</sup>)  
 $\sigma'_n$  : Effective normal stress after excavation work (tf/m<sup>2</sup>)  
OCR : Overconsolidation ratio after excavation  
 $\alpha$  : Constant parameter of strength decrease,  $Su/Sn=OCR^\alpha$   
 $\mu_A$  : Bjerrum's correction factor  
 $\mu_B$  : Correction factor ( $=OCR^{-5}$ )  
Su : Shear strength from F.V. test data (tf/m<sup>2</sup>)  
Su\* : Shear strength for design (tf/m<sup>2</sup>),  $Su^* = \mu_A \mu_B Su$

Fig.4.2.4 Ratio of Strength Decrease and Design Parameters for Non-treatment Slope

Fig.4.2.3 Strength Decrease Zone for Non-treatment Slopes

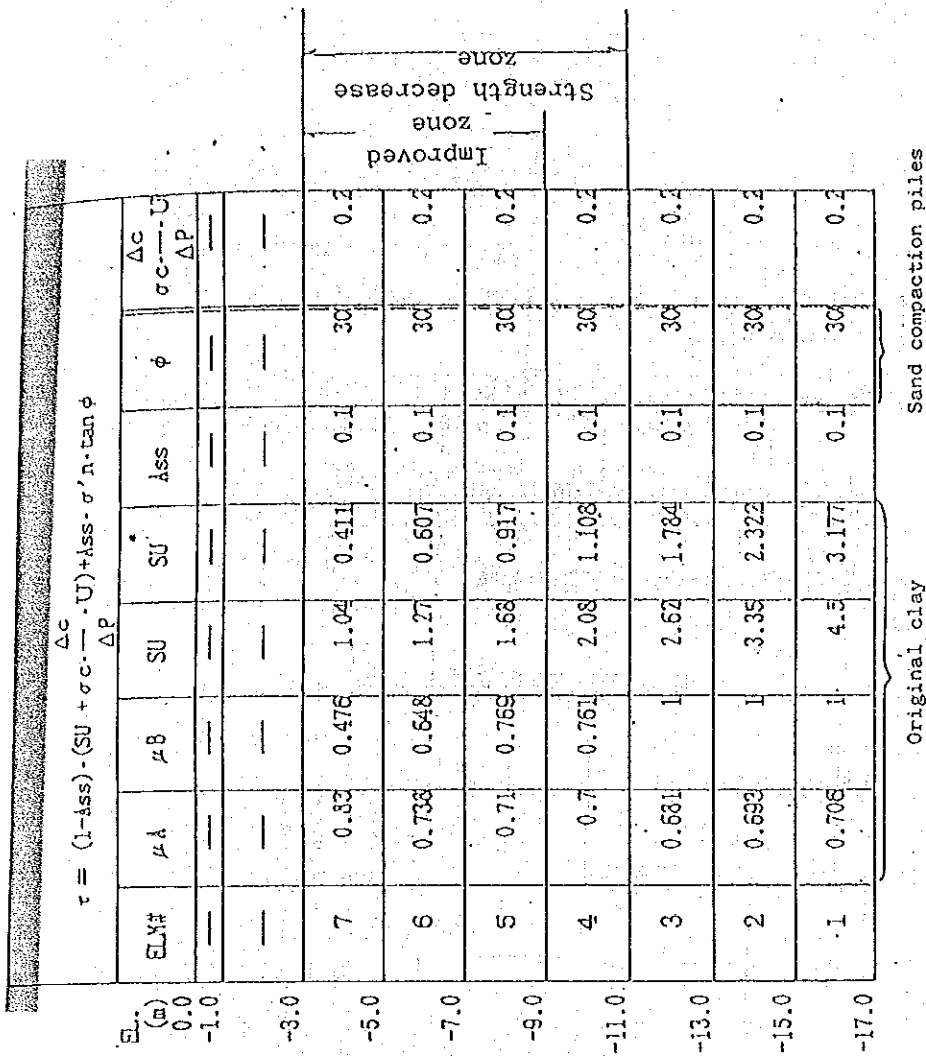


Fig.4.2.5 Strength Decrease Zone and Improved Zone by Sand Compaction Piles

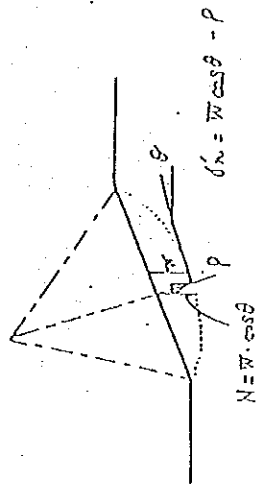


Fig.4.2.6 Design Parameters of Improved Zone by Sand Compaction Piles

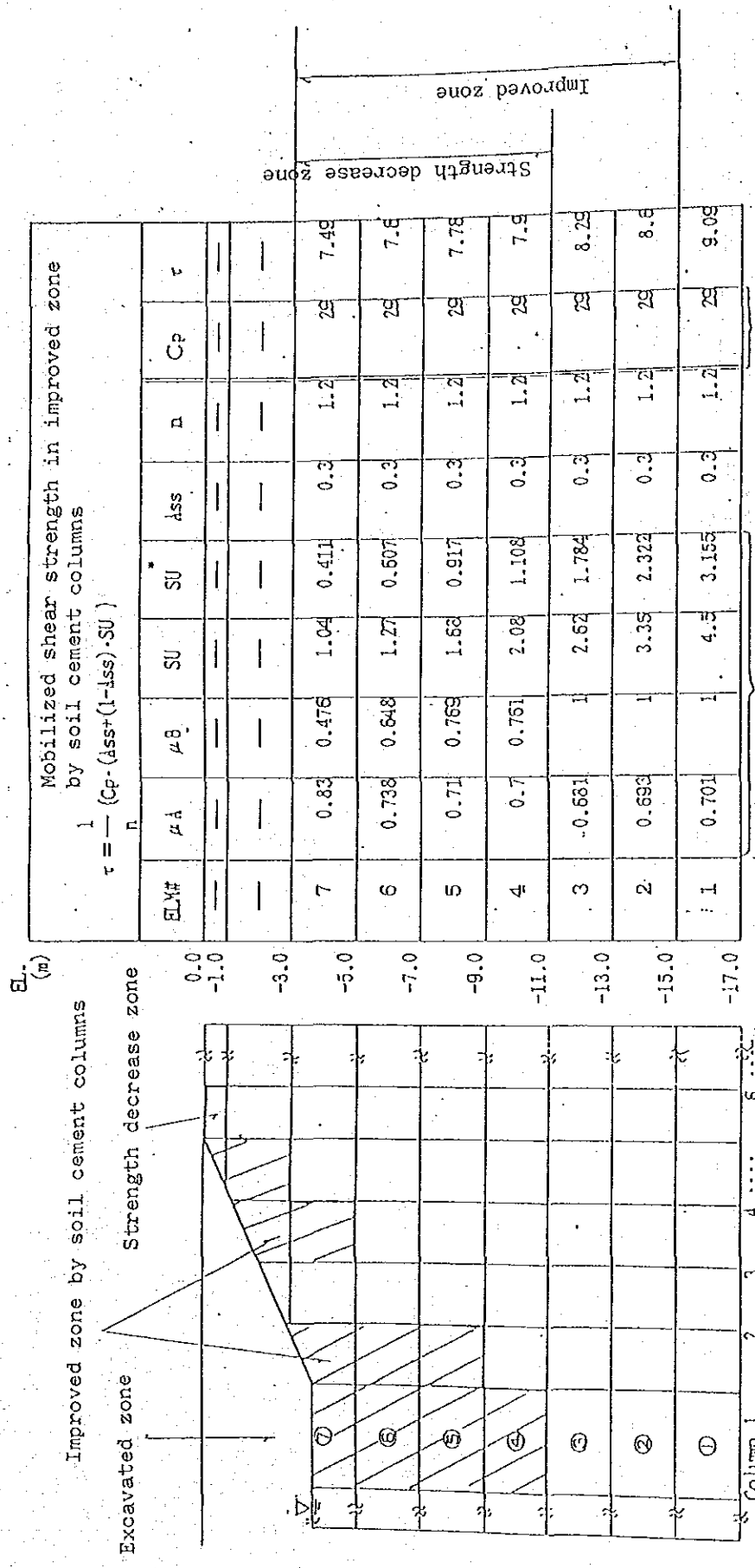


Fig. 4.2.7 Strength Decrease Zone and Improved Zone by Soil Cement Columns

A : Bjerrum's correction factor  
 B : Correction factor (=OCR, =0.3) (tf/m<sup>2</sup>)  
 Su : Shear strength F.V test data (tf/m<sup>2</sup>)  
 Su\* : Design shear strength (tf/m<sup>2</sup>)  
 Ass : Volume ratio  
 n : Safety factor  
 Cp : Shear strength of soil cement column

Fig. 4.2.8 Design Parameters of Improved Zone by Soil Cement Columns

3) Result of Stability analysis

The result of stability analysis of each case is shown in Fig. 4.2.9 ~ Fig. 4.2.12.

Although safety factors obtained in this time become a little bit smaller than factors obtained by the preliminary analysis where only the test data of Boring No. 1 was used, both of them are judged to have almost the same tendency as a whole, therefore, the design slope gradient determined in the preliminary analysis is judged to be adequate to be applied to the test slope gradients.

The minimum safety factor for long term slope stability indicates somewhat a small value because the strength of the clay is decreased to the critical point as close as possible considering strength decrease caused by excavation work and strength decrease due to anisotropy occurring in the original ground, therefore, the great care must be taken in the construction.

Table 4.2.2 Minimum Safety Factors of Slope Stability Analysis

Case of Analysis	Minimum Safety Factor (SF)	
	Data based only on Boring No. 1	Average data of all of Borings
1. Short term Stability of non-treatment slope	0.966	0.931
2. Long term Stability of non-treatment slope	1.056	1.006
3. Improved Slope by Sand Compaction Pile	1.279	1,077 (Slope Surface)
4. Improved Slope by Soil Cement Column	1.277	1.292

Fig. 4.2.9 Critical Slip Circle in Non-treatment  
Slope for Short Term Slope Stability

Slope Gradient 1:4

F.S.=0.981

R=9.96

(X,Y)=(47.5,22.5)

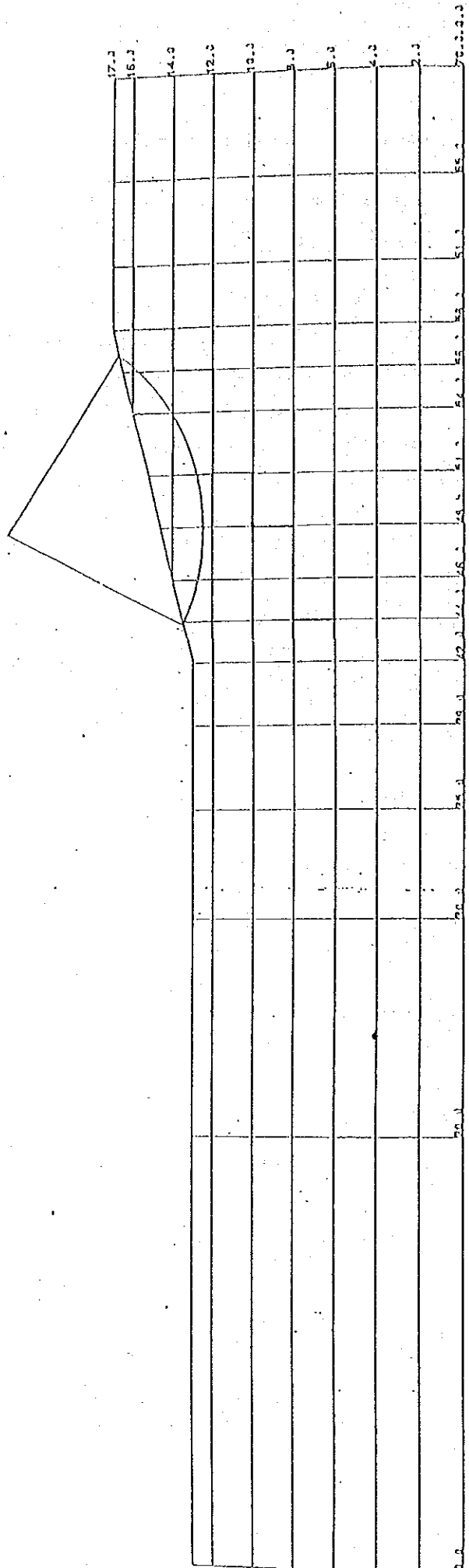


Fig. 4.2.10 Critical Slip Circle in Non-treatment  
Slope for Short Term Slope Stability

Slope Gradient 1:6

F.S.=1.006

R=14.97

(X,Y)=(50.0,25.0)

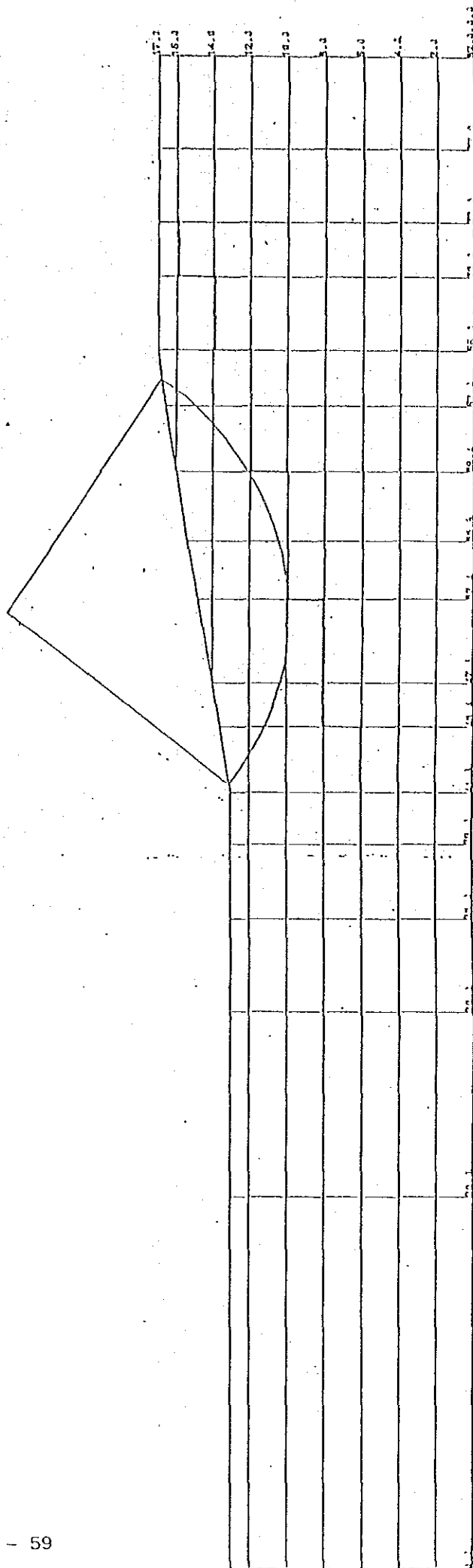




Fig.4.2.11 Critical Slip Circle in Improved Slope  
by Sand Compaction Piles

Slope Gradient 1:3

F.S=1.309

R=19.56

(X,Y)=(53.13,16.25)

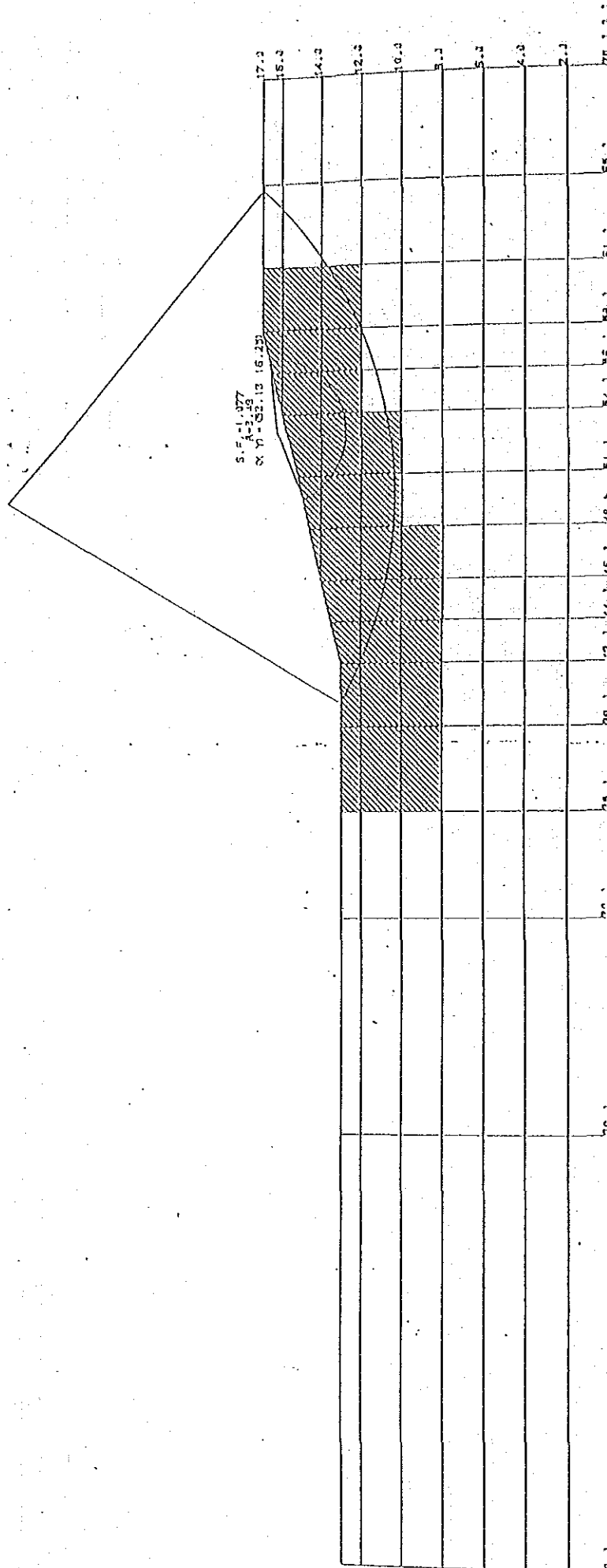


Fig.4.2.12 Critical Slip Circle in Improved Slope  
by Soil Cement Columns

Slope Gradient 1:4

F.S=1.408

R=40.0

(X, Y) = (45.0, 30.0)

F.S=1.292

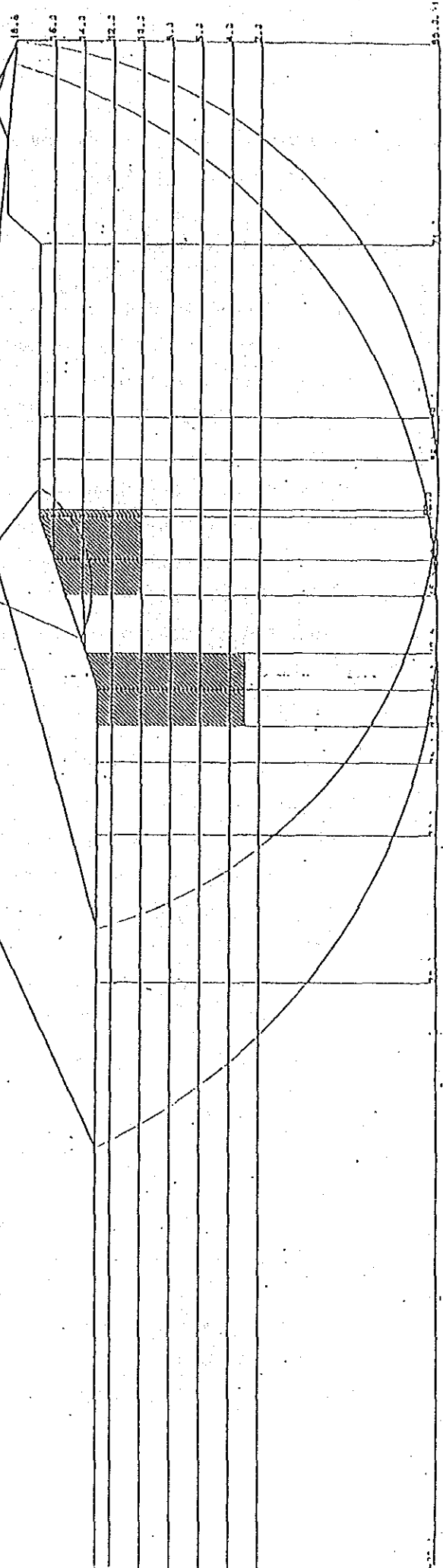
R=31.25

(X, Y) = (53.75, 21.25)

F.S=9.402

R=8.64

(X, Y) = (47.0, 22.0)



#### 4-3 Simulation on Slope Behavior by Finite Element Method using Elasto-viscoplastic Model

##### 1) Method of Analysis

When dealing with deformation of soft soil foundation, especially deformation caused by excavation work, swelling of viscous soil (clay) due to unloading is a big problem in geotechnical engineering. However, there are some limitation in the existing theory of one-dimensional consolidation where geometric configuration and loading condition of consolidation and swelling problems can not be considered in the two or three dimensional consolidation. Therefore, one of constitutive equations (stress-strain relation equations) which can express alteration of stress-strain relation and accompanied alteration of properties of materials such as coefficient of dilatancy and time dependency of creep, relaxation, etc. is adopted, and then analysis by finite element method is performed.

In the analysis this time Sekiguchi-Ota Model, one of elasto-viscoplastic models which can consider induced anisotropy is applied referring its recent record of performance (cf. Appendix 1 & 2). In addition, the model adopts the theory of multi dimensional consolidation by Akai et al., therefore effective stress analysis on relationship between skeleton of soil particle and pore water can be performed in this analysis.

##### 2) Determination of Parameters for Analysis

Parameters for the analysis should be determined referring the results of laboratory tests and in situ tests obtained in Chapter 3 in order to carry out the analysis on elasto-viscoplastic consolidation and swelling. There are fifteen (15) parameters necessary for the analysis as shown in Table 4.3.1.

The parameters are determined mainly based on data directly from Ko-note triaxial compression tests ( $\overline{CKoCU}$ ), standard consolidation tests and tests on physical properties performed for each depth.

A flow chart of determination of parameters for analysis is shown in Fig. 4.3.1.

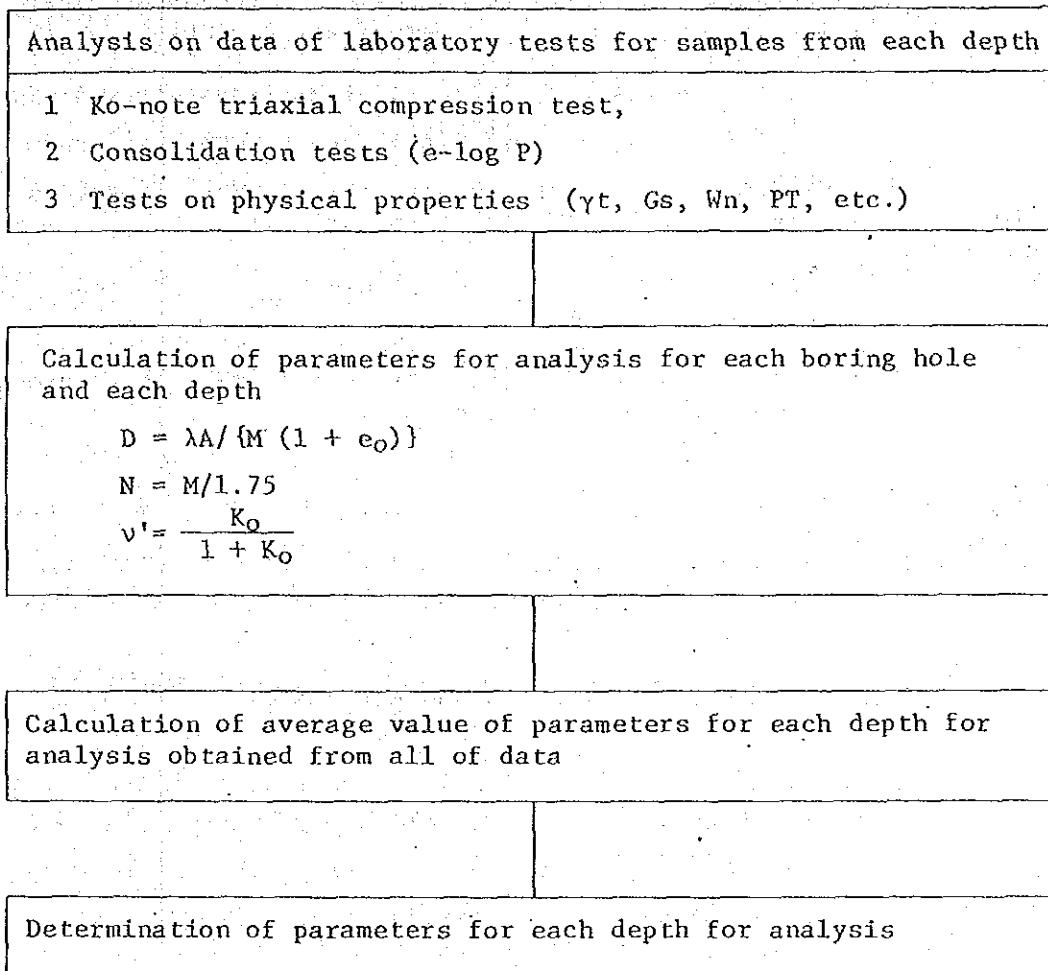


Fig. 4.3.1 Flow Chart of Determination of Parameters for Analysis

Table 4.3.1 Parameters for Analysis and its Test Method

	Parameters for Analysis	Laboratory Test	Remarks
Mechanical Properties	D : Coefficient of dilatancy	Drained triaxial compression test *1 (CD)	$D = \frac{\lambda - K}{M(1 + e_0)}$ 1)
	$\Lambda$ : Irreversibility ratio	Standard consolidation test	$\Lambda = 1 - K/\lambda$ or $M/1.75$
	M : Critical state parameter	Ko-note triaxial compression test	$M = \frac{6 \sin \phi'}{3 - \sin \phi'}$
	$v'$ : Effective Poisson ratio	- ditto -	
	$\alpha$ : Coefficient of secondary compression	Standard consolidation test	$\alpha = dv/d(\ln t)$
	$v =$ Initial volumetric strain rate	- ditto -	$V_0 = \alpha/t_c$ 2)
Pre-load	$\sigma_{v0}$ : Pre-consolidation vertical pressure	Standard consolidation test	
	$\kappa_0$ : Coefficient of earth pressure at rest	Ko-note triaxial compression test *2	
Initial Stress	$\sigma'_{vi}$ : Effective overburden pressure	Consolidation test	$\sigma'_{vi} = \sigma$ sub Z
	$K_i$ : Coefficient of in-situ earth pressure at rest	Triaxial Ko-swelling test	
	K : Coefficient of permeability	Standard consolidation test	$K = \gamma W_m v C_v$

Parameter of stress	$\eta^* = \sqrt{\frac{3}{2} (\eta_{ij} - \eta_{ij0})(\eta_{ij} - \eta_{ij0})}$ $\eta_{ij} = \frac{S_{ij}}{P}, S_{ij} = \sigma'_{ij} - \rho \sigma'_{ij}$ $P^i = \frac{1}{3} \sigma'_{ij}$
---------------------	---

Where 1)  $\lambda = 0.434 C_c$ ,  $K = 0.434 C_s$  (in case of natural logarithm)

2)  $t_c$  : When one dimensional consolidation completed

3)  $\sigma'$  : Weight of soil in water

4)  $\sigma'_{ij}$  : Effective stress tensor

\*1 In this project undrained triaxial compression test is not performed, therefore, D is obtained from calculation.

\*2 The value of  $\kappa_0$  is obtained by Alpan's method (1967).

As to the determination of parameters for analysis of Bangkok Clay, results of soil tests are taken seriously and used in order to heighten accuracy of analysis, and presumptive equation for each parameter was tried to be not applied as far as possible, except for the value of coefficient of earth pressure at rest  $K_0$  corresponding to pre-load, which is obtained by Alpan's method (1967) as follows.

$$K_0 = 0.19 + 0.233 \times \log PI$$

where, PI: Plasticity index (%)

The above equation has been verified to be able to obtain approximate value of  $K_0$  tolerable enough for engineering use through the past performance on Bangkok Clay and on Kibushi Clay in Japan as shown in Appendix 3.

As to values obtained from each soil test, the geological components at the project site are judged to be horizontally almost homogeneous as mentioned in chapter 3, an average value of data of samples taken from each depth of all the boring holes is adopted as the representing value of parameters for each layer of each depth.

Each average value of parameters is determined based on depth distribution of data of each test, and the representing value of each depth (layer) is determined.

The adopted values of parameters for analysis are shown in Table 4.3.2.

As there are no data on stiff clay below EL. 17 m, estimated values shown in Table 4.3.2 are applied to stiff clay assuming that stiff clay is linear elastic body.

There are two cases of analysis. One is non-treatment excavated slope of case I (slope gradient : 1 : 4, excavation depth: 4 m), and the other is improved slope by soil cement columns (slope gradient : 1 : 3, excavation depth : 4 m) (cf. Fig. 4.3.2).

Table 4.3.2 Summary of Design Parameters for F.E.M. Analysis

LEAYER	DEPTH (m)	① $D = \lambda \Delta / (M(1+s_0))$				② $\Delta$	③ $\nu = \frac{k_0}{1+k_0}$	④ $b_x$ ⑤ $b_y$ ⑥ $b_z$ (m/day)	⑦ $\sigma' v' d$ (t/m <sup>2</sup> )	⑧ $k_0$	⑨ $\sigma' v' i$ (t/m <sup>2</sup> )	⑩ $K_i = k_0(OCR)$	⑪ $0.54 \exp(-P/L/122)$							
		⑫ $e_0$	⑬ $M$	⑭ $\kappa$	D								$N = 1 - k/\lambda$	$\lambda = M/1.75$	$\frac{\sigma' v \sigma}{\sigma' v i}$	P.I.(%)				
11	-1.0	0.16	2.1	1.22	0.08	0.021	0.029	0.029	0.5	0.697	0.373	$4.32 \times 10^{-4}$	2	0.595	0.24	1.236	8.33	55	0.0028	$1 \times 10^{-4}$
10	-3.0	0.2	2.2	1.1	0.07	0.037	0.036	0.036	0.53	0.529	0.372	$6.05 \times 10^{-4}$	2	0.594	0.96	0.766	2.083	54.4	0.003	$1 \times 10^{-4}$
9	-5.0	0.26	2.25	0.98	0.068	0.06	0.049	0.049	0.738	0.56	0.376	$6.05 \times 10^{-4}$	2.4	0.602	1.92	0.649	1.25	58.8	0.0059	$1 \times 10^{-4}$
8	-7.0	0.28	2.3	0.98	0.048	0.072	0.048	0.048	0.829	0.56	0.377	$5.27 \times 10^{-4}$	3.2	0.604	2.88	0.625	1.111	59.8	0.0059	$1 \times 10^{-4}$
7	-9.0	0.32	2.5	0.96	0.043	0.082	0.052	0.052	0.866	0.55	0.379	$4.75 \times 10^{-4}$	4	0.611	3.84	0.619	1.042	64.4	0.0059	$1 \times 10^{-4}$
6	-11.0	0.35	2.7	0.99	0.04	0.085	0.054	0.054	0.886	0.56	0.385	$3.54 \times 10^{-4}$	5.2	0.625	4.8	0.64	1.082	73.3	0.0131	$1 \times 10^{-5}$
5	-13.0	0.36	2.65	1.02	0.036	0.087	0.056	0.056	0.9	0.562	0.387	$2.59 \times 10^{-4}$	6.8	0.632	5.76	0.662	1.181	79.2	0.0073	$1 \times 10^{-5}$
4	-15.0	0.34	2.35	1.02	0.034	0.09	0.058	0.058	0.9	0.562	0.387	$1.73 \times 10^{-4}$	8	0.764	6.72	0.662	1.19	77.2	0.0097	$1 \times 10^{-5}$
3	-17.0	0.3	2	0.98	0.04	0.088	0.057	0.057	0.867	0.56	0.385	$1.73 \times 10^{-4}$	10	0.625	7.68	0.676	1.302	73.4	0.0102	$1 \times 10^{-4}$
2	-25.0	0	0	0.98	0	0.080	0.055	0.055	0.559	0.56	0.367	$6.7 \times 10^{-4}$	11.3	0.58	10.56 (tt=1.5)	0.595	1.07	47	0.007	$1 \times 10^{-4}$
1	-30.0	---	---	---	---	---	---	---	---	---	---	$1.0 \times 10^{-4}$ (9.8 x 10 <sup>-4</sup> )	---	---	14.46 (tt=1.6)	0.595	---	---	---	---

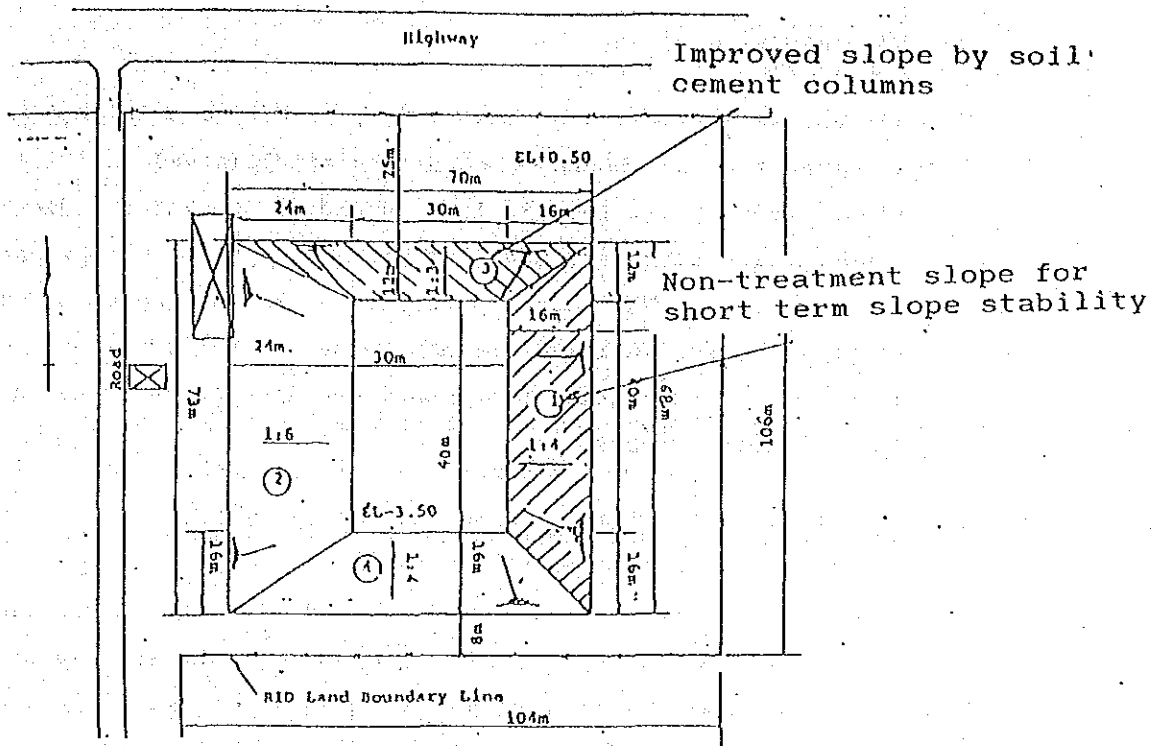


Fig. 4.3.2 Plan of Testing Canal

Parameters for the analysis obtained this time shown in Table 4.3.2 are compared with parameters adopted for other analyses in the past. Parameters for analysis shown in Table 4.3.3 were adopted by Asaoka et al. (1985) for the analysis of undrained normally consolidated clay ground. Parameters shown in Table 4.3.4 were adopted for the analysis of visco-elasto-plastic secondary consolidation of highway constructed in Higashi Komesato area, Hokkaido, Japan. Although above each clay is different from each other, parameters for each analysis has similar tendency to each other except for the high  $e_0$  value bigger than 2.1 and somewhat small value of swelling index smaller than 0.10 in Bangkok Clay.

The values of  $e_0$  and  $n$  can be judged quite appropriate considering that the soft clay foundation of the test site is new marine clay foundation, and the parameters for the analysis of Bangkok Clay shown in Fig. 4.3.2 are judged adequate.



### 3) Determination of Mesh Model

For the determination of mesh model, boundary condition (geometrical condition and boundary condition of drainage), initial condition (ground water level), load (un-load) condition indicating construction stage and model of ground composition for analysis are necessary. The boundary conditions and the model of ground composition for analysis are determined as follows from the results of construction plan mentioned in Chapter 6 and in-situ and laboratory tests.

#### ① Model of ground composition

As described in preliminary analysis for the slope stability in chapter 4, the ground composition of the soft layers are divided into soft clay portion (EL. 0.0 ~ EL. -17.0) and stiff clay portion (EL. -17.0 ~ EL. -30.0). Furthermore, the ground composition are subdivided into horizontal sedimentary layers in detail as shown in Fig. 4.3.3.

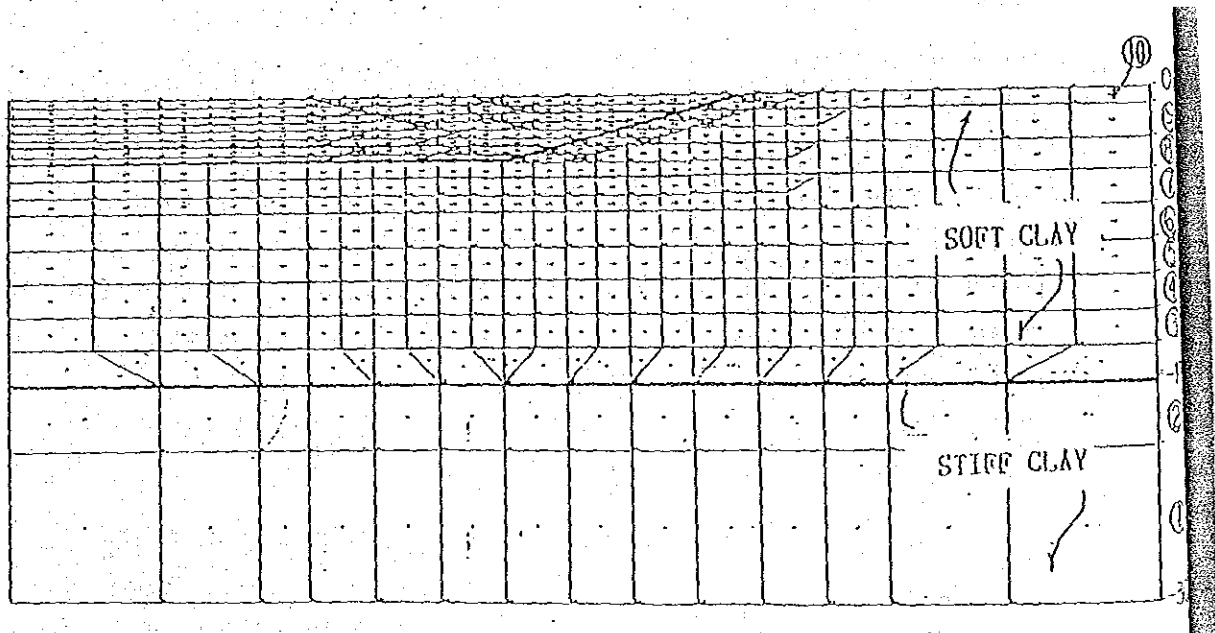


Fig. 4.3.3 Model of Layer Deposit Component

The soft clay portion is estimated to be almost in a state of normal consolidation except for the surface layer showing an overconsolidation ratio (OCR) of 8.033. Physical properties of each layer is shown in the preceding Table 4.3.2.

② . Boundary conditions

i) Excavation stage

Excavation work is divided into two stages. One is the 1st excavation stage (EL. -0.50 m ~ EL. -1.50m) and the other is the 2nd excavation stage (EL. -1.50m ~ EL. -3.50m) as shown in the construction plan in Chapter 6.

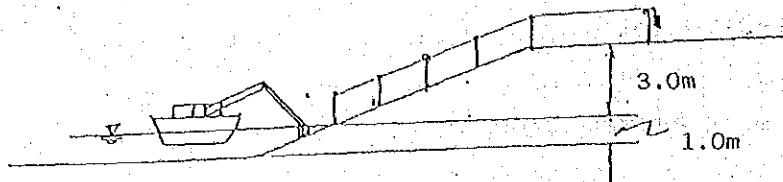
a. 1st excavation stage

Construction is carried out by Backhoes, clamshells and by dump tracks in dry condition in 1st excavation stage. Steel plates are put under backhoes and clamshells so as to decrease their contact pressures to the ground, however, degree of soil disturbance caused by vibration of the machines is not grasped at the present time. Consequently, alteration (deterioration) in physical properties of soft clay by vibration caused by heavy equipments is not considered in this analysis.

b. 2nd excavation stage

Construction is carried out by backhoes on a pontoon in wet condition so as not to give any contact pressure on excavated surface. The depth of water in the test canal is gradually decreased for the installation of extensometers on the slope, however about 1m of the depth of draft for pontoon should be secured. Eventually, installation of extensometer is possible down to EL. -2.50 m in accordance with excavation.

After excavating the remaining 1m, the water inside the test canal is pumped out to install the remaining extensometers.



- ii) Alteration of boundary conditions of drainage and ground water level with the progress of excavation stages.

As excavation progresses, boundary conditions and ground water level change correspondingly as shown in Fig. 4.3.5 ~ Fig. 4.3.6. Up to the excavation stage 7, excavation work is in dry condition, therefore original ground surface become drainage boundary.

Secondary, as excavation stage 8 to 13 are done in wet condition, water level for the operation of pontoon is considered for the analysis.

The excavation stages and progress of excavation are shown in Fig. 4.3.4 and Table 4.3.5 respectively.

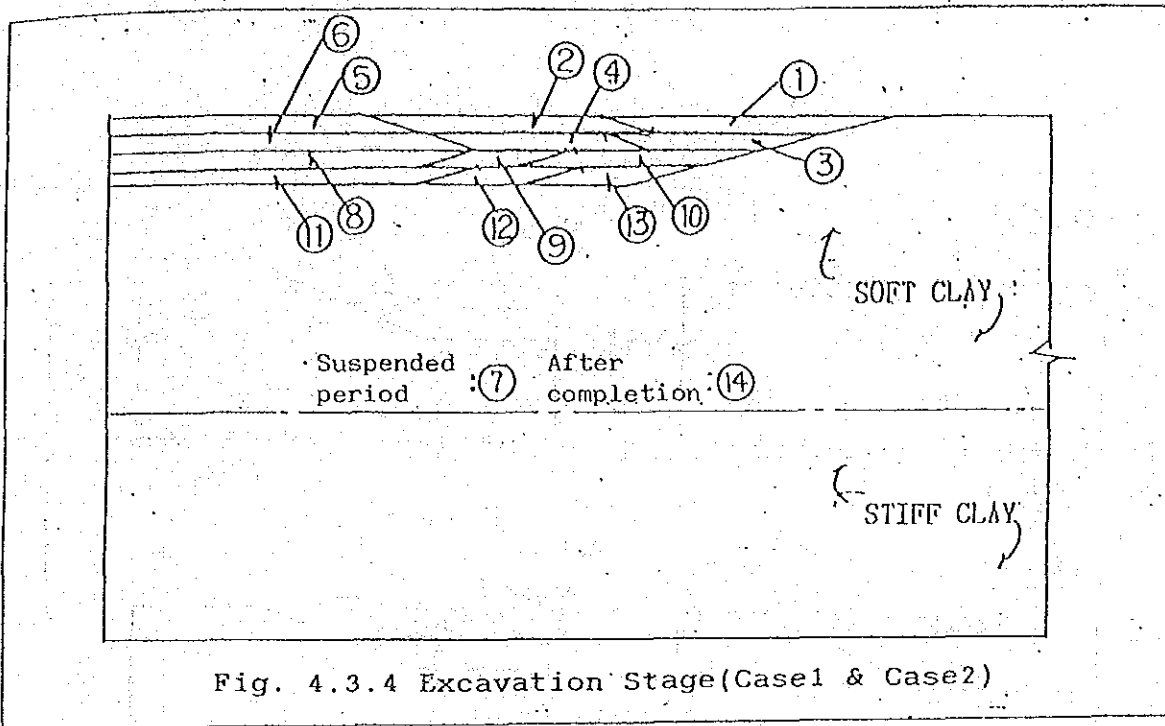


Table 4.3.5 Progress of Excavation

	Excavation Method	Stage No.	Duration of stage (days)	Total lapsed days (days)	Remarks
First excavation stage	Dry excavation	1	6	6	
		2	9	15	
		3	6	21	
		4	11	32	
		5	15	47	
		6	15	62	
Suspended period		7	6	68	
Second excavation stage	Wet excavation	8	5	73	
		9	3	76	
		10	3	79	
		11	3	82	
		12	3	85	
		13	3	88	
		14	20	108	

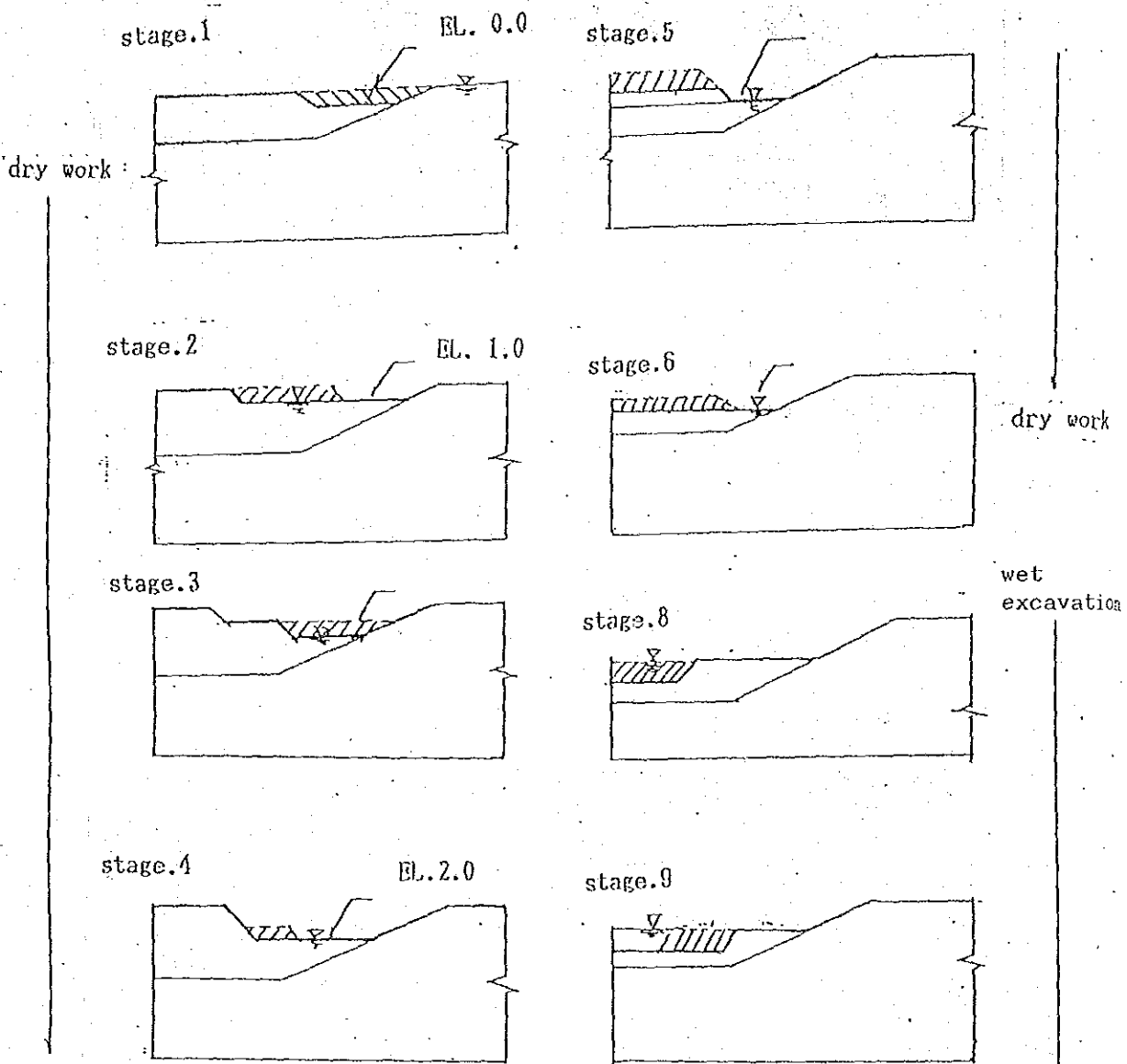


Fig.4.3.5 Excavation Stage and Boundary Condition of Ground Water Level (1)

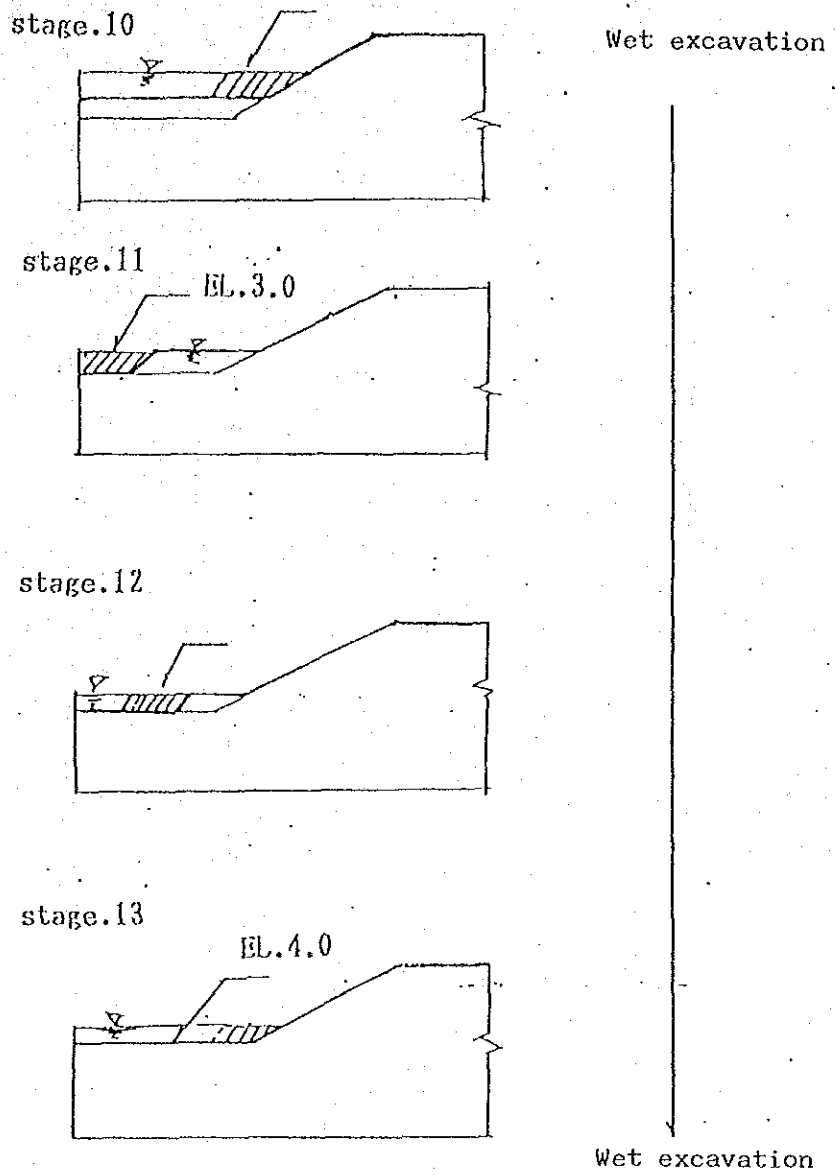


Fig.4.3.6 Excavation Stage and Boundary Condition of Ground Water Level (2)

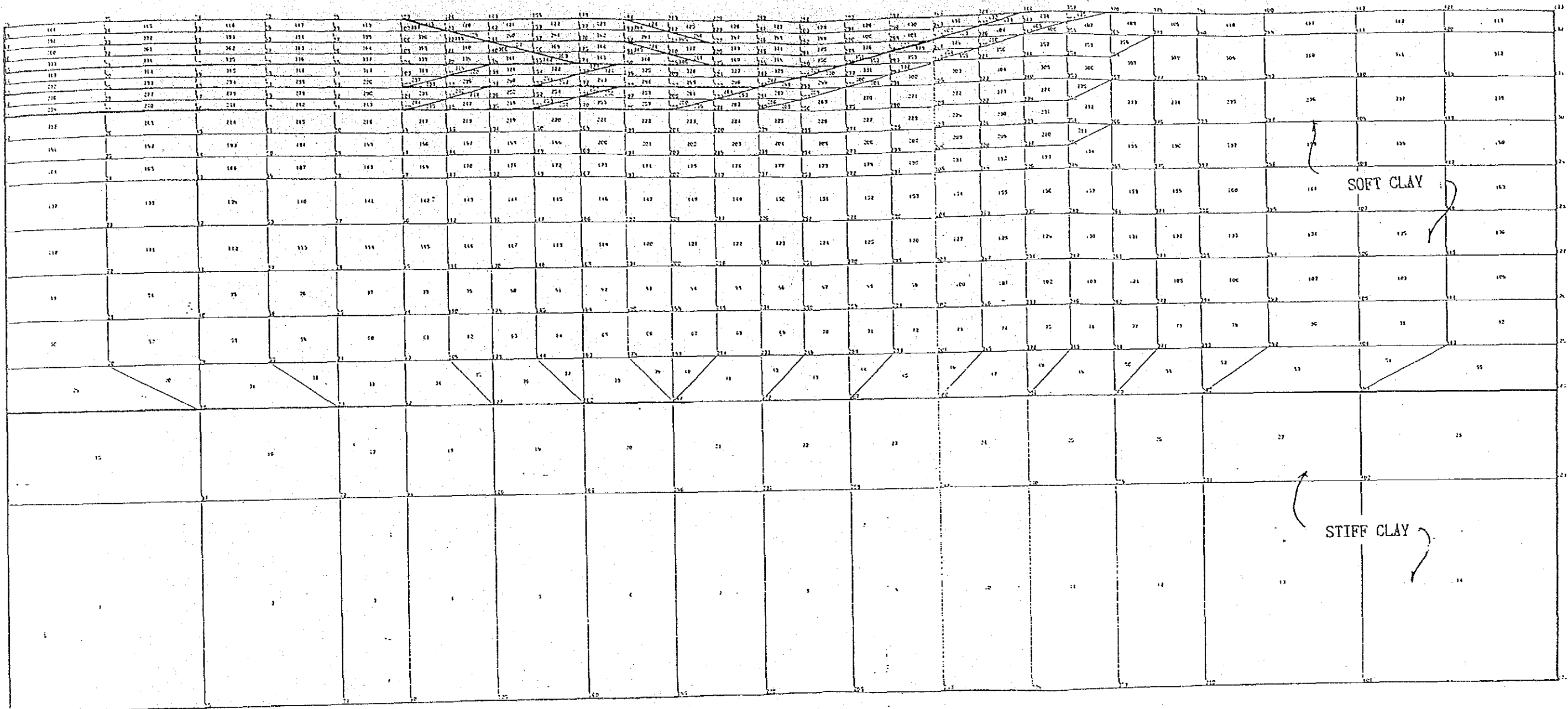


Fig.4.3.7 Analysis Model of F.E.M. for Non-treatment Slope For Short Term Slope Stability (Slope Gradient, 1:4)

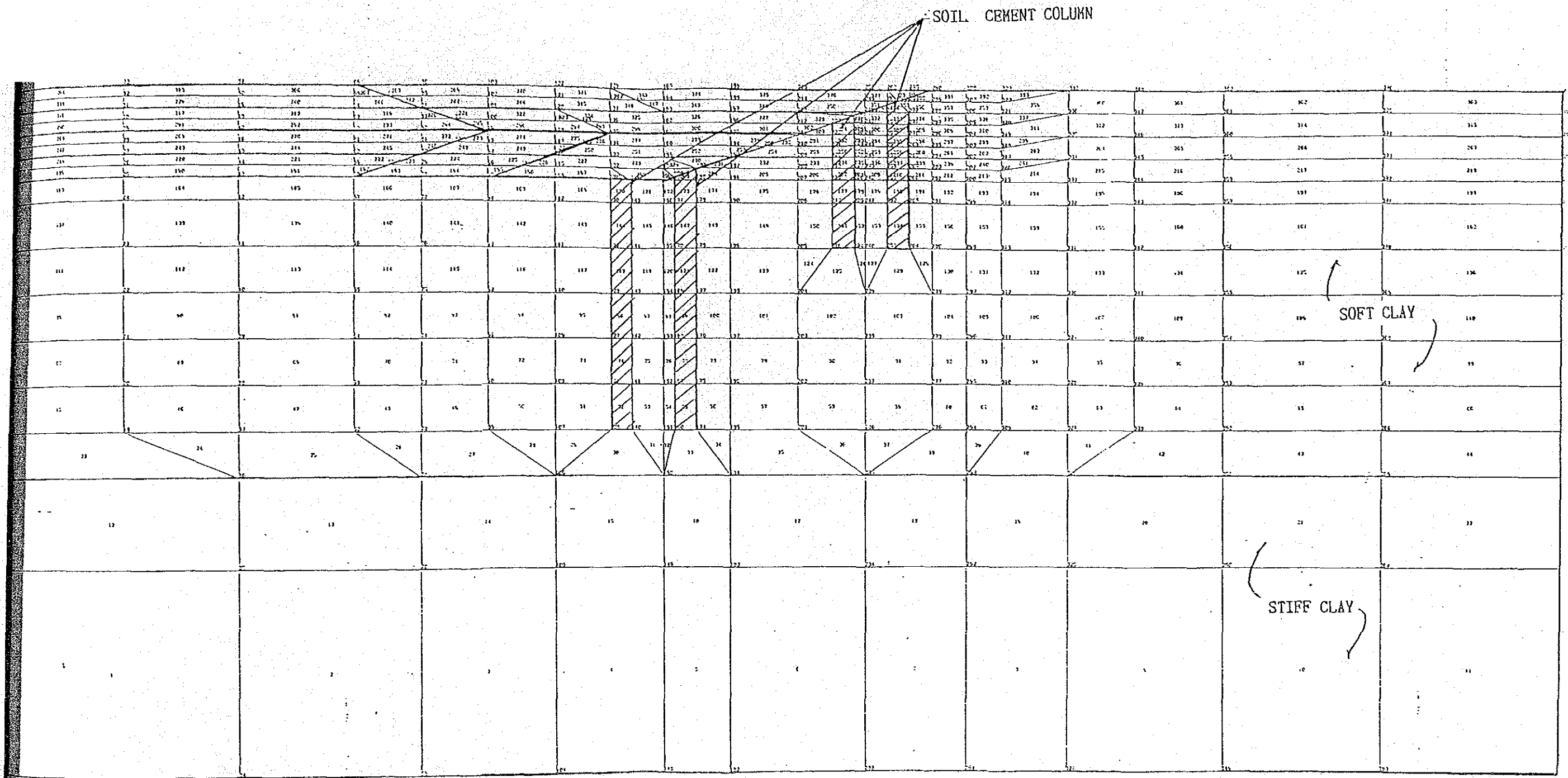


Fig.4.3.8 Analysis Model of F.E.M. for Improved Slope by Soil Cement Columns (Slope Gradient, 1:3)



#### 4) Results of Analysis and Evaluation

- 1) Non-treatment slope for short term stability (slope gradient 1 : 4) (1 ~ 62 days)

Results of simulation for each stage of excavation work for non-treatment slope for the study of short term stability are shown in Fig. 4.3.9 ~ Fig. 4.3.27.

- a. First excavation stage (dry condition)

Studying on overall deformation behaviour of ground from the figures of overall displacement, degree of deformation is about 20 ~ 30 cm vertically and horizontally in the dry work stage of 2 m excavation in depth which can be considered of no problem. There is no place showing symptoms of slope failure seeing the process of deformation in the figure of deformation vector. Furthermore, there is no big change in pore water pressure in the ground. Seeing from the figures of principal stress, there is no disorder in distribution of principal stress and is no place of failure. Therefore, it is judged that there is no problem up to the first excavation stage.

- b. Second excavation stage (wet condition : 80 days)

Tendency of swelling is found at around the toe of the slope (EL. -1.5 m) more less during the transitional period from the first excavation stage in dry condition to the second excavation stage of wet condition, however, sliding failure is still not occurred. This tendency increases gradually as wet excavation progresses but doesn't reach to formation of slip surface to the 14th stage, the completion stage of excavation.



c. After completion of excavation (80 ~ 110 days)

When the test canal is in dried condition just after the water remaining in the canal is pumped out after the excavation work is completed, swelling is found in the excavated slope around EL. -2.0 ~ -3.0, and in such condition slope failure is predicted to occur with high possibility. Moreover, disorder in principal stress distribution and in pore water pressure is found.

Following the results of simulation on excavation procedure mentioned in the above, construction of non-treatment slope with a gradient of 1 : 4 should be carefully carried out from the second excavation stage below EL. -1.50 m paying serious attention to any disorder indicated by displacement gauges and piezometer.

ii) Improved slope by soil cement column (gradient 1 : 3)

a. First excavation Stage (dry condition)

Seeing the figures of overall displacement, Fig. 4.3.28 ~ Fig. 4.3.33, lateral flow in the excavated slope is well prevented by improved zone by soil cement columns showing remarkable effect of the said method. Figures of deformation vector and principal stress in Fig. 4.3.35 ~ Fig. 4.3.37 also prove that the soil cement column method has great effect on prevention of deformation.

b. Second excavation stage (wet excavation : 80th day)

Lateral flow in the slope is almost completely prevented as well as the first excavation stage as shown in the figures of overall displacement, Fig. 4.3.33 ~ Fig. 4.3.34. However, swelling caused by unloading is found in the excavated surface of the canal bed, and the strength of the said position is predicted to be decreased. In the final stage of excavation, it is necessary to pay strong

attention to the non-treatment portion, between two improved zones by soil cement columns, where heaving is slightly found.

Lateral flow is prevented well by soil cement columns, which can be said to prove superiority of this improvement method.

Judging from the above results from the F.E.M analyses for the short term stability of the non-treatment slope (slope gradient 1 : 4), big lateral flow is predicted to occur from the middle part to the toe of the slope, probably at or after the time of completion of excavation.

These results can be said to satisfy the initial aim to grasp the short term stability of this non-treatment slope. As to the improved slope by soil cement column (slope gradient 1 : 3), lateral displacement in the slope and in the toe of the slope is almost prevented, which can be judged to prove the adequacy of this improvement method, however, in both cases (non-treatment slope and improved slope) swelling caused by unloading by excavation is found in the canal bed, strength in the surface of the canal bed is seemed to be decreased.

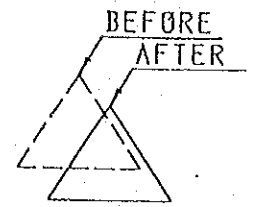
The arrangement plan of sensors for the monitoring system is made considering the results of elasto-visco-plastic analysis (cf. chapter 5).

DISPLACEMENT

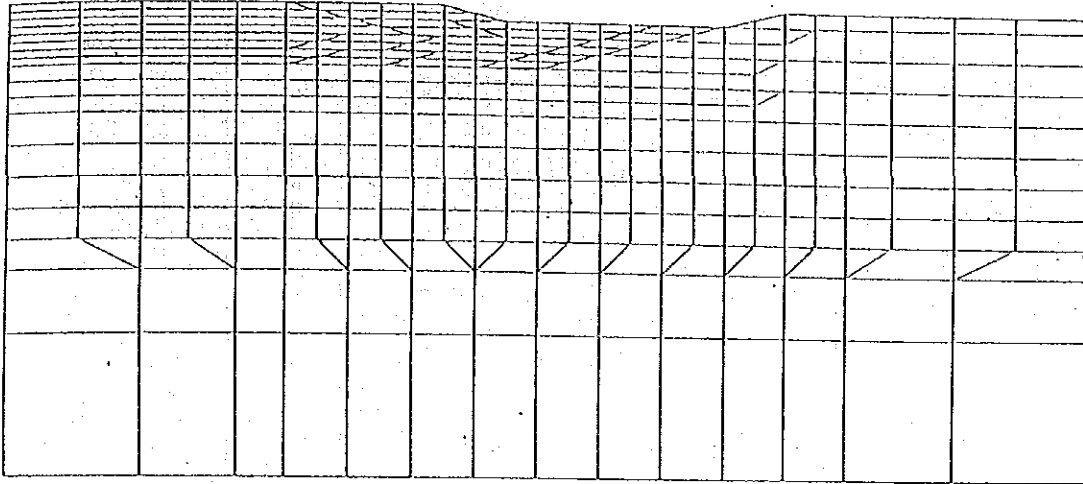
MODEL SCALE (m)  
0.0 16.00

DISPLACEMENT SCALE (m)  
0.0 64.00

LEGEND



STEP=2.0  
TIME=7.0



STEP=3.0  
TIME=16.0

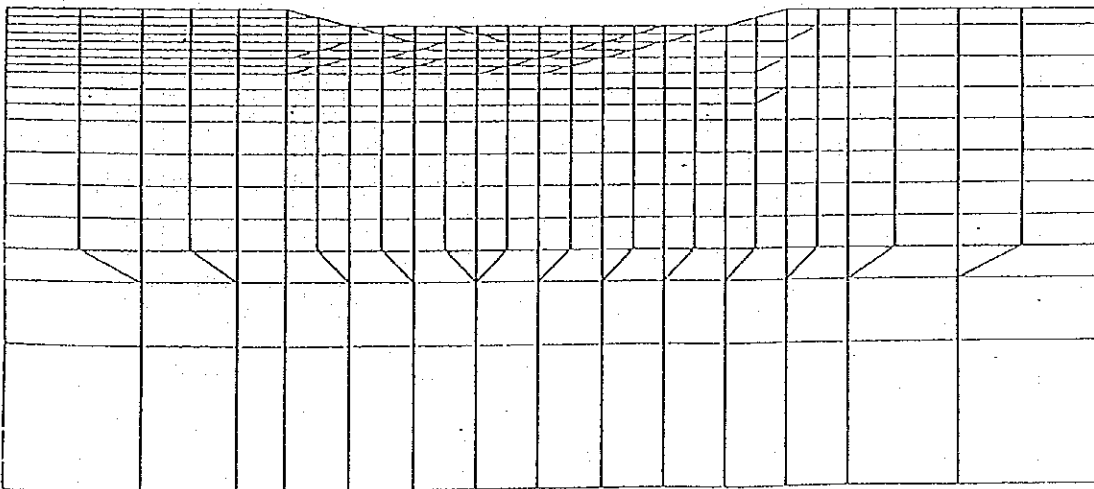


Fig.4.3.9 Overall Displacement in Non-treatment Slope for Short Term Slope Stability

DISPLACEMENT.

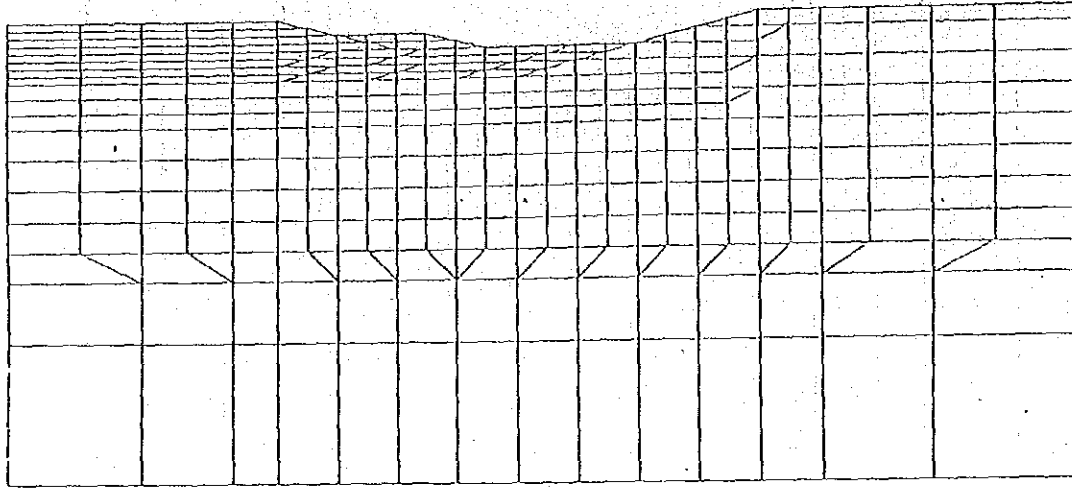
LEGEND

MODEL SCALE (m)  
0.0 16.00

DISPLACEMENT SCALE (m)  
0.0 64.00



STEP=4.0  
TIME=22.0



STEP=5.0  
TIME=33.0

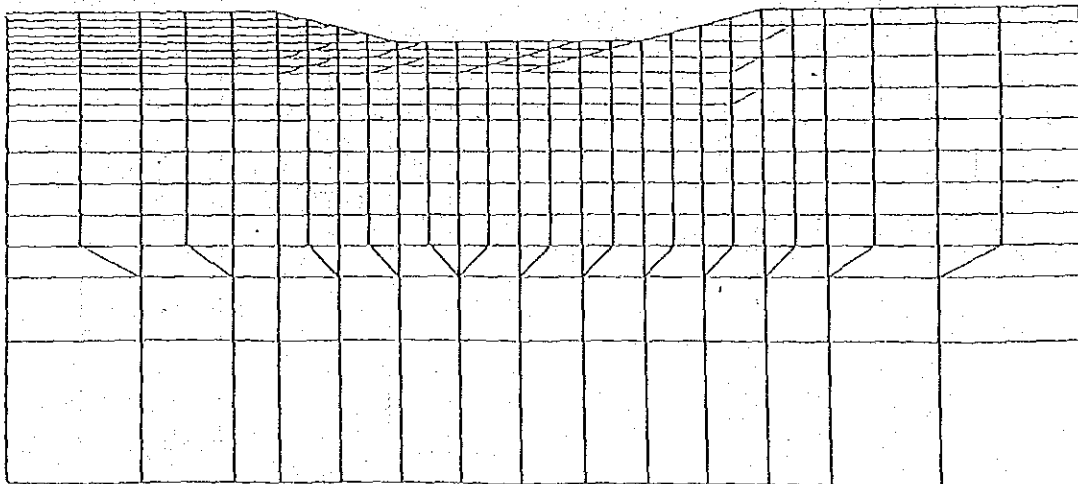
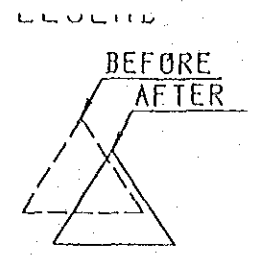


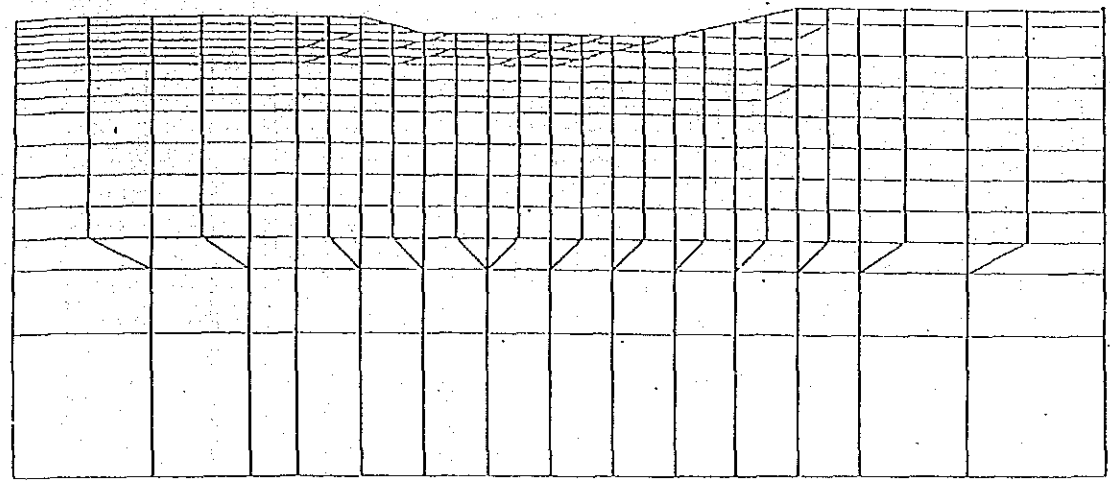
Fig.4.3.10 Overall Displacement in Non-treatment Slope for Short Term Slope Stability

DISPLACEMENT  
MODEL SCALE (m)  
0.0 16.00

DISPLACEMENT SCALE (m)  
0.0 64.00



STEP=6.0  
TIME=39.0



STEP=7.0  
TIME=54.0

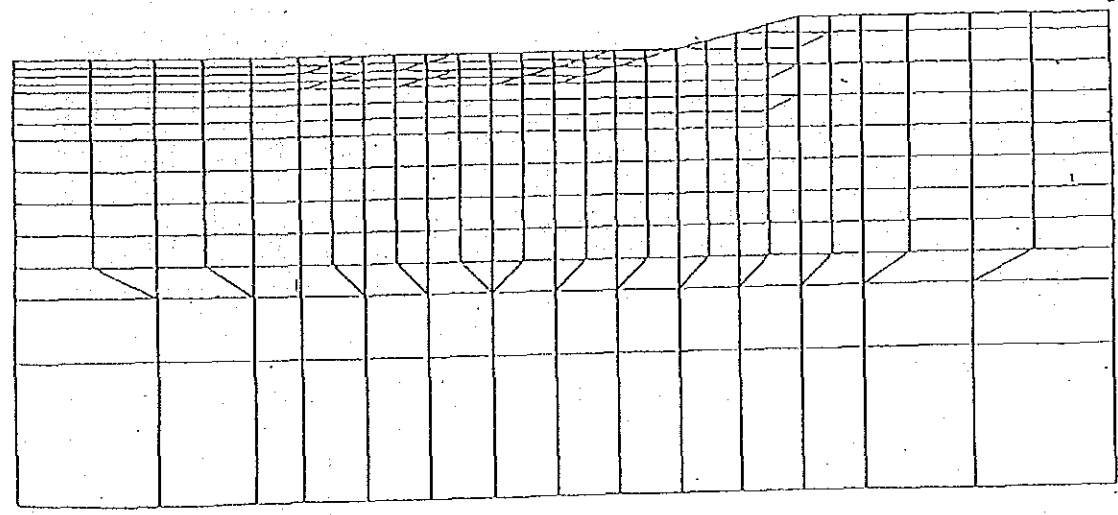
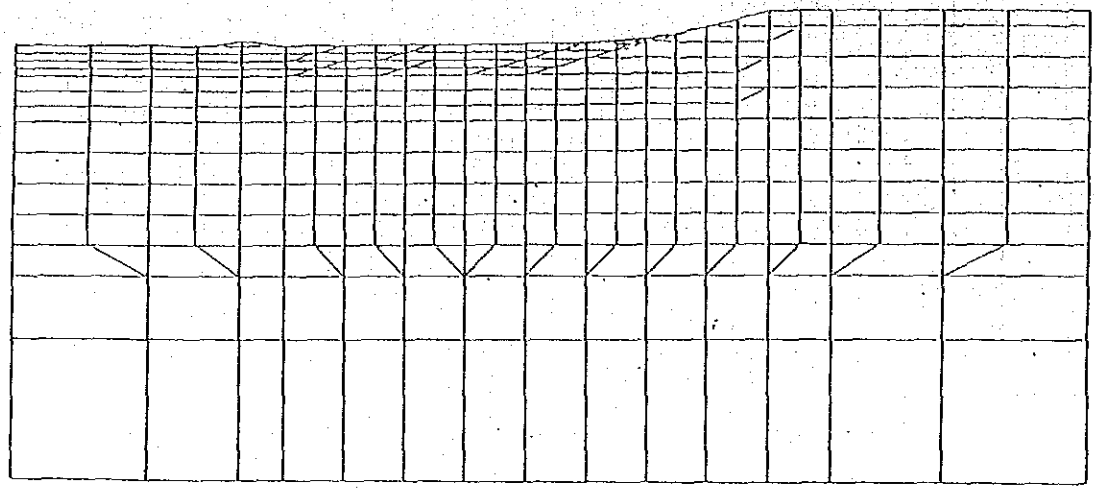


Fig.4.3.11 Overall Displacement in Non-treatment Slope for Short Term Slope Stability

DISPLACEMENT  
MODEL SCALE (m)  
0.0 16.00  
DISPLACEMENT SCALE (m)  
0.0 64.00

LEGEND  
BEFORE  
AFTER  
STEP=8.0  
TIME=60.0



STEP=9.0  
TIME=65.0

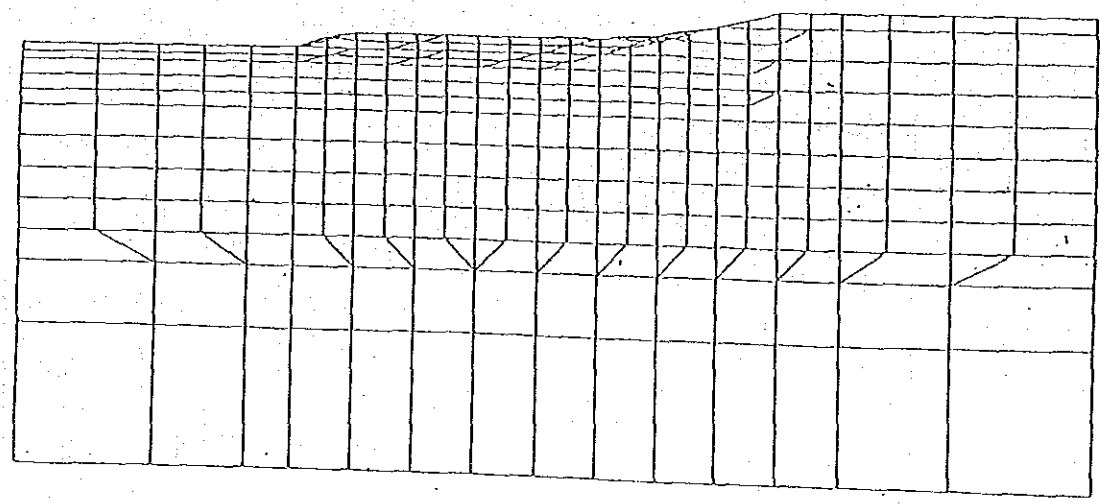
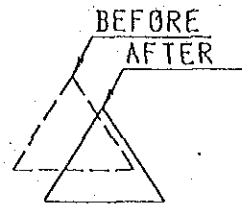
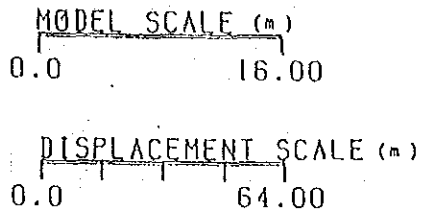


Fig.4.3.12 Overall Displacement in Non-treatment Slope for Short Term Slope Stability

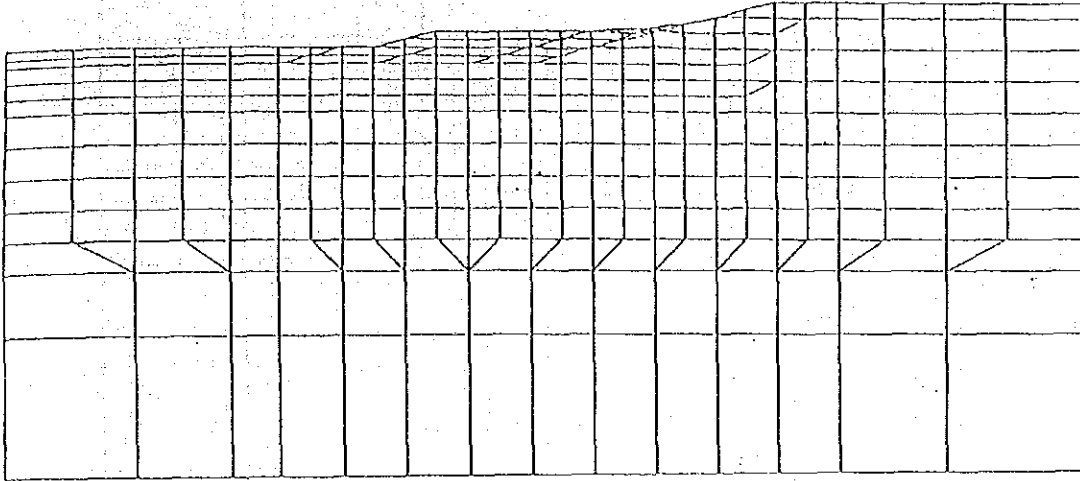


DISPLACEMENT

LEGEND



STEP=10.0  
TIME=68.0



STEP=11.0  
TIME=71.0

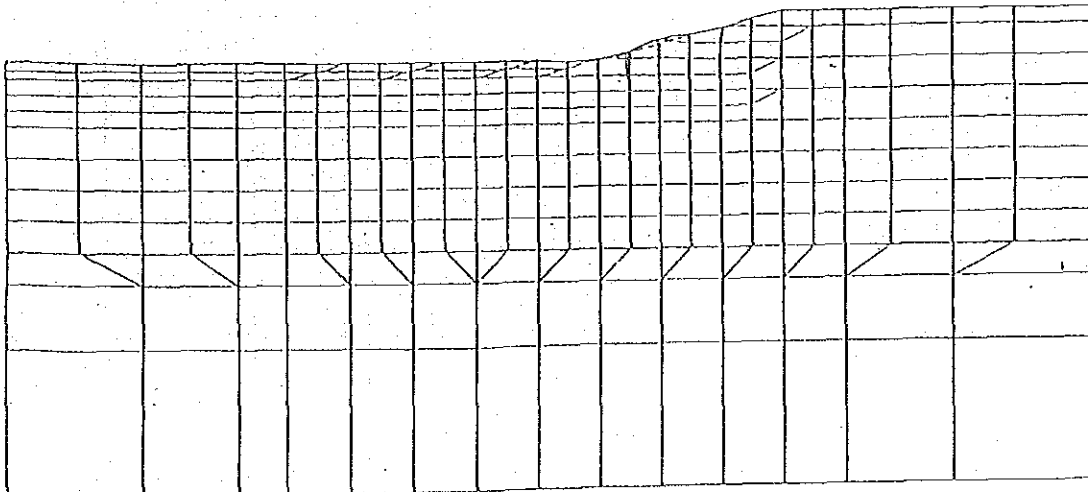


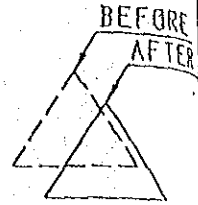
Fig.4.3.13 Overall Displacement in Non-treatment Slope for Short Term Slope Stability

DISPLACEMENT

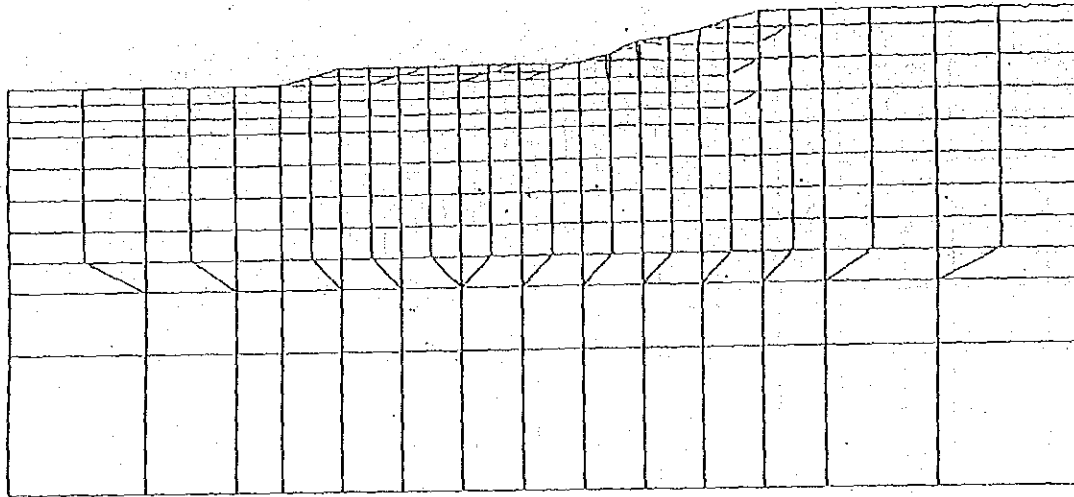
LEGEND

MODEL SCALE (m)  
0.0 16.00

DISPLACEMENT SCALE (m)  
0.0 64.00



STEP=12.0  
TIME=74.0



STEP=13.0  
TIME=77.0

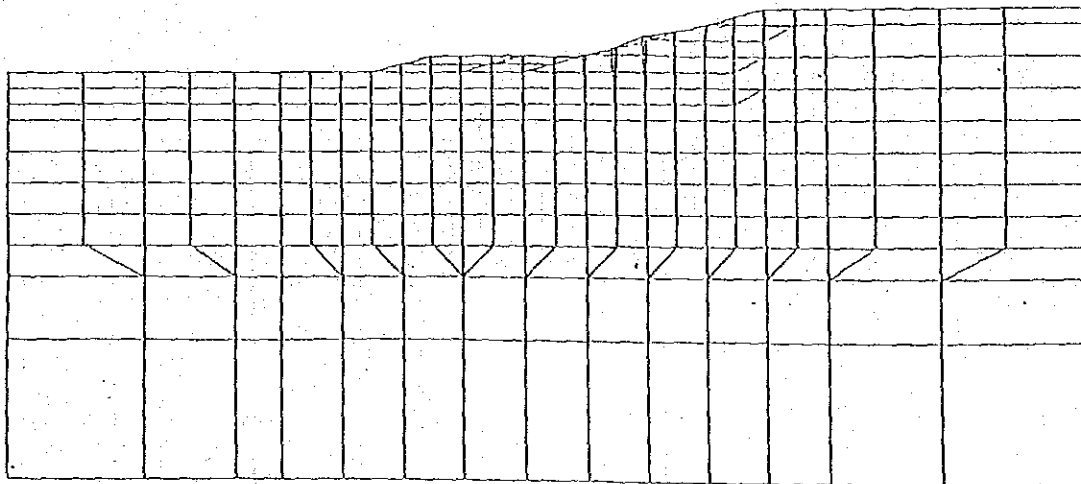
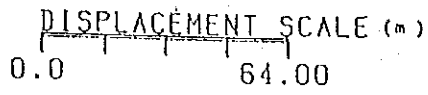
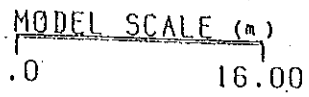
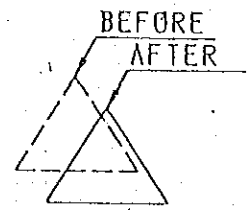


Fig.4.3.14 Overall Displacement in Non-treatment Slope for Short Term Slope Stability

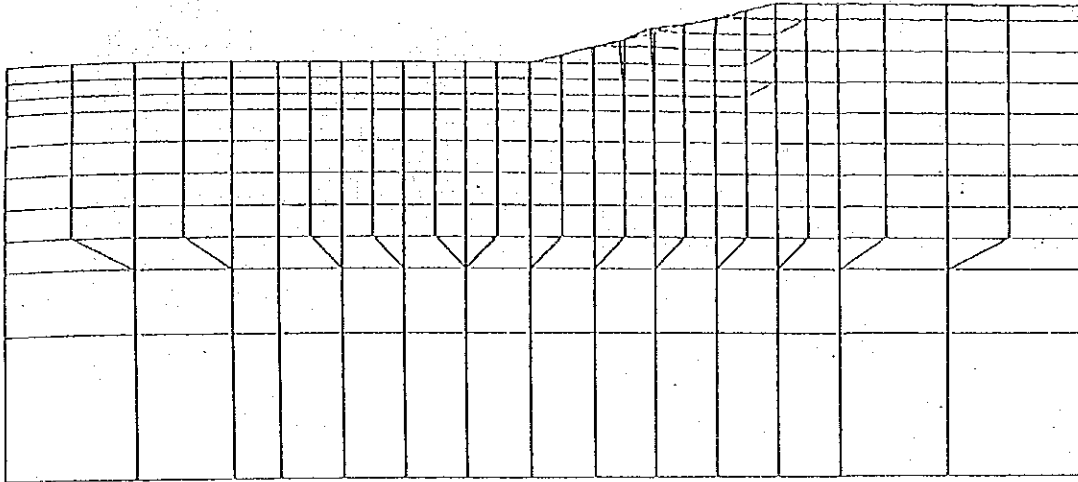
DISPLACEMENT



LEGEND



STEP=14.0  
TIME=80.0



STEP=15.0  
TIME=110.0

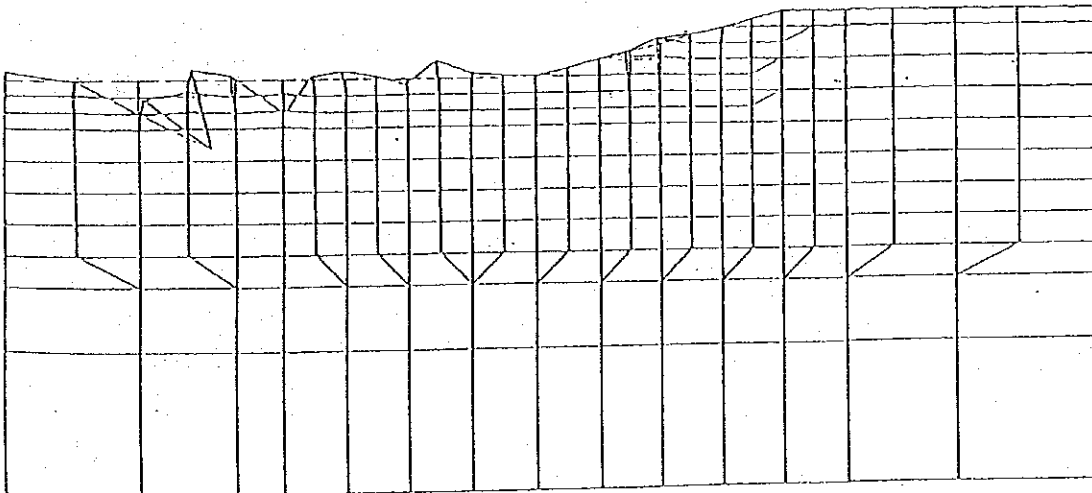
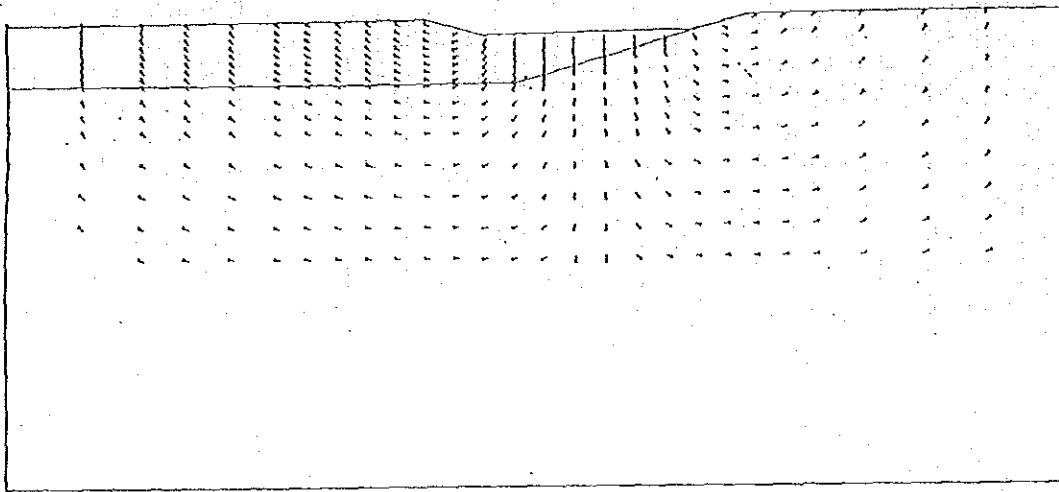


Fig.4.3.15 Overall Displacement in Non-treatment Slope for Short Term Slope Stability

Model Scale (ft)  
0.0 0.16

Displacement Scale (cm)  
0.0 160.00

STEP=2.0  
TIME=7.0



STEP=3.0  
TIME=16.0

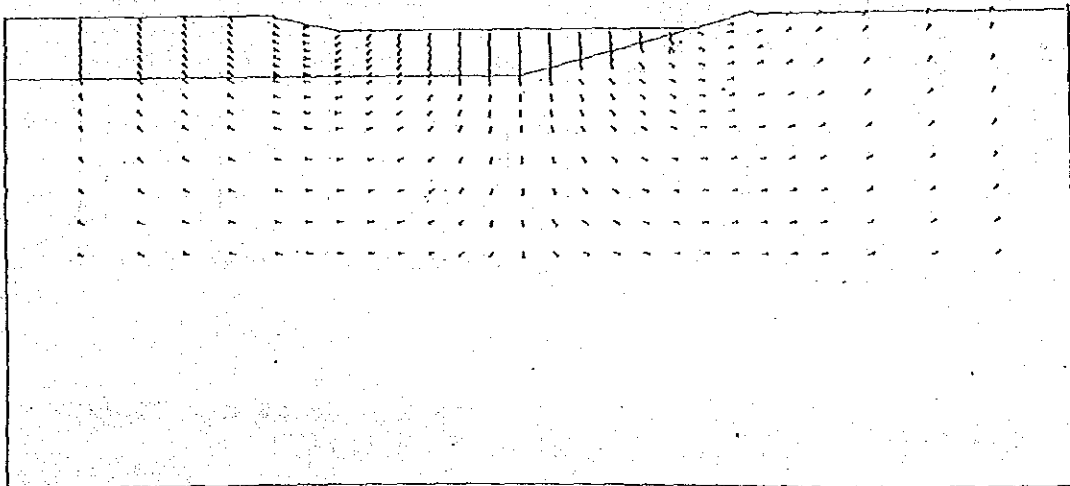
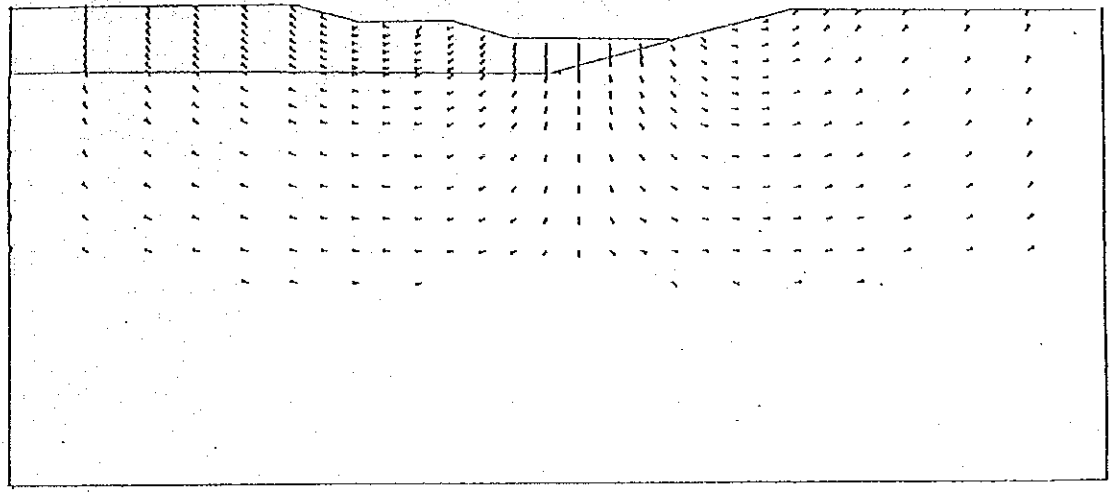


Fig.4.3.16 Deformation Vector in Non-treatment Slope for Short Term Slope Stability

Model Scale (m)  
0.0 0.16

Displacement Scale (cm)  
0.0 160.00

STEP=4.0  
TIME=22.0



STEP=5.0  
TIME=33.0

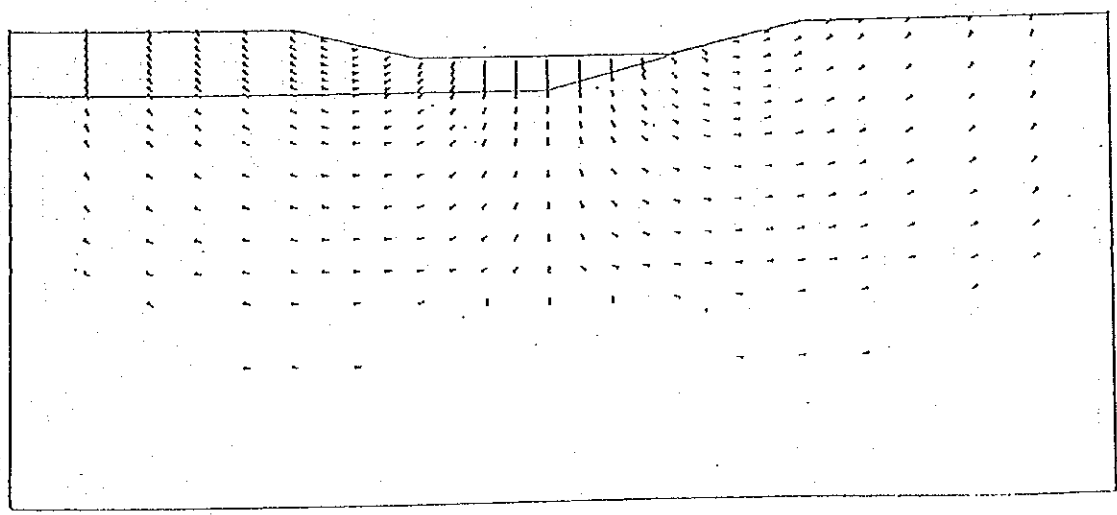
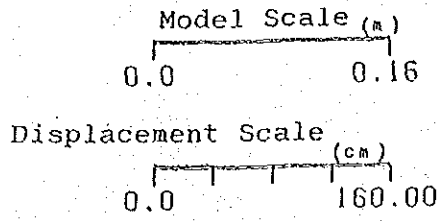
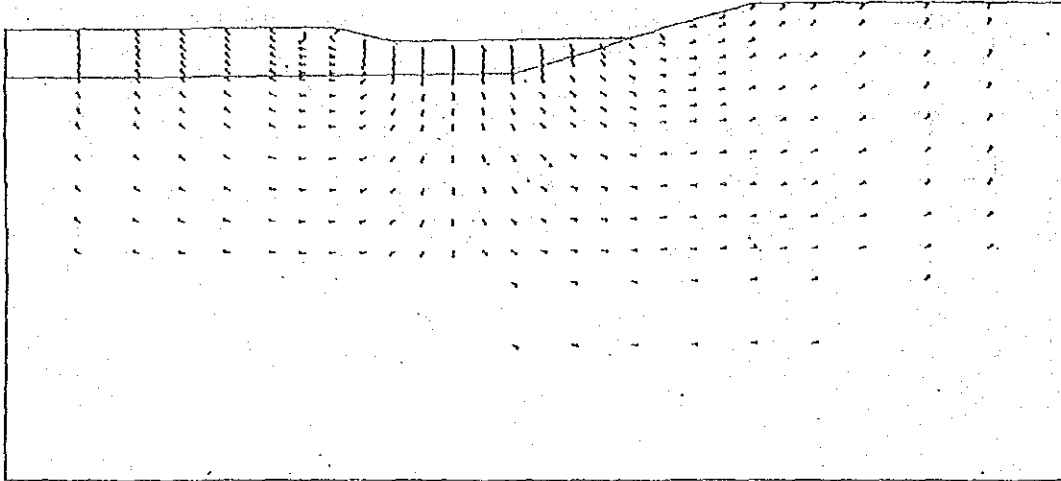


Fig.4.3.17 Deformation Vector in Non-treatment Slope for Short Term Slope Stability



STEP=6.0  
TIME=39.0



STEP=7.0  
TIME=54.0

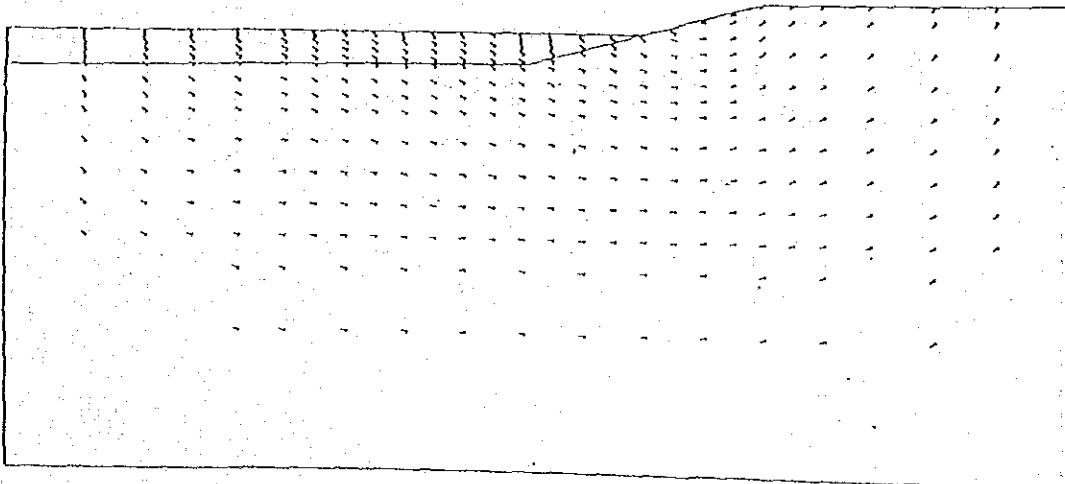
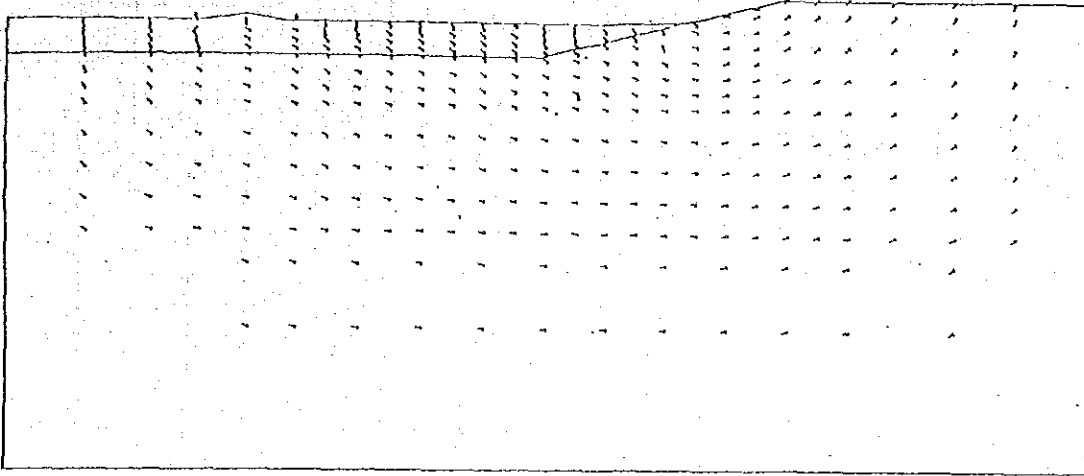


Fig.4.3.18 Deformation Vector in Non-treatment Slope  
for Short Term Slope Stability

Model Scale (m)  
0.0 0.16

Displacement Scale (cm)  
0.0 160.00

STEP=8.0  
TIME=60.0



STEP=9.0  
TIME=65.0

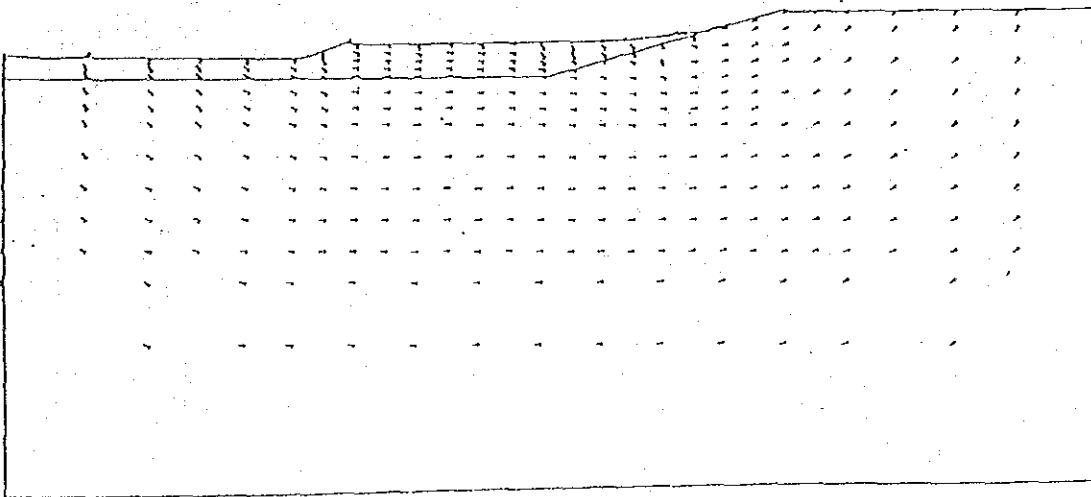
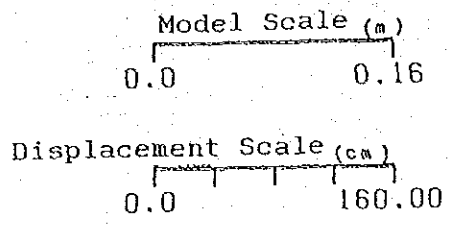


Fig.4.3.19 Deformation Vector in Non-treatment Slope for Short Term Slope Stability



STEP=10.0  
TIME=68.0

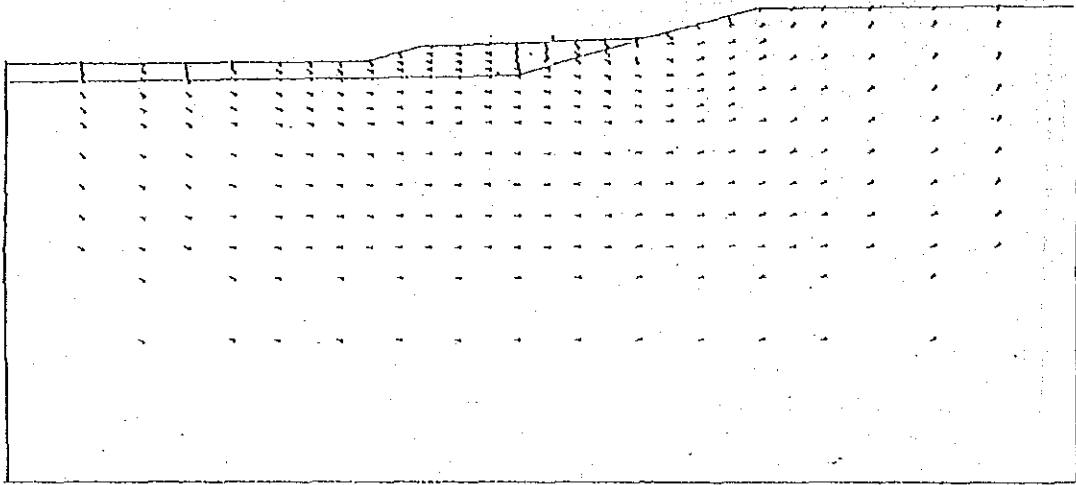


Fig.4.3.20 Deformation Vector in Non-treatment Slope for Short Term Slope Stability

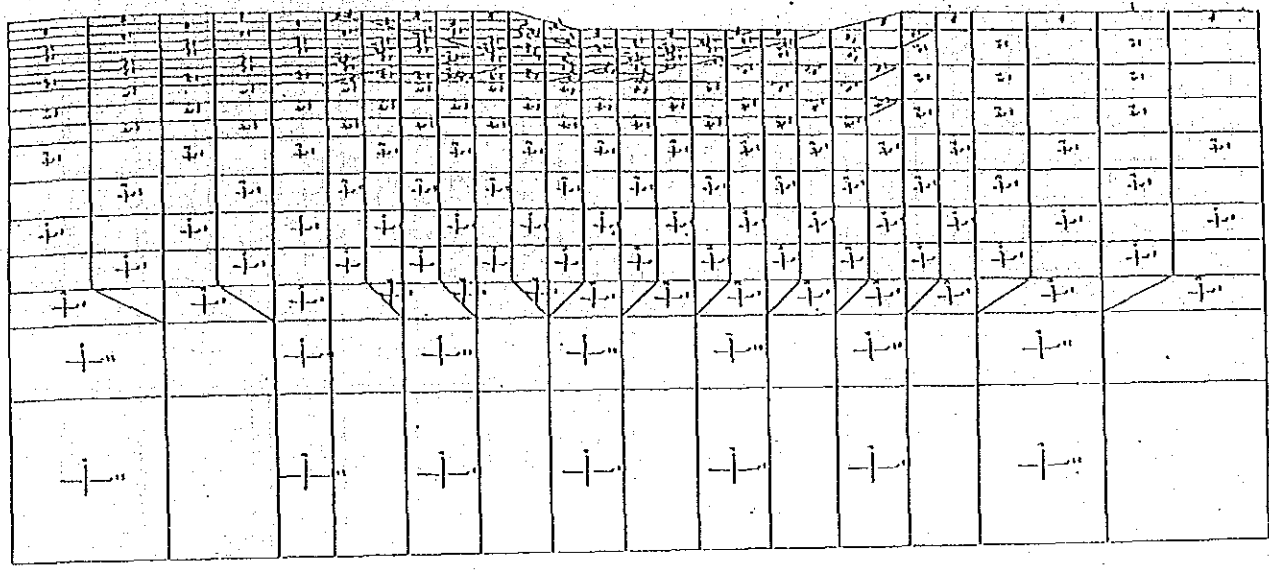
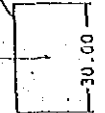


Model Scale  
0.0 8.00H

Unit  
( 1/HZ )

Compression Stress  
Tensile Stress

STEP=2.0  
TIME=7.0



STEP=3.0  
TIME=16.0

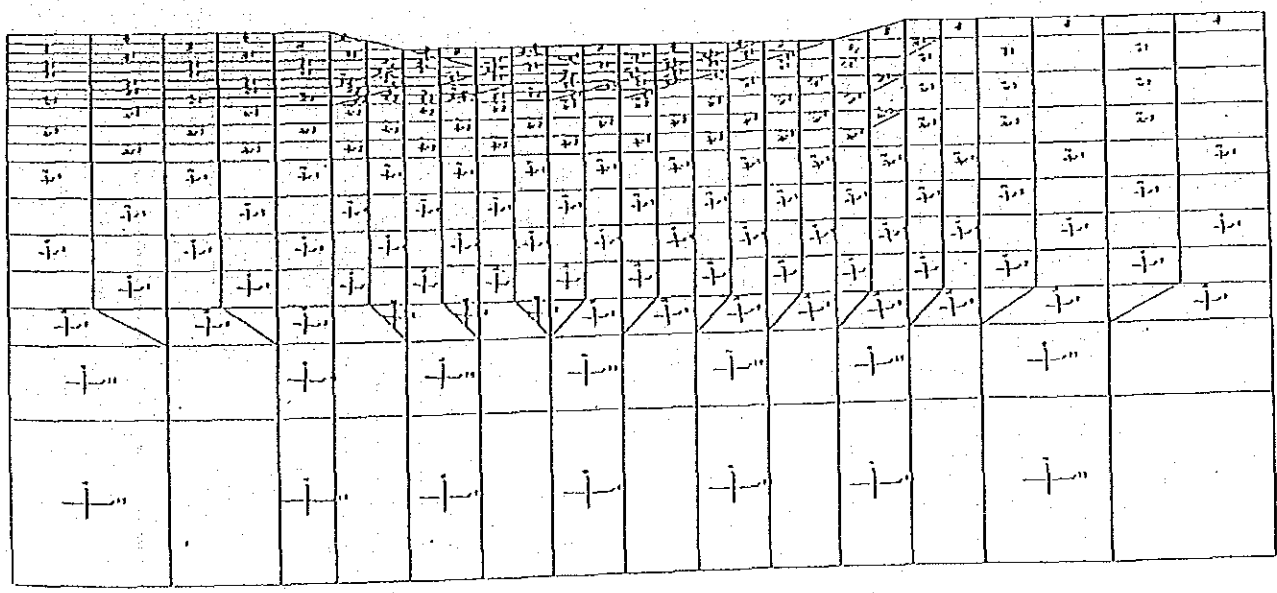
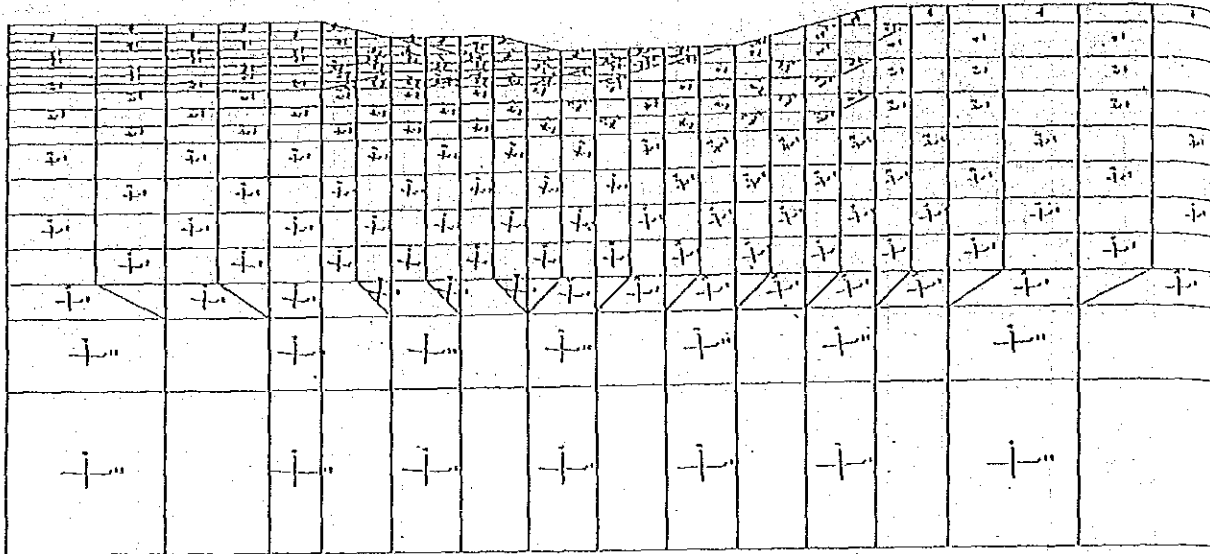


Fig.4.3.21 Stress Occuring in Non-treatment Slope for Short Term Slope Stability

Model Scale  
0.0

Unit  
(1/112)  
Compression Stress  
Tensile Stress

STEP=4.0  
TIME=22.0



STEP=5.0  
TIME=33.0

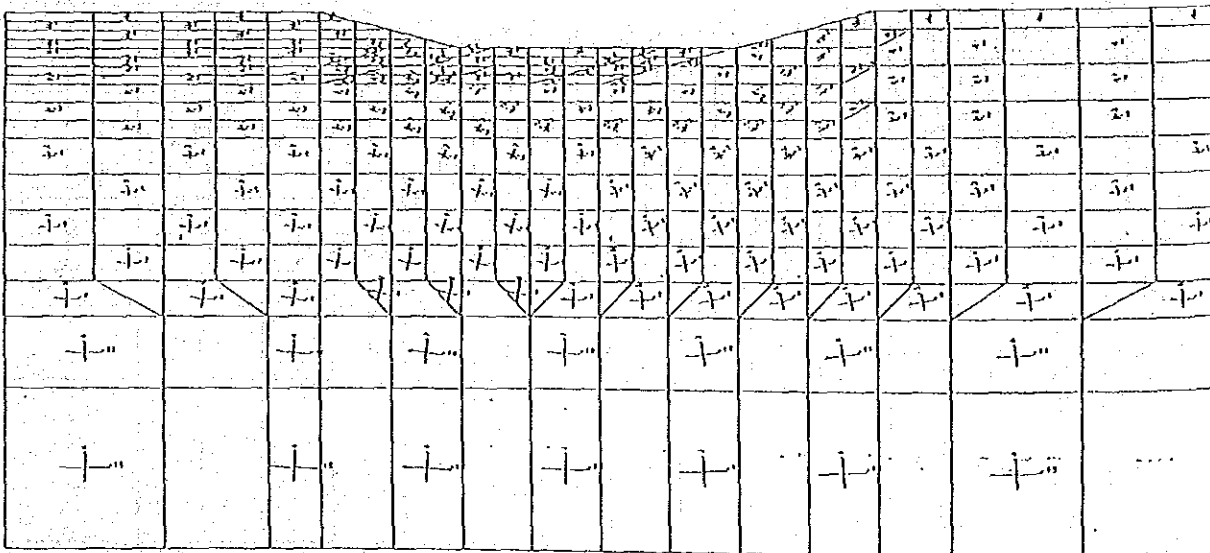


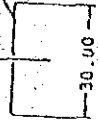
Fig.4.3.22 Stress Occuring in Non-treatment Slope  
for Short Term Slope Stability

Model Scale  
0.0 3.00ft

Unit  
C/IN<sup>2</sup>

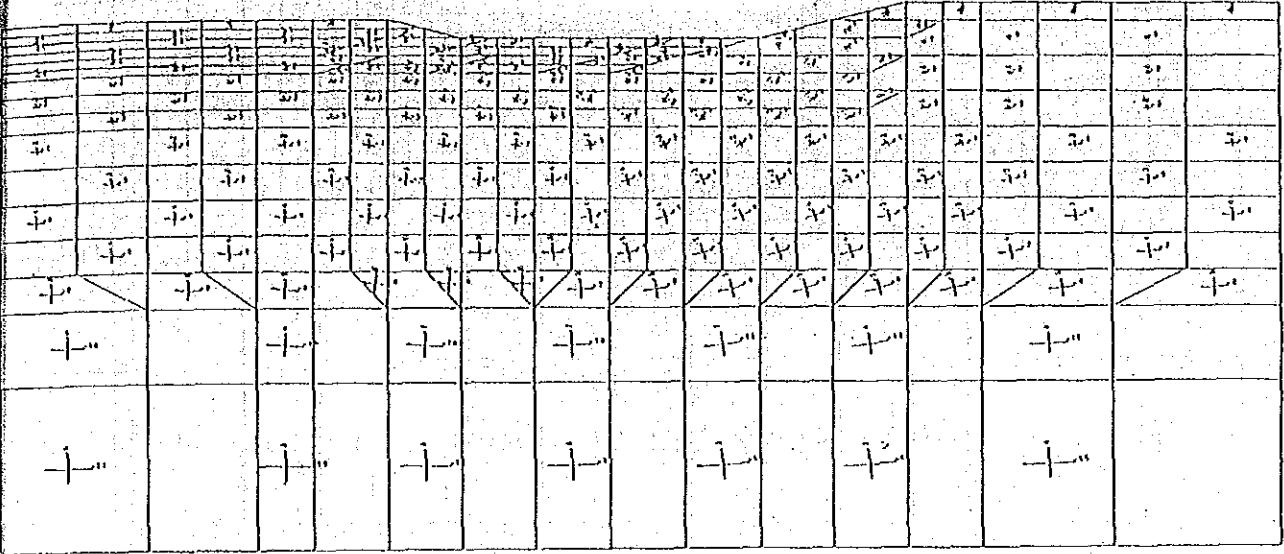
Compression Stress

Tensile Stress



STEP=6.0

TIME=39.0



STEP=7.0

TIME=54.0

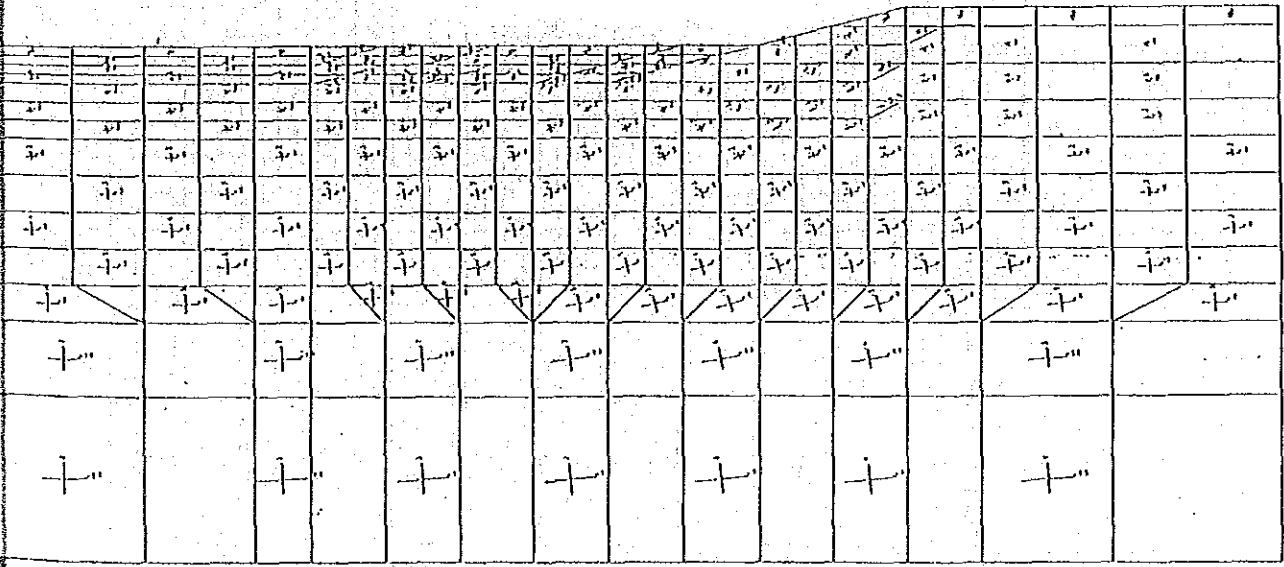
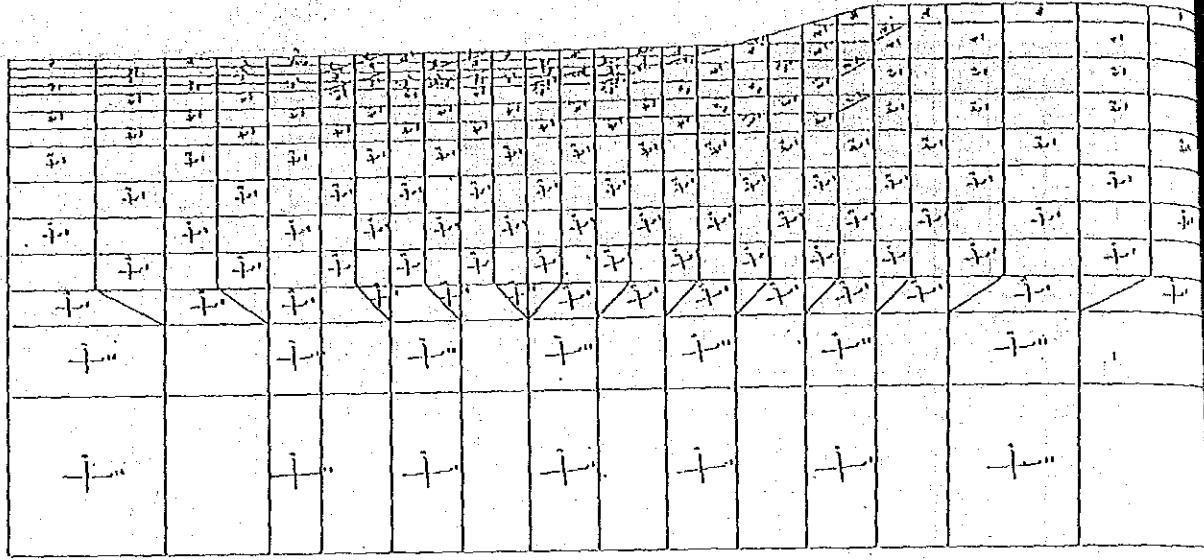


Fig.4.3.23 Stress Occuring in Non-treatment Slope for Short Term Slope Stability

Model Scale  
0.0 3.00

Unit  
(1/42)  
Compression Stress  
Tensile Stress

STEP=8.0  
TIME=60.0



STEP=9.0  
TIME=65.0

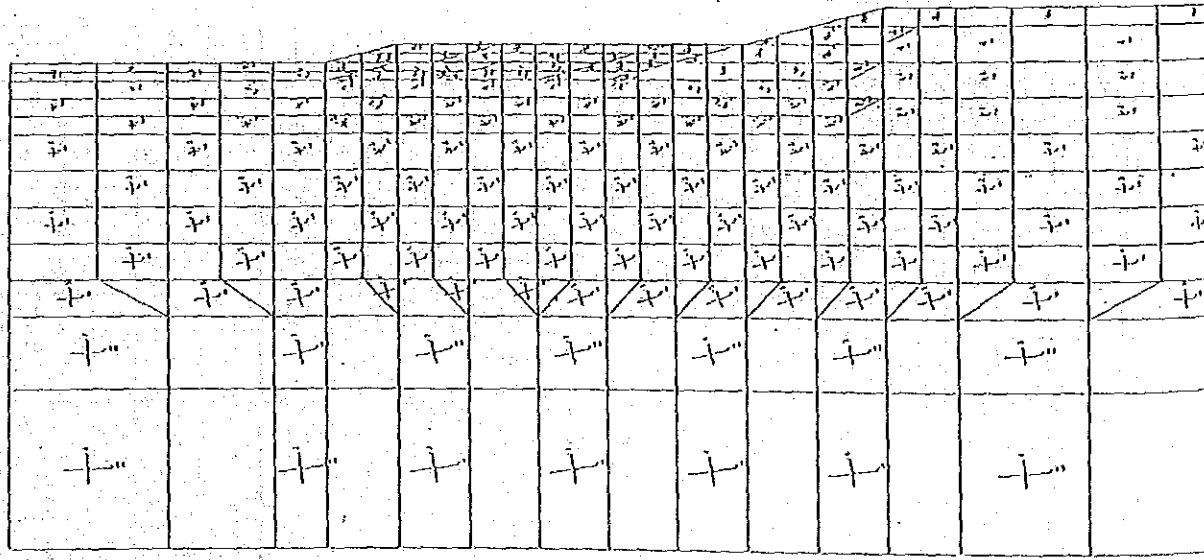
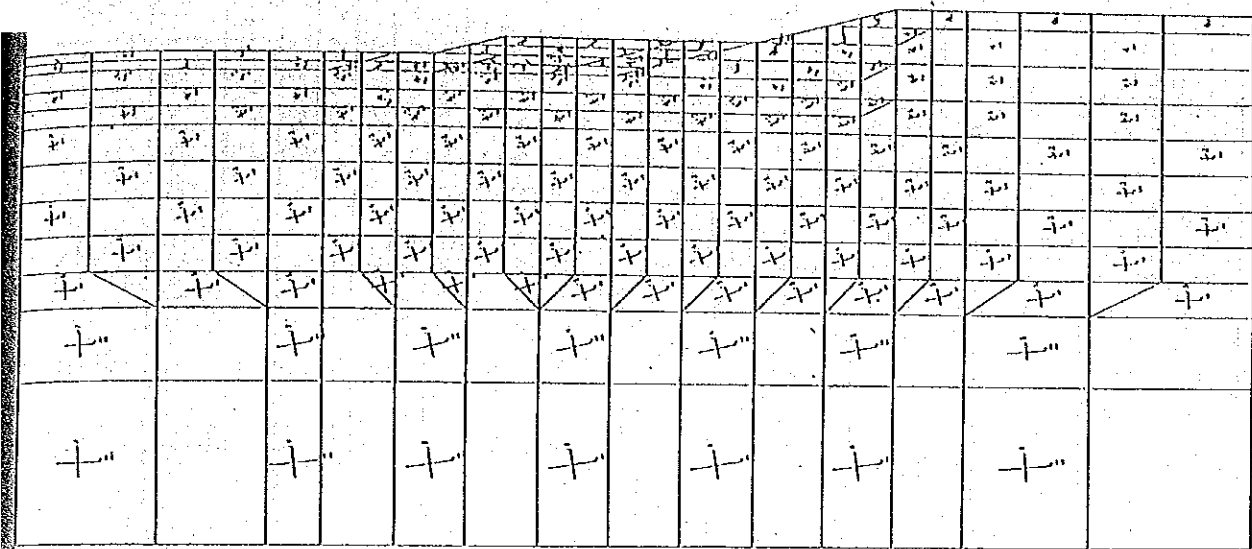


Fig.4.3.24 Stress Occuring in Non-treatment Slope for Short Term Slope Stability

Model Scale  
0.0 5.00H

Unit  
( T/H<sup>2</sup> )  
Compression Stress  
Tensil Stress  
30.00

STEP=10.0  
TIME=68.0



STEP=11.0  
TIME=71.0

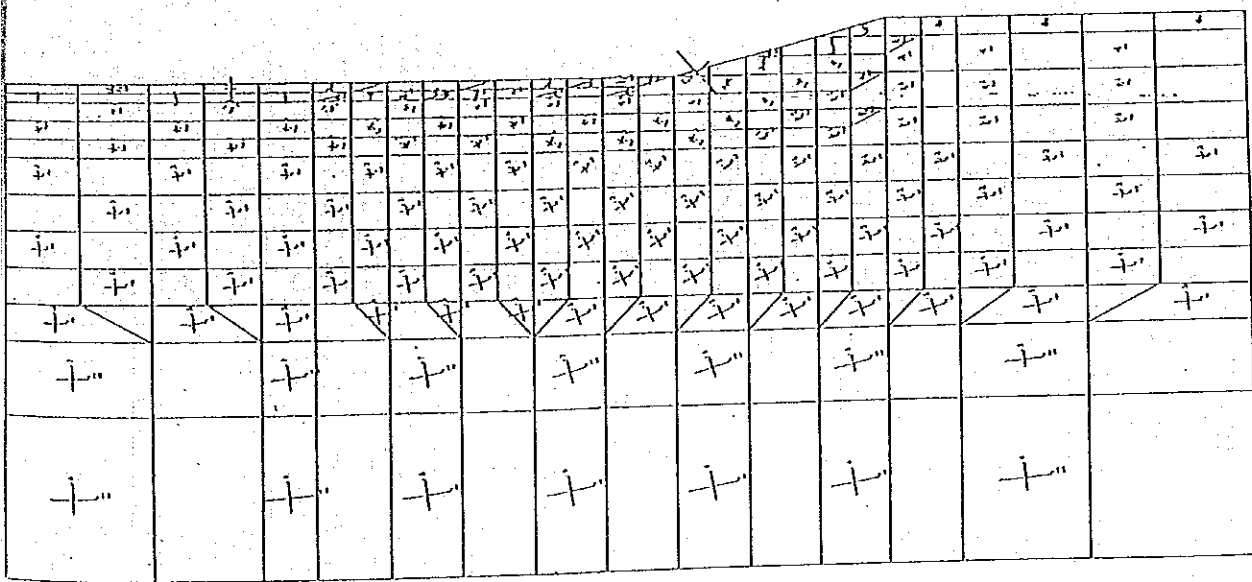


Fig.4.3.25 Stress Occuring in Non-treatment Slope for Short Term Slope Stability

Model Scale  
0.0 3.000

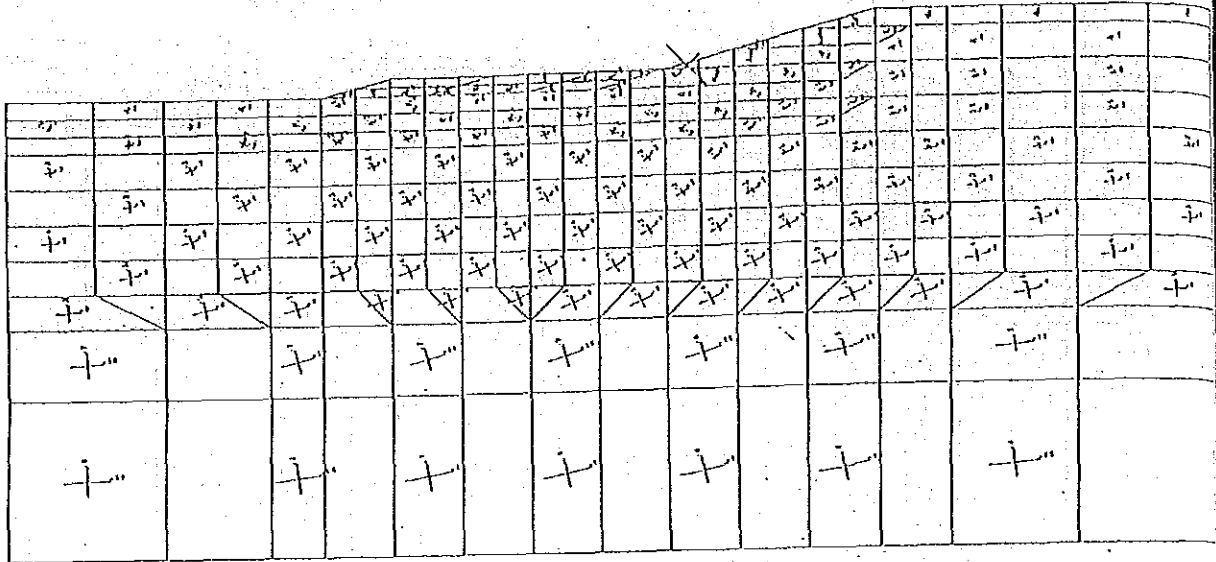
Unit  
( 1/H2 )

Compression Stress

Tensil Stress

STEP=12.0

TIME=74.0



STEP=13.0

TIME=77.0

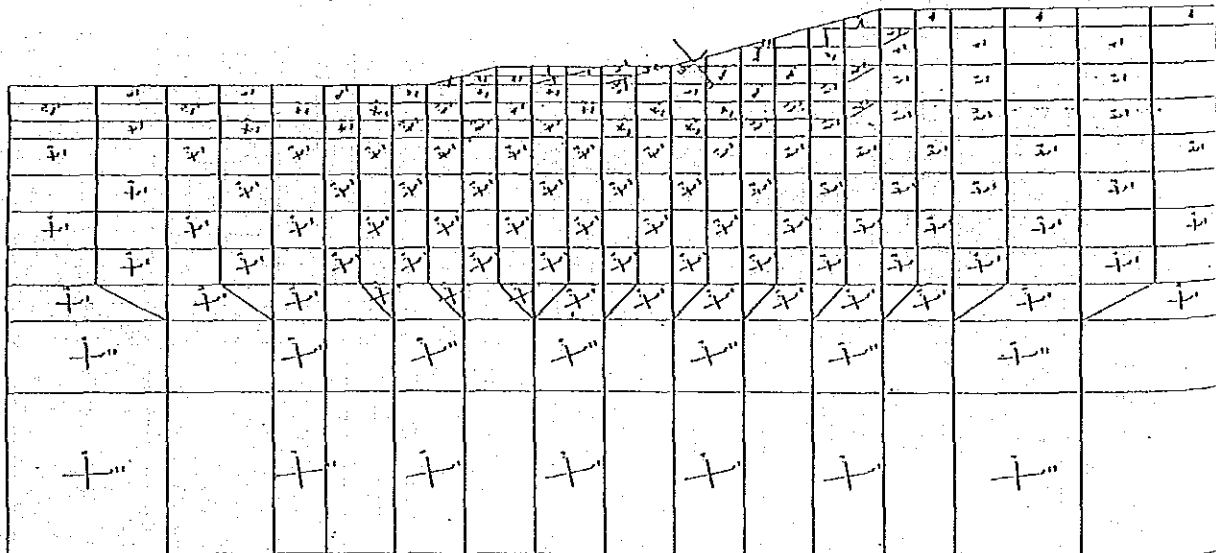
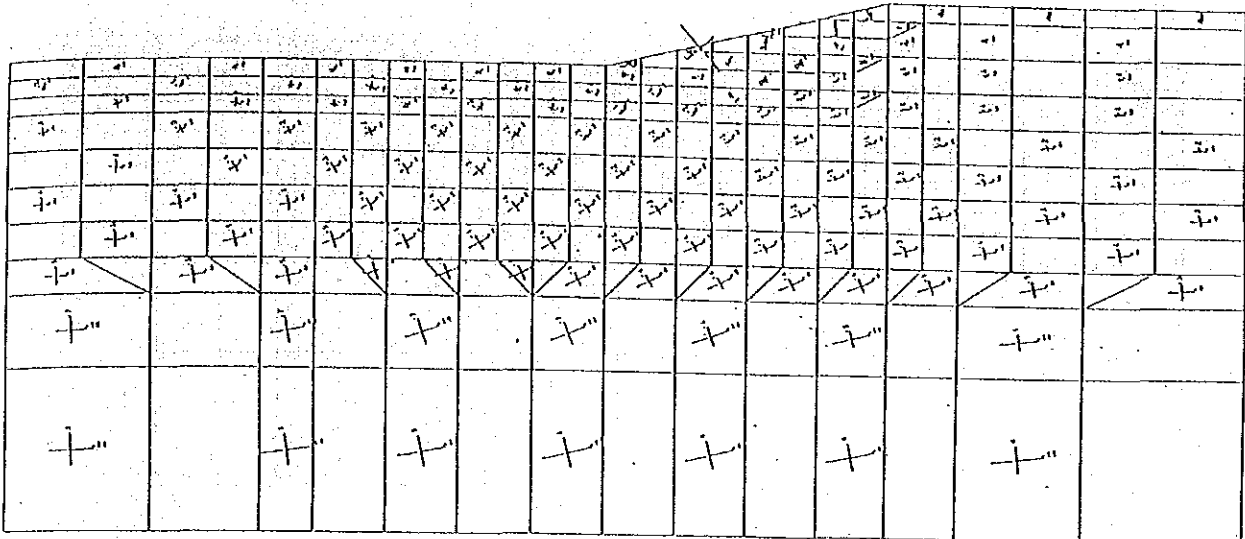


Fig.4.3.26 Stress Occuring in Non-treatment Slope for Short Term Slope Stability

Model Scale  
0.0 3.00H

Unit  
(t/m<sup>2</sup>)  
STEP=14.0  
TIME=80.0  
Compression Stress  
Tensile Stress



STEP=15.0  
TIME=110.0

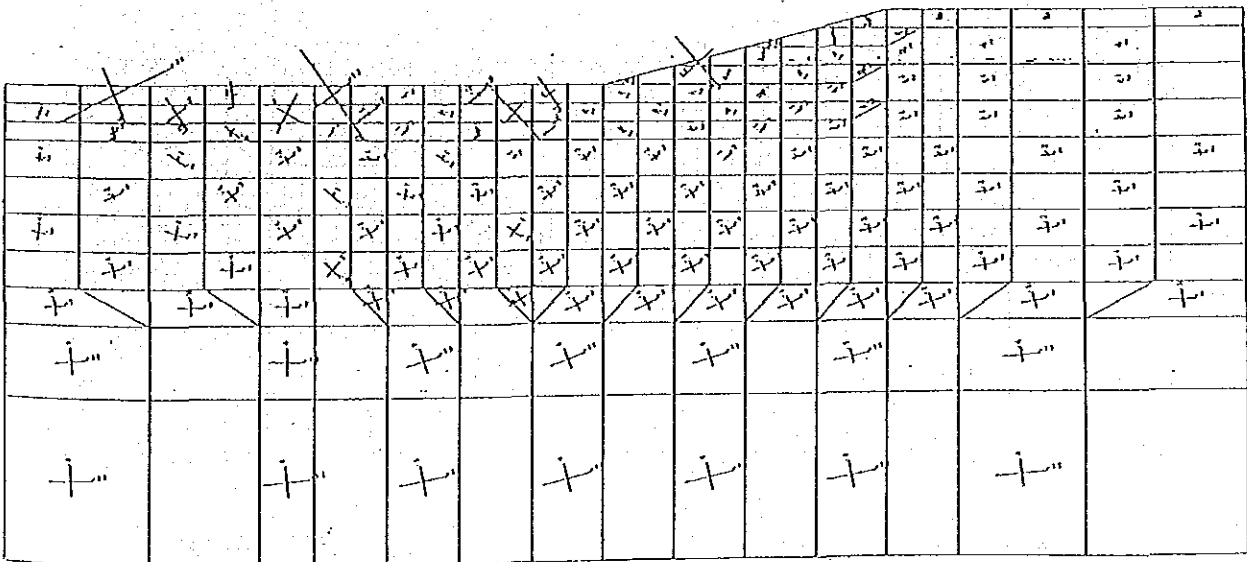


Fig.4.3.27 Stress Occuring in Non-treatment Slope  
for Short Term Slope Stability

DISPLACEMENT

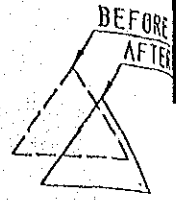
MODEL SCALE (m)

0.0 16.00

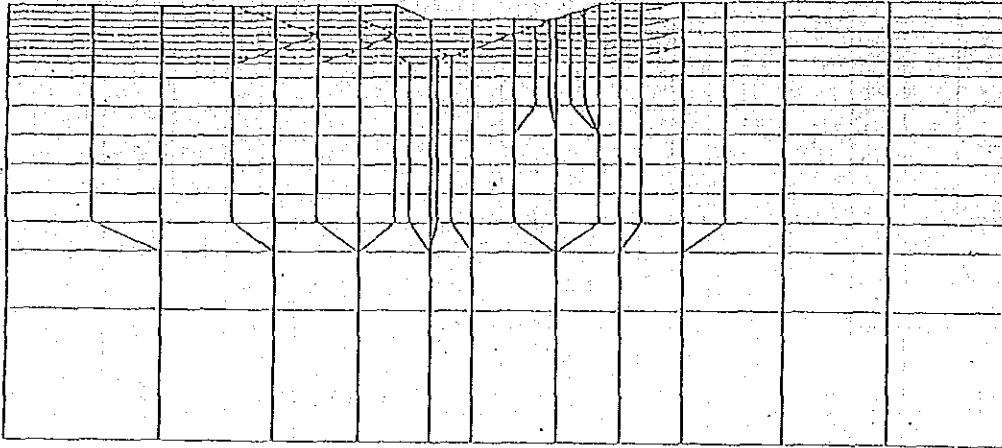
DISPLACEMENT SCALE (m)

0.0 64.00

LEGEND



STEP=2.0  
TIME=7.0



STEP=3.0  
TIME=16.0

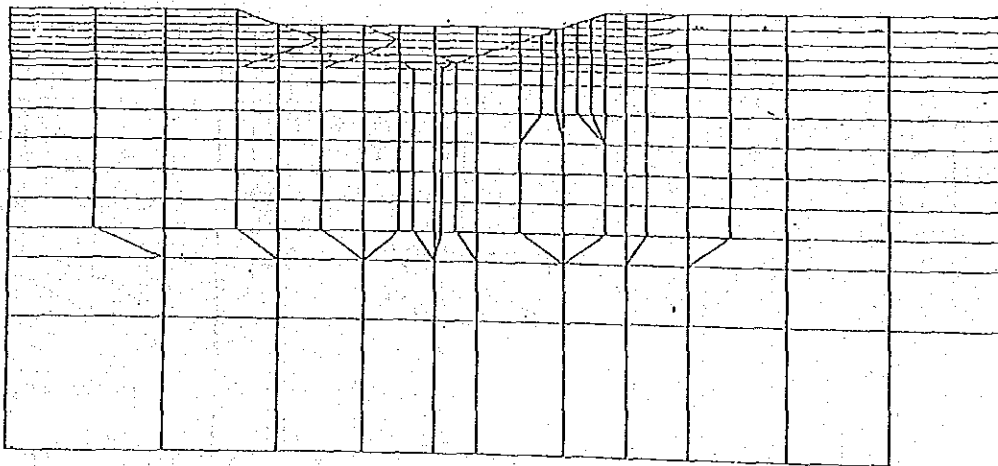


Fig.4.3.28 Overall Displacement in Improved Slope by Soil Cement Columns



DISPLACEMENT

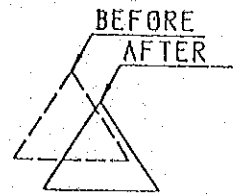
MODEL SCALE (m)

0.0 16.00

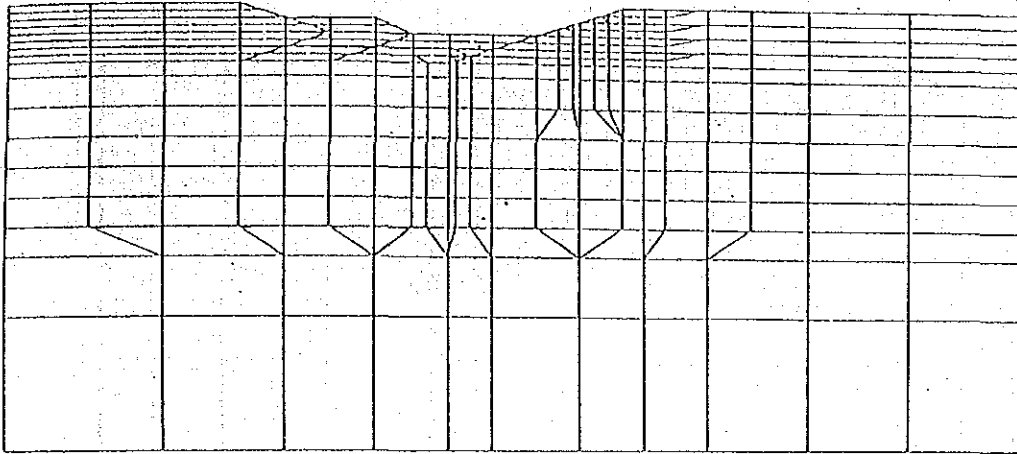
DISPLACEMENT SCALE (m)

0.0 64.00

LEGEND



STEP=4.0  
TIME=22.0



STEP=5.0  
TIME=33.0

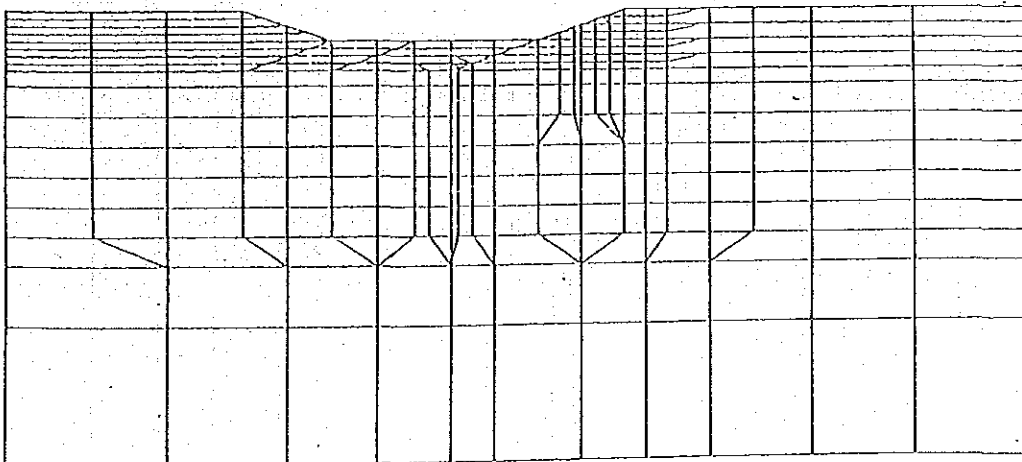
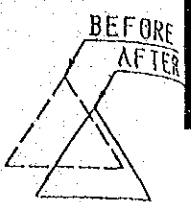


Fig.4.3.29 Overall Displacement in Improved Slope  
by Soil Cement Columns

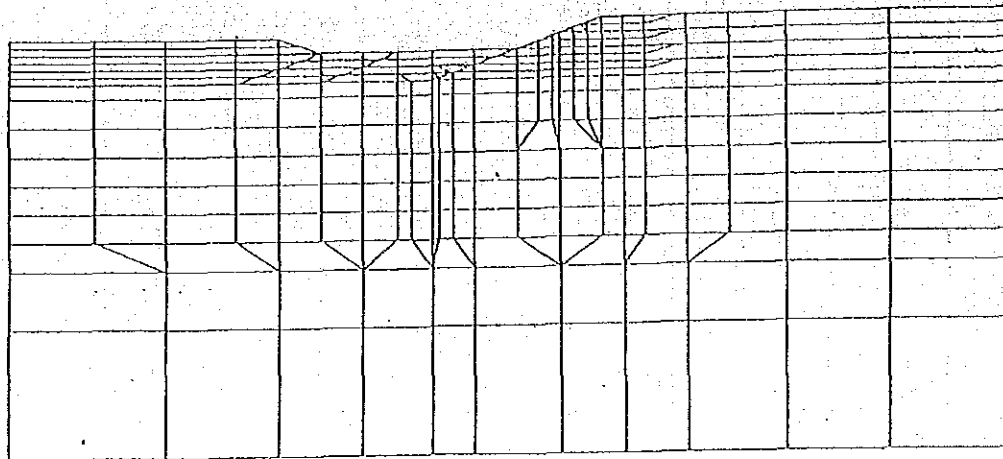
DISPLACEMENT  
 MODEL SCALE (m)  
 0.0 16.00

DISPLACEMENT SCALE (m)  
 0.0 64.00

LEGEND



STEP=6.0  
 TIME=48.0



STEP=7.0  
 TIME=63.0

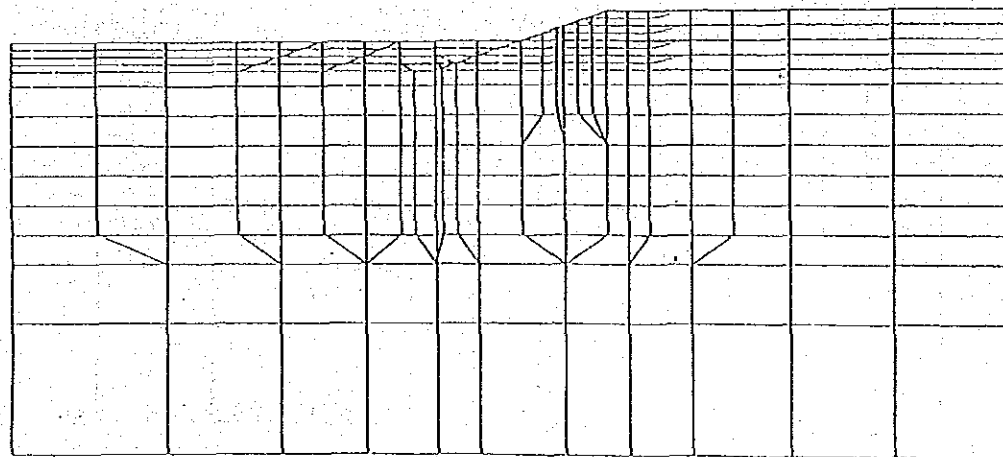


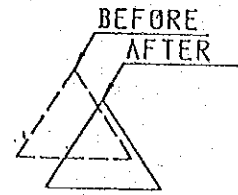
Fig.4.3.30 Overall Displacement in Improved Slope by Soil Cement Columns

DISPLACEMENT

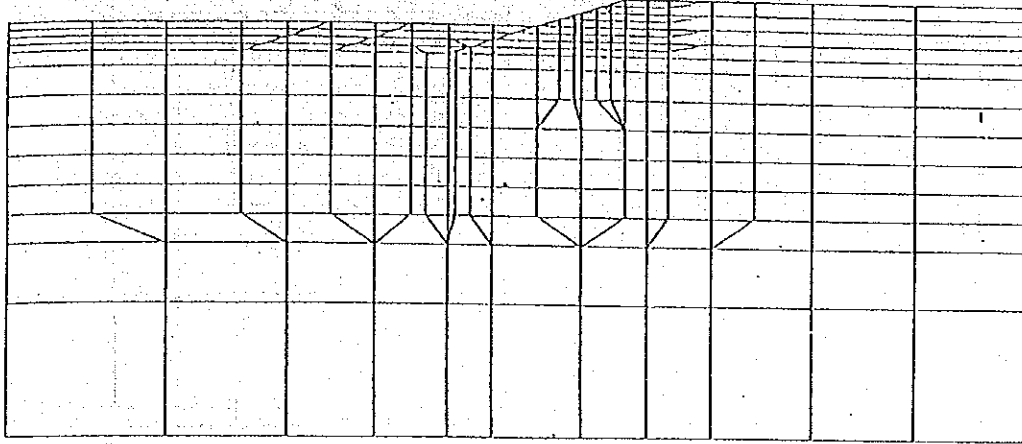
MODEL SCALE (m)  
0.0 16.00

DISPLACEMENT SCALE (m)  
0.0 64.00

LEGEND



STEP=8.0  
TIME=69.0



STEP=9.0  
TIME=74.0

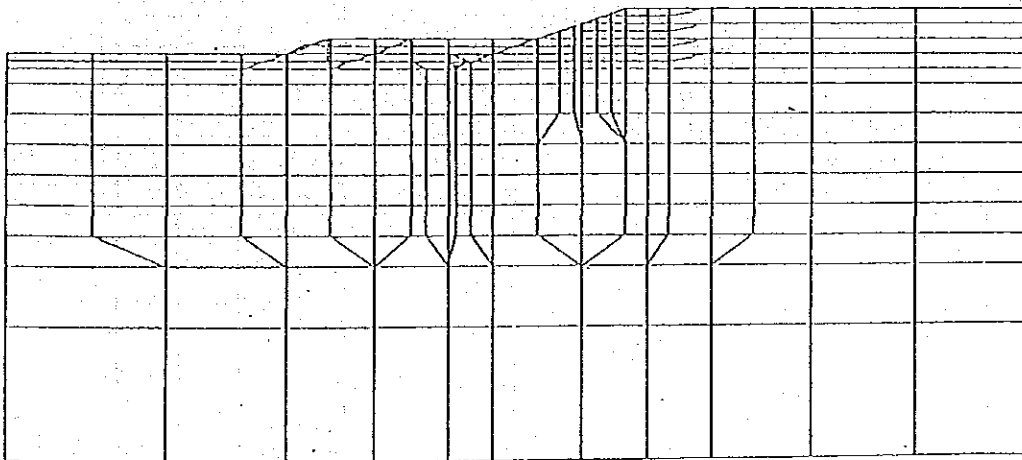


Fig.4.3.31 Overall Displacement in Improved Slope by Soil Cement Columns

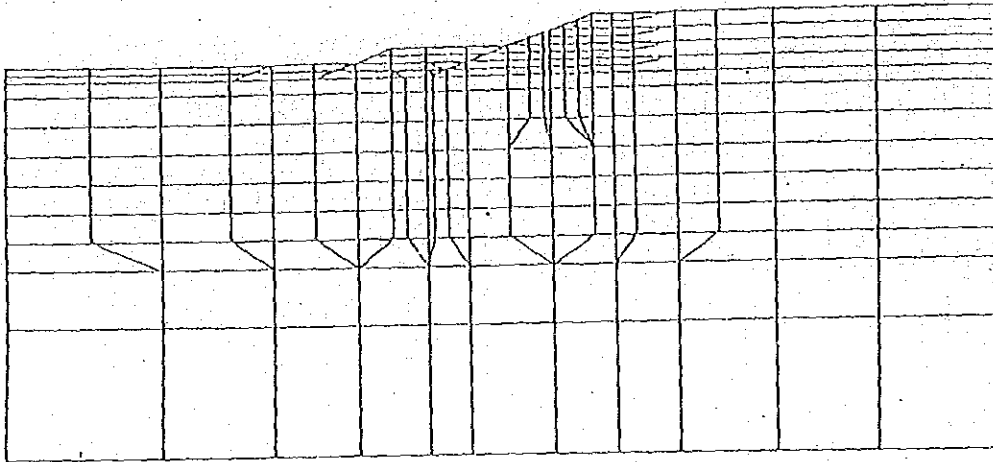
DISPLACEMENT  
MODEL SCALE (m)  
0.0 16.00

DISPLACEMENT SCALE (m)  
0.0 64.00

LEGEND



STEP=10.0  
TIME=77.0



STEP=11.0  
TIME=80.0

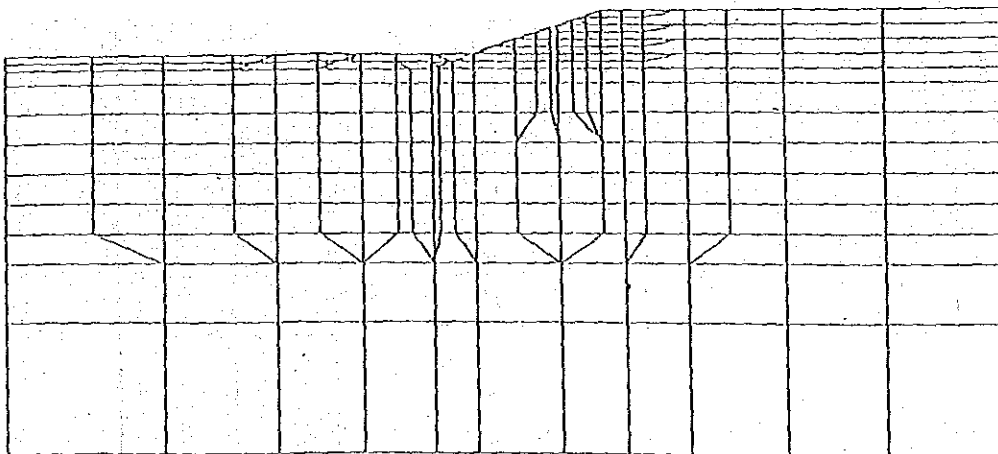


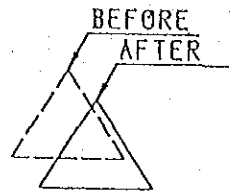
Fig.4.3.32 Overall Displacement in Improved Slope  
by Soil Cement Columns

DISPLACEMENT

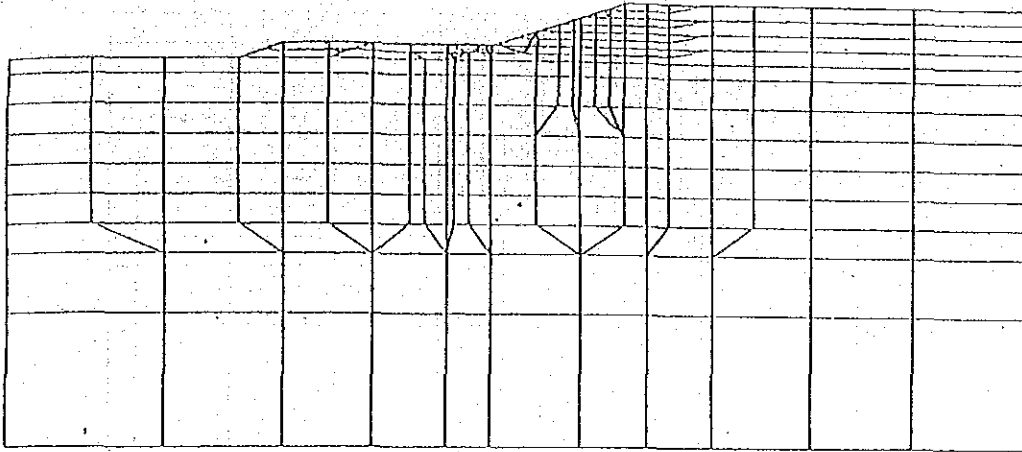
MODEL SCALE (m)  
0.0 16.00

DISPLACEMENT SCALE (m)  
0.0 64.00

LEGEND



STEP=12.0  
TIME=83.0



STEP=13.0  
TIME=86.0

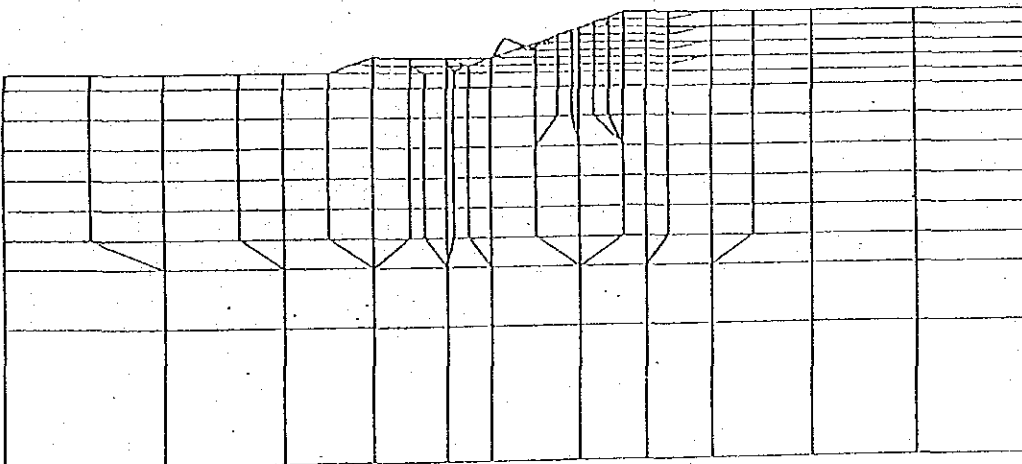


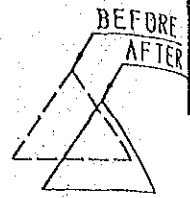
Fig.4.3.33 Overall Displacement in Improved Slope  
by Soil Cement Columns

DISPLACEMENT

MODEL SCALE (m)  
0.0 16.00

DISPLACEMENT SCALE (m)  
0.0 64.00

LEGEND



STEP=14.0  
TIME=89.0

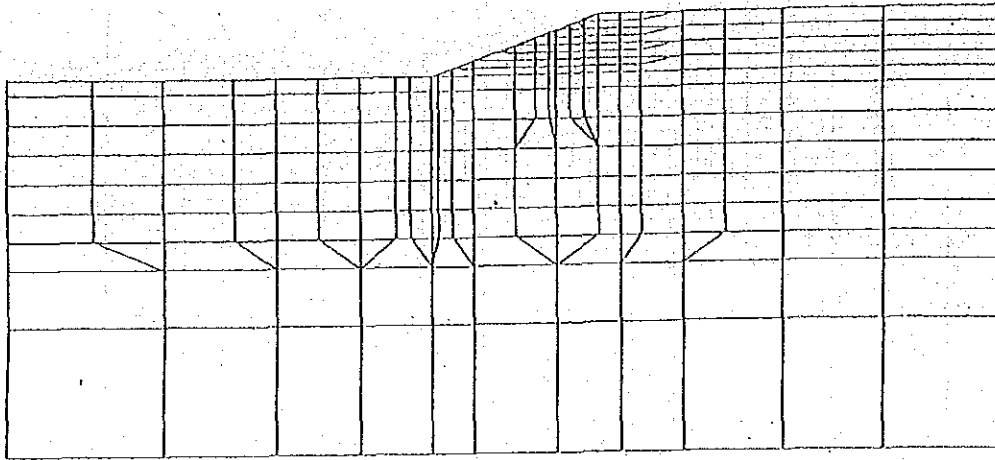
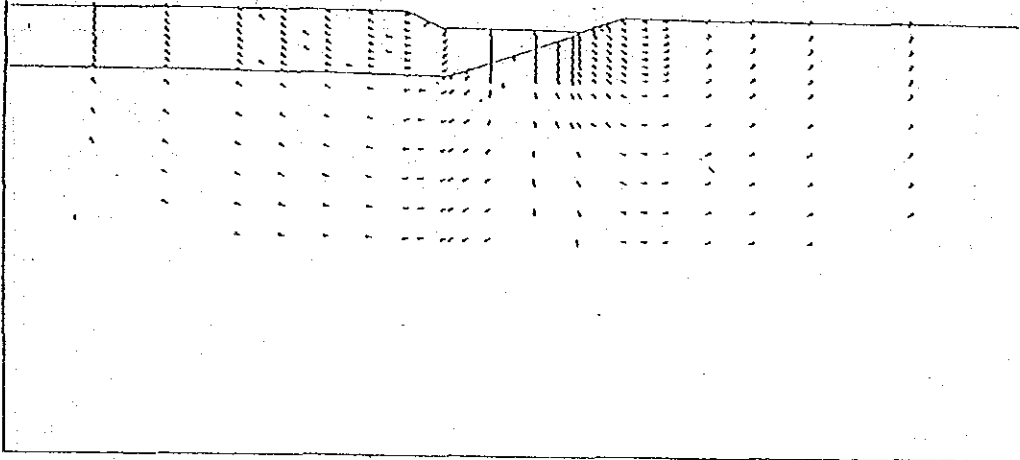


Fig.4.3.34 Overall Displacement in Improved Slope  
by Soil Cement Columns

STEP=2.0  
TIME=7.0



STEP=3.0  
TIME=16.0

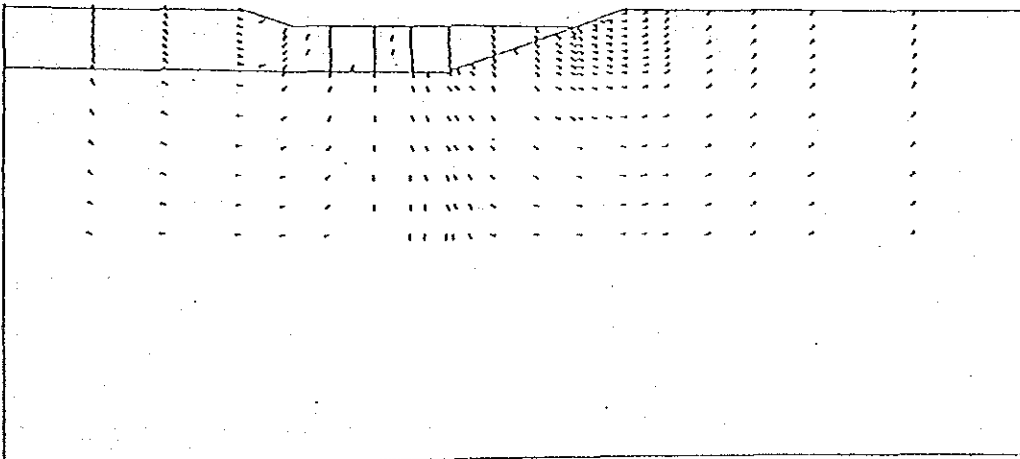
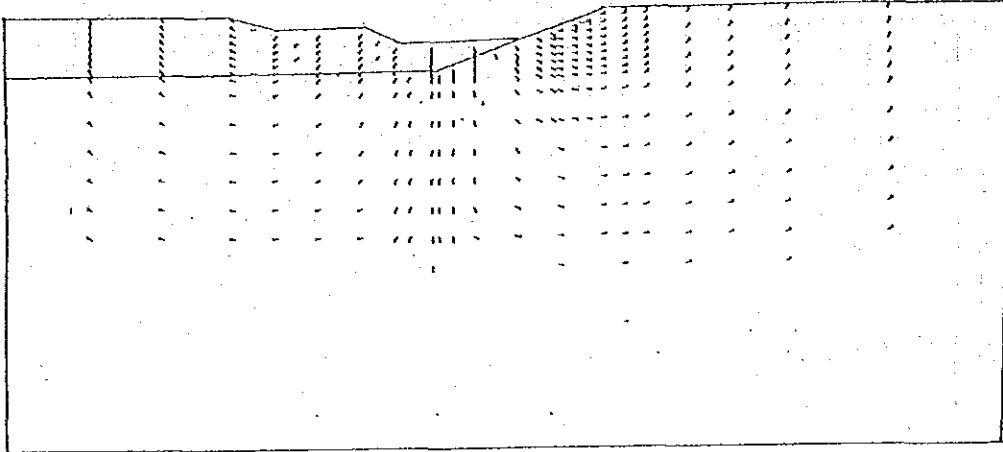


Fig.4.3.35 Deformation Vector in Improved Slope  
by Soil Cement Columns

STEP=4.0  
TIME=22.0



STEP=5.0  
TIME=33.0

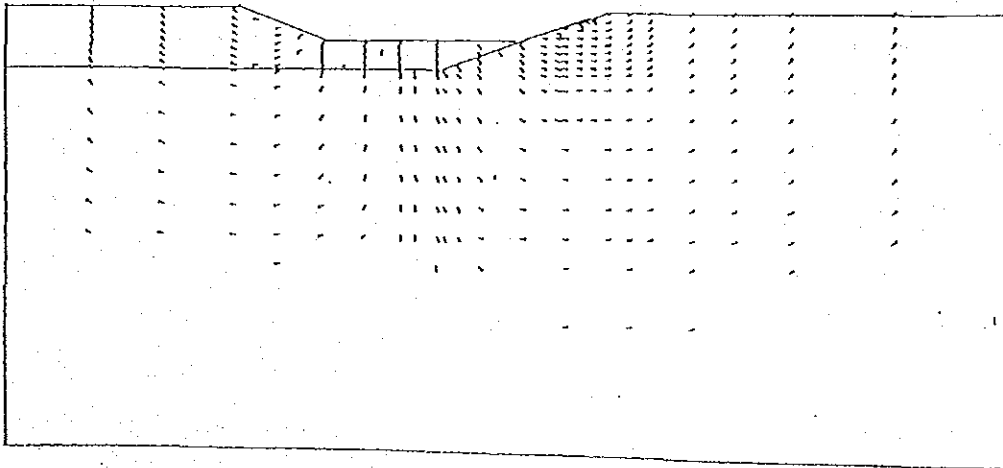
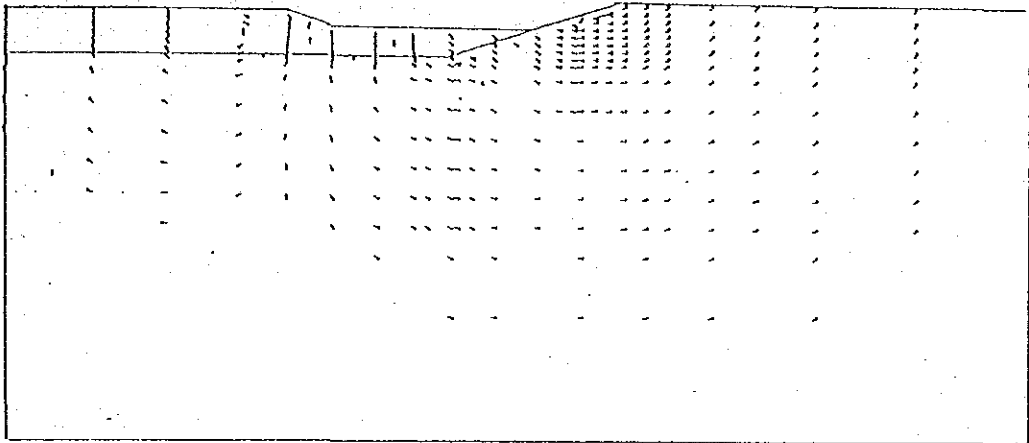


Fig.4.3.36 Deformation Vector in Improved Slope  
by Soil Cement Columns



STEP=6.0  
TIME=48.0



STEP=7.0  
TIME=63.0

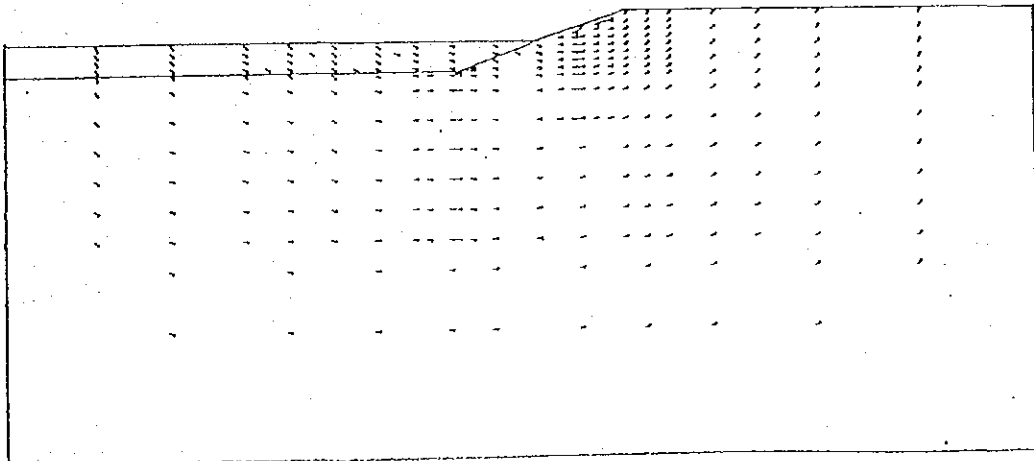
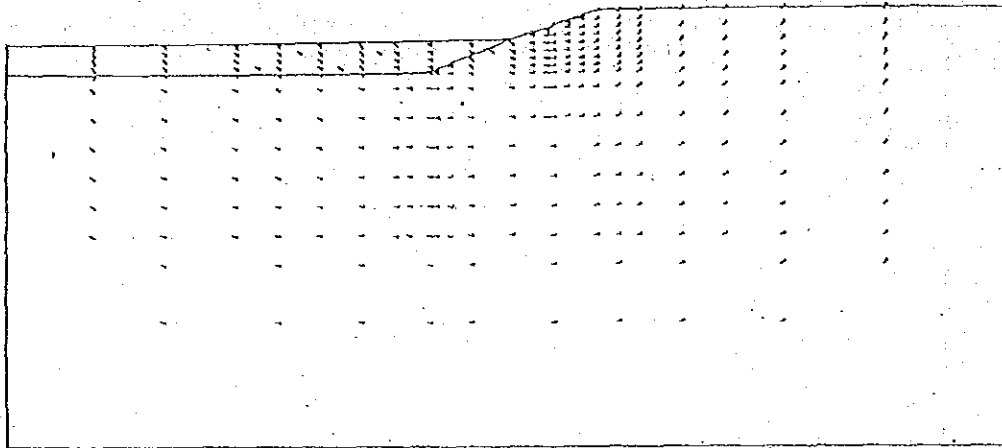


Fig.4.3.37 Deformation Vector in Improved Slope  
by Soil Cement Columns

STEP=8.0  
TIME=69.0



STEP=9.0  
TIME=74.0

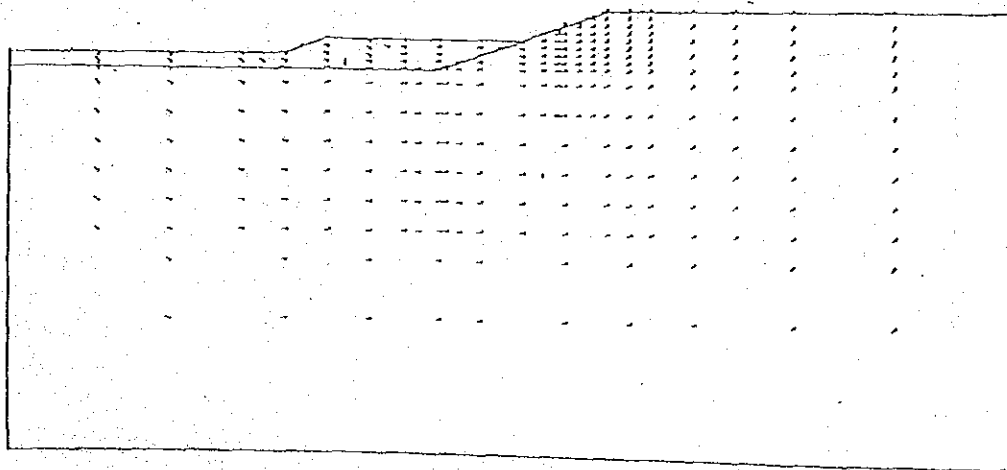
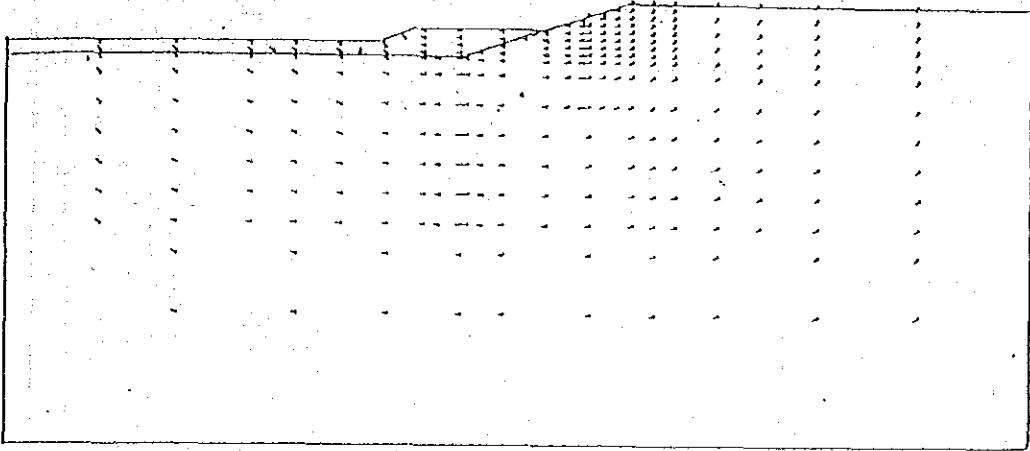


Fig.4.3.38 Deformation Vector in Improved Slope  
by Soil Cement Columns.

STEP=10.0  
TIME=77.0



STEP=11.0  
TIME=80.0

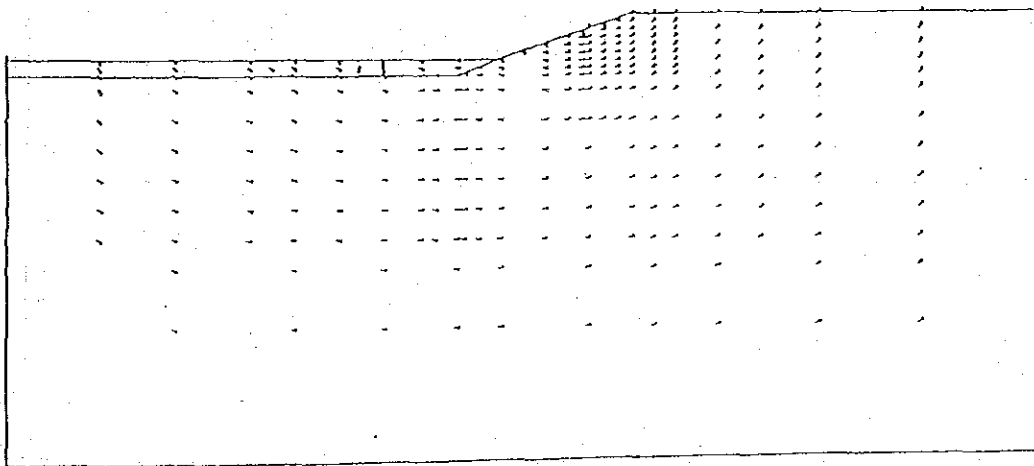
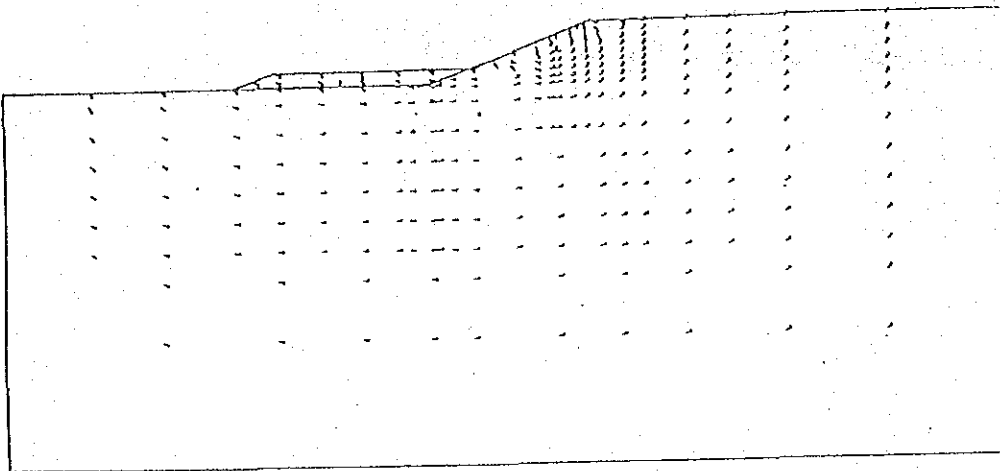


Fig.4.3.39 Deformation Vector in Improved Slope  
by Soil Cement Columns

STEP=12.0  
TIME=83.0



STEP=13.0  
TIME=86.0

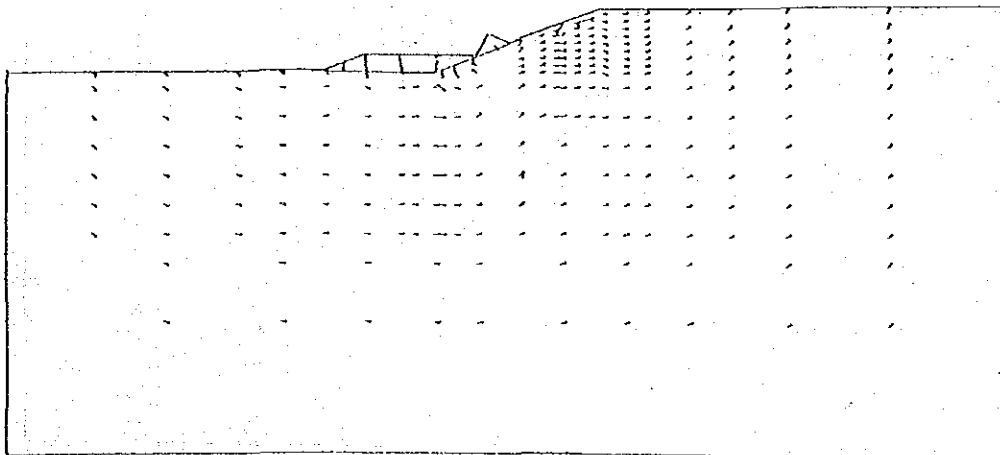


Fig.4.3.40 Deformation Vector in Improved Slope  
by Soil Cement Columns

STEP=14.0  
TIME=89.0

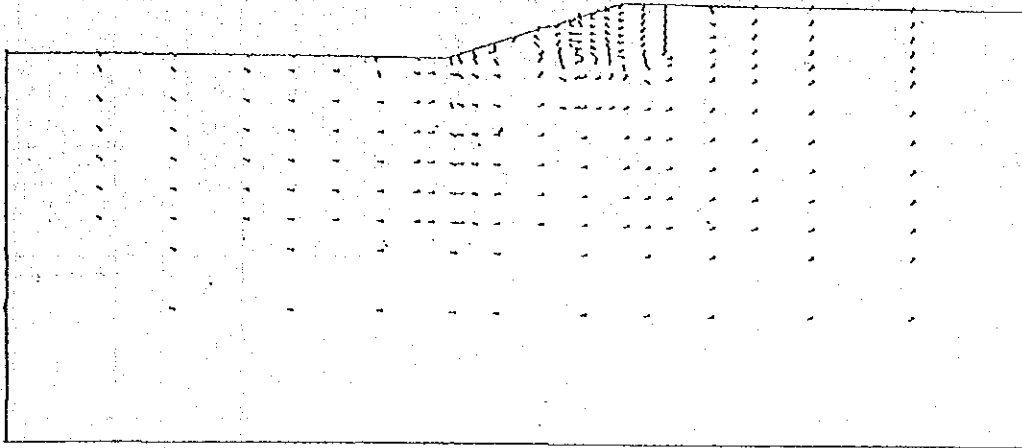
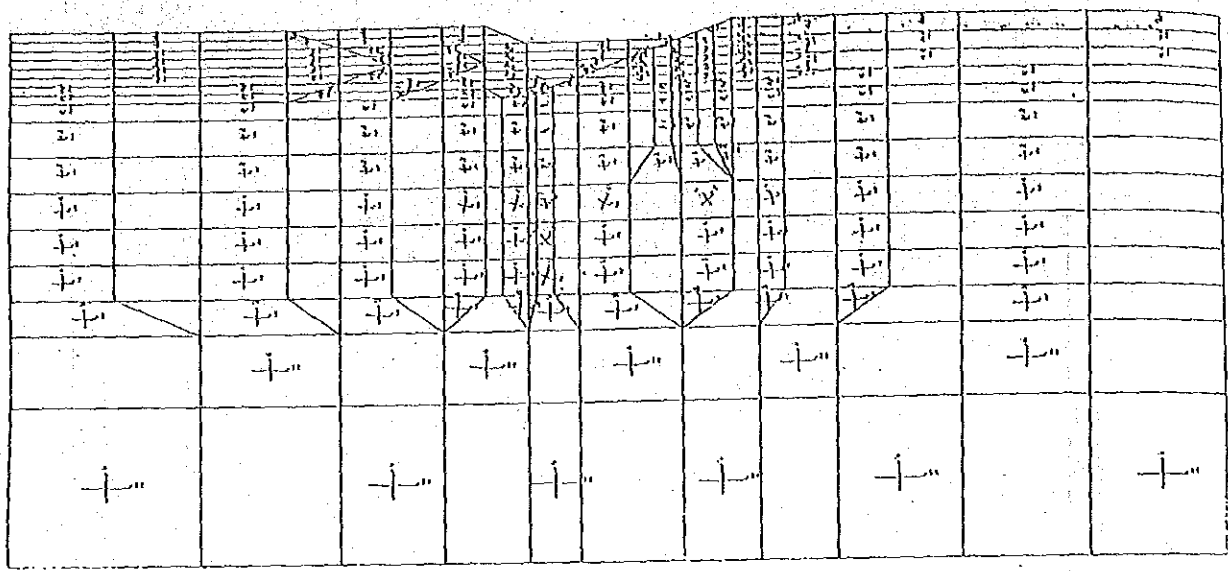
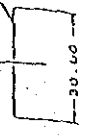


Fig.4.3.41 Deformation Vector in Improved Slope  
by Soil Cement Columns

Model Scale  
0.0 3.00H

Unit  
( T/M<sup>2</sup> )  
Compression Stress  
Tension Stress

STEP=2.0  
TIME=7.0



STEP=3.0  
TIME=16.0

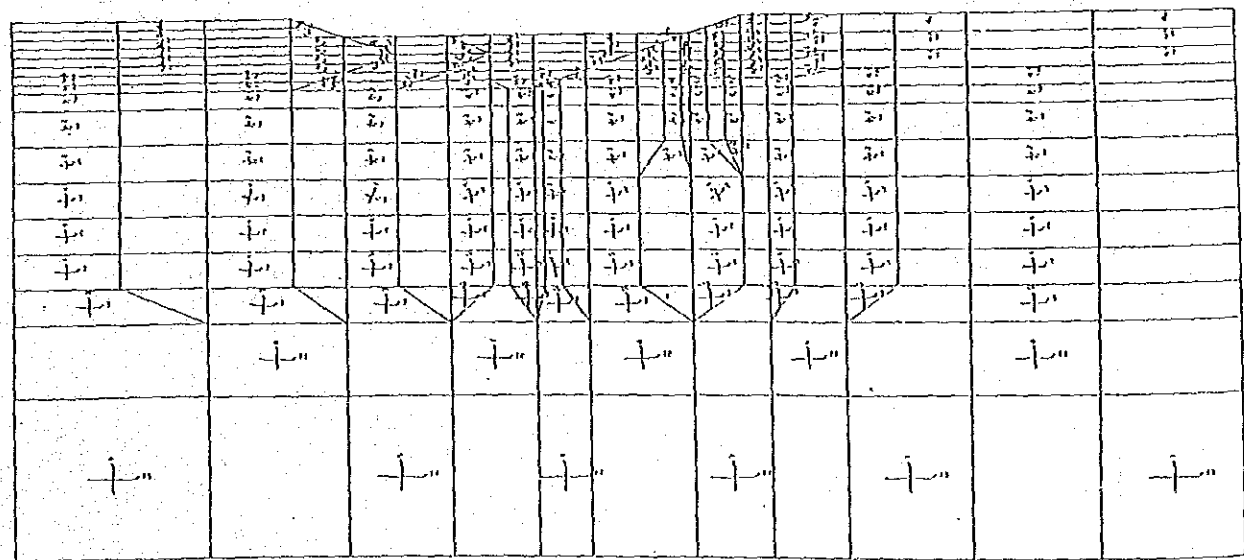


Fig.4.3.42 Stress Occuring in Improved Slope

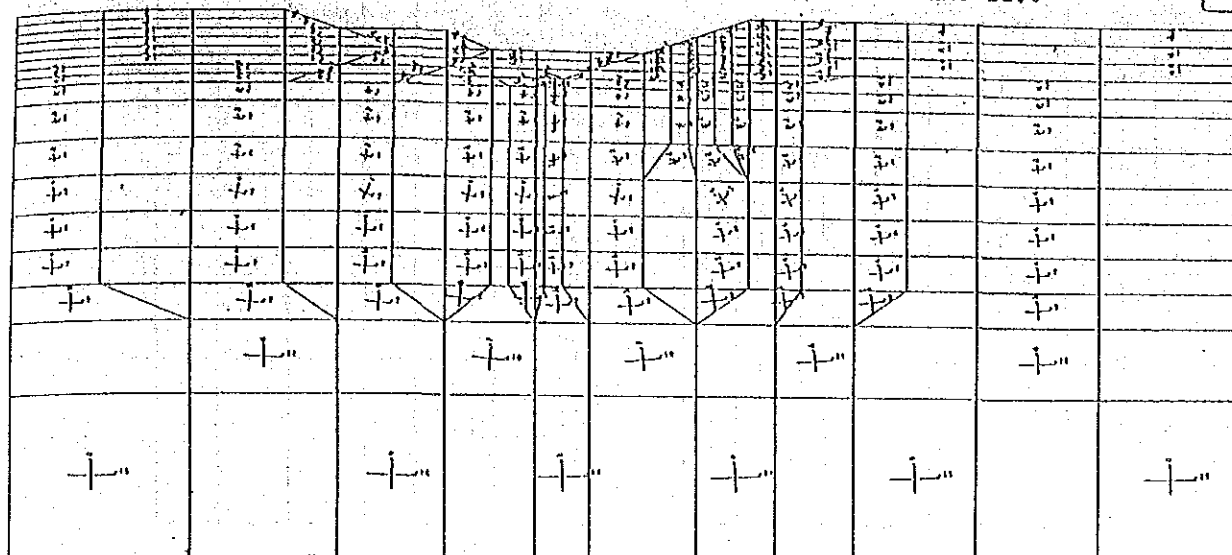
Model Scale  
0.0 8.00H

Unit  
( 1/82 )  
Compression Stress

Tensil Stress  
30.00

STEP=4.0

TIME=22.0



STEP=5.0

TIME=33.0

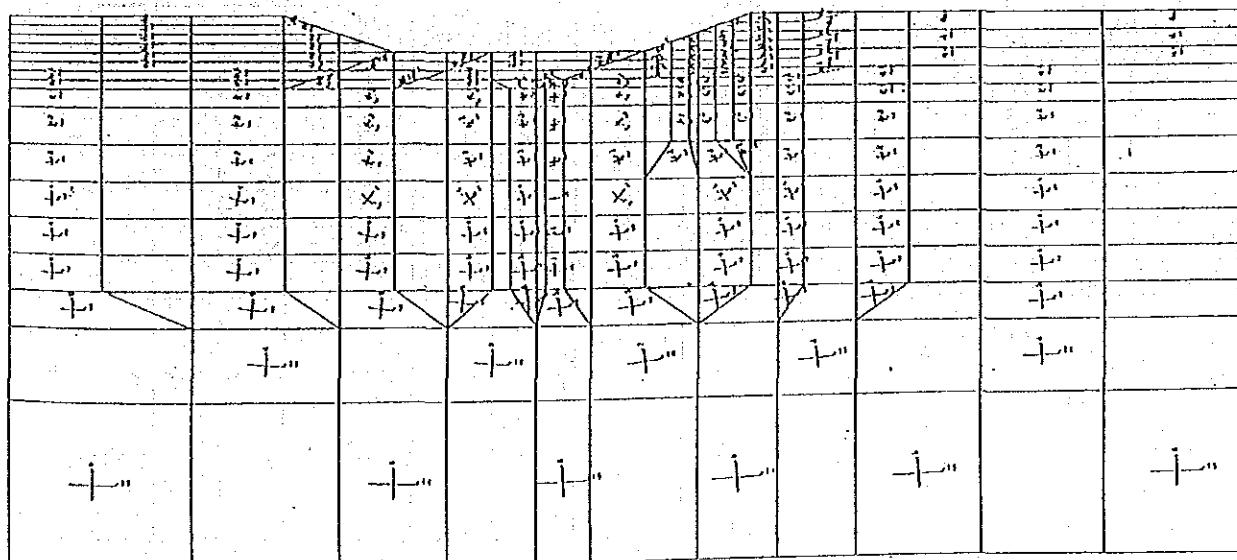
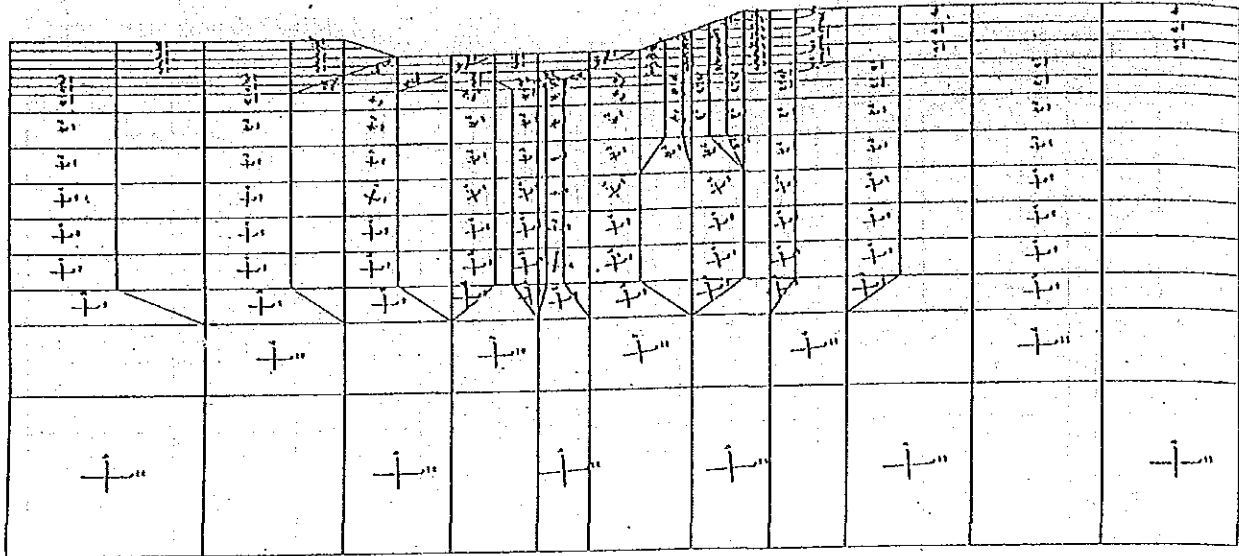
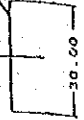


Fig.4.3.43 Stress Occuring in Improved Slope  
by Soil Cement Columns

Model Scale  
0.0 6.00H

Unit  
( T/M<sup>2</sup> )  
Compression Stress  
Tensile Stress

STEP=6.0  
TIME=48.0



STEP=7.0  
TIME=63.0

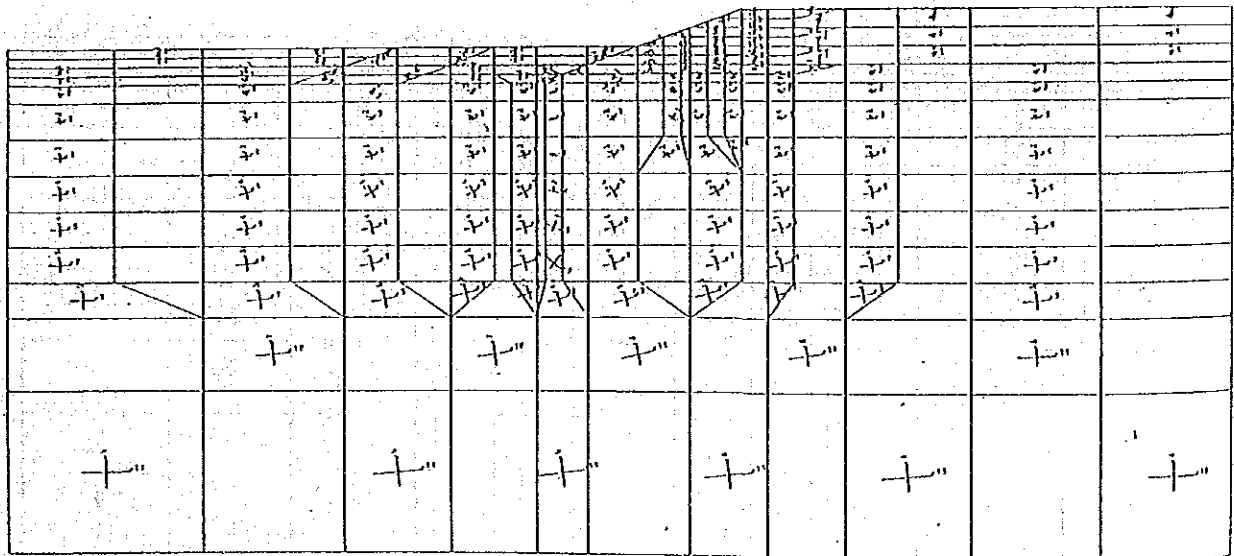


Fig.4.3.44 Stress Occuring in Improved Slope  
by Soil Cement Columns



Model Scale  
0.0 3.00H

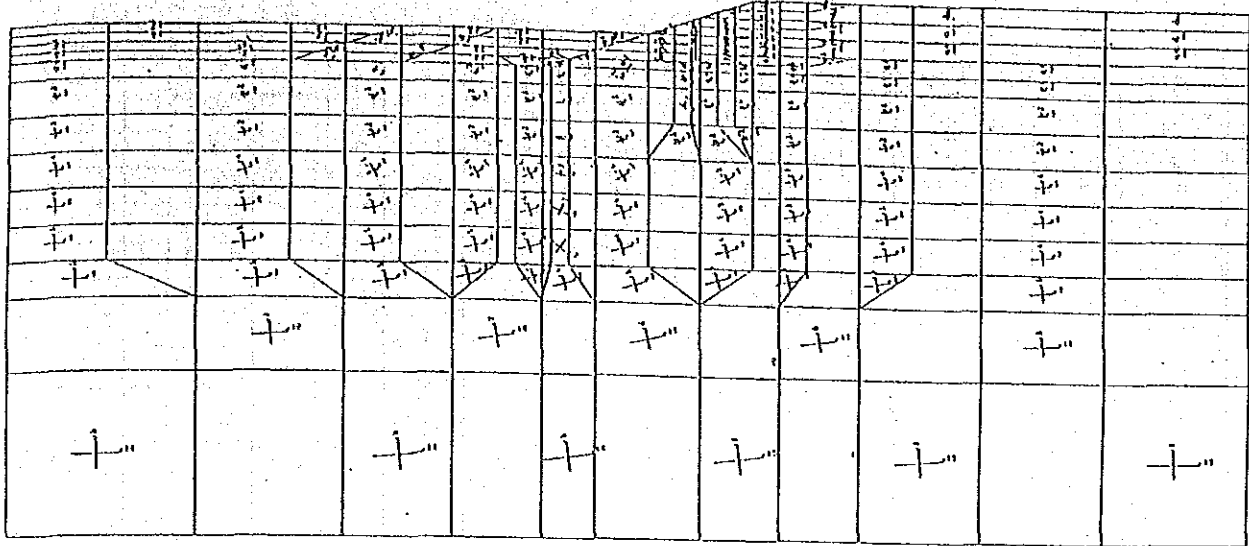
Unit  
( 1/H<sup>2</sup> )

Compression Stress

Tensil Stress

STEP=8.0

TIME=69.0



STEP=9.0

TIME=74.0

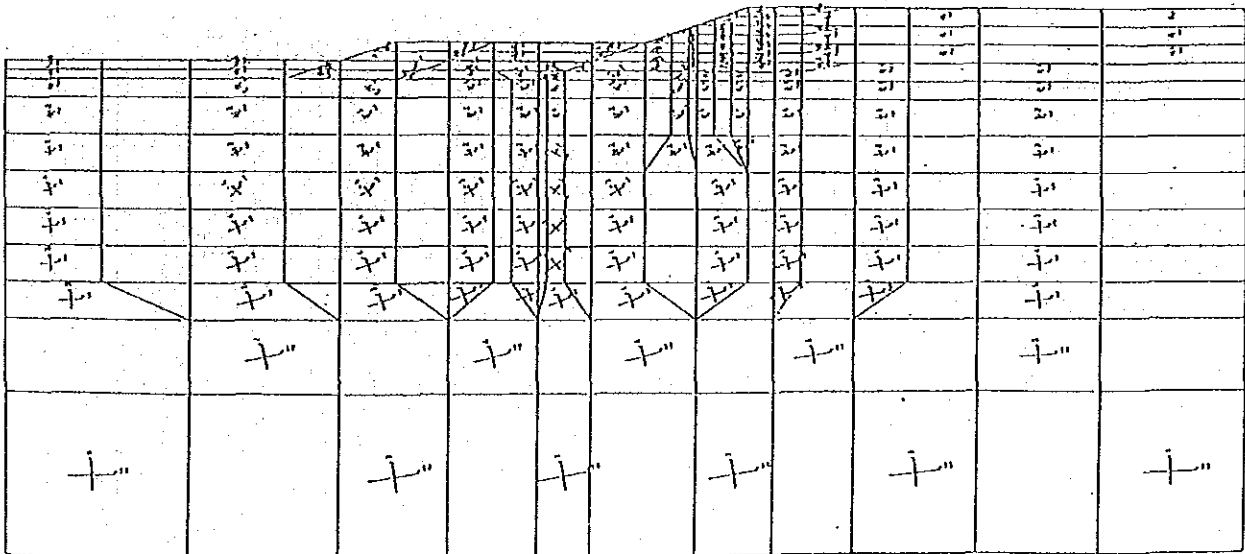
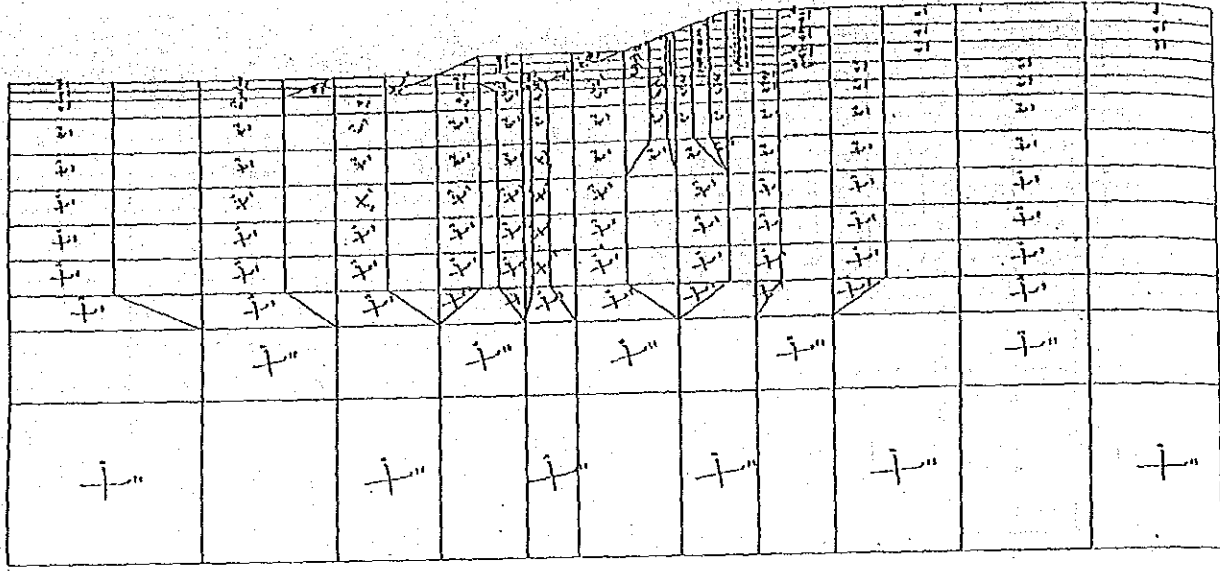


Fig.4.3.45 Stress Occuring in Improved Slope by Soil Cement Columns

Model Scale  
0.0 8.00

Unit  
( 1/K2 )  
Compression Stress  
Tensil Stress

STEP=10.0  
TIME=77.0



STEP=11.0  
TIME=80.0

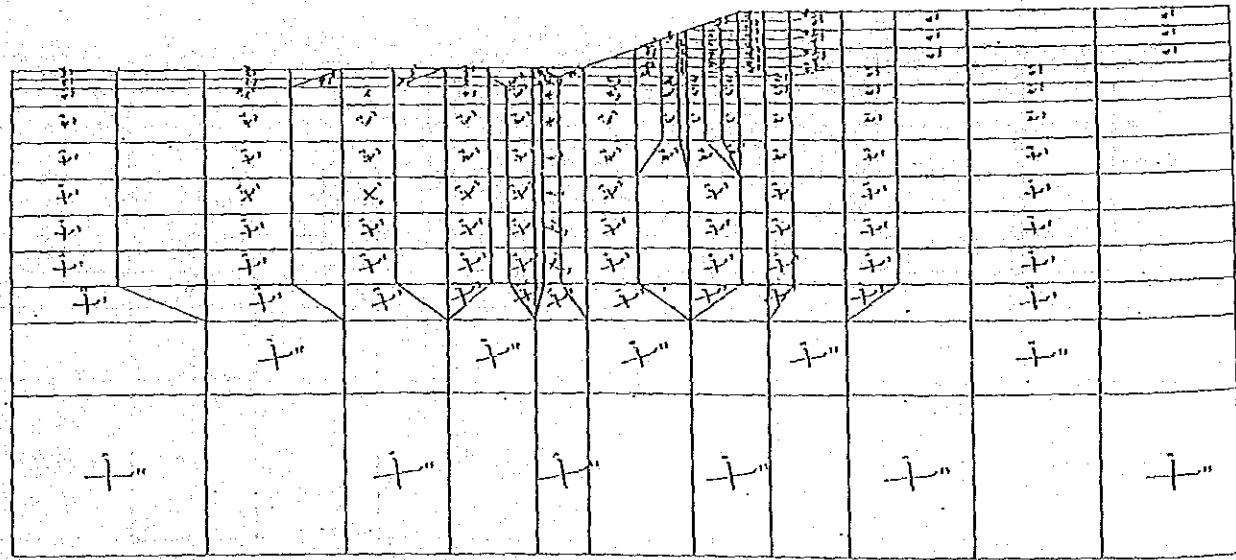
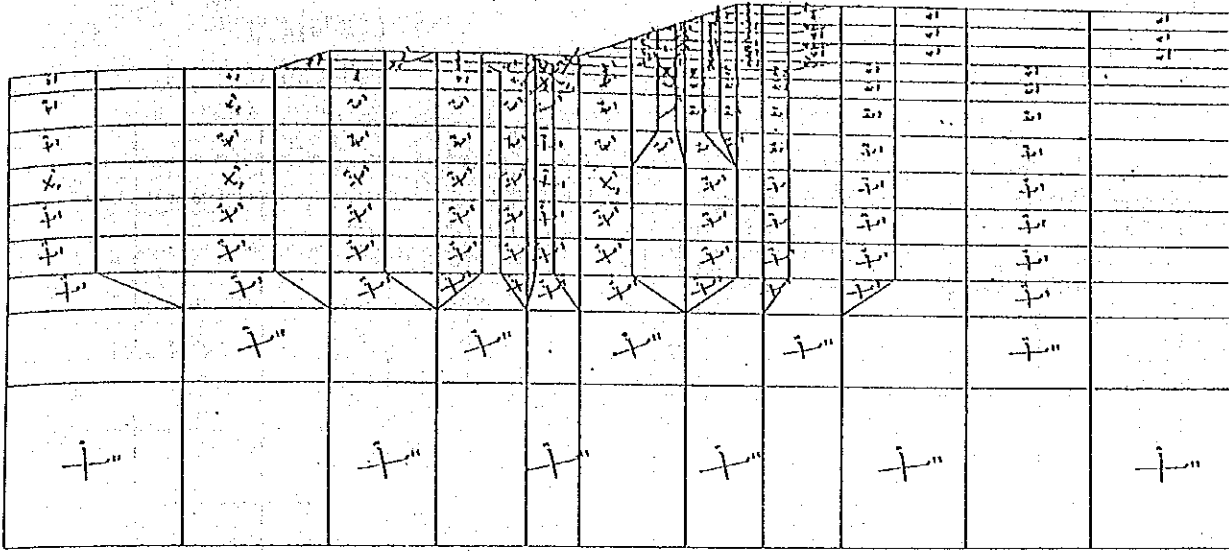


Fig.4.3.46 Stress Occuring in Improved Slope  
by Soil Cement Columns

STEP=12.0

TIME=83.0



Model Scale  
0.0 5.00H

Unit  
( 1/112 )  
Compression Stress  
Tensile Stress  
30.00

STEP=13.0

TIME=86.0

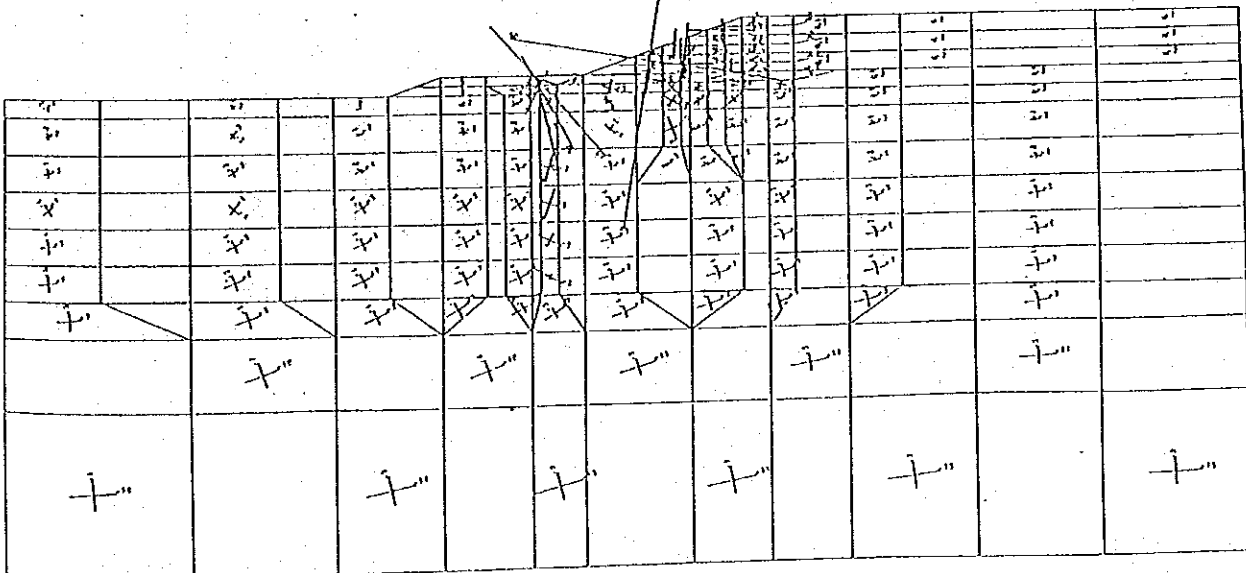


Fig.4.3.47 Stress Occuring in Improved Slope by Soil Cement Columns

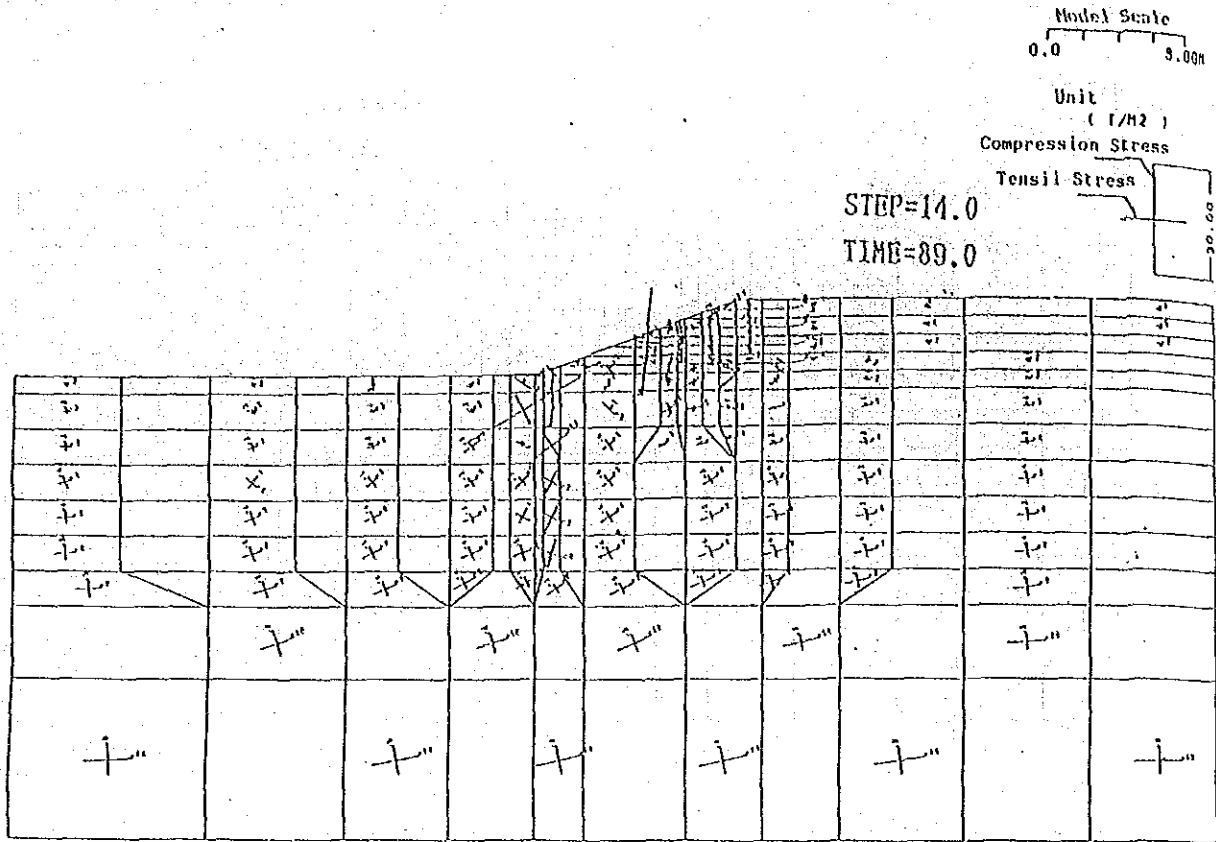


Fig.4.3.48 Stress Occuring in Improved Slope  
by Soil Cement Columns

Appendix 1 Sekiguchi-Ohta Model (Elasto-viscoplastic model)

1. Ohta Constitutive Model

Ohta (1967) introduced the yield function of clay and the elasto-plastic strain according to the normality rule. He assumed that volume change of soil element under consolidation and shearing depends the mean effective stress and the octahedral shear stress,  $\gamma_{oct}$ , is defined by invariant of the effective stress components.

The octahedral shear stress is expressed by the following equation.

$$\gamma_{oct} = \frac{1}{3} \sqrt{(\sigma_1' - \sigma_2')^2 + (\sigma_2' - \sigma_3')^2 + (\sigma_3' - \sigma_1')^2} \quad \dots(1)$$

Where,  $\sigma_1'$ ,  $\sigma_2'$  and  $\sigma_3'$  are principal stress and under the triaxial compression condition ( $\sigma_1' \geq \sigma_2' = \sigma_3'$ ),  $\gamma_{oct}$  is expressed in the following equation.

$$\gamma_{oct} = \frac{2}{3} (\sigma_1' - \sigma_3') \dots\dots\dots(2)$$

On this basis, dilatancy is defined as volume changes which occur under loading with P being held constant as follows.

$$\frac{-\Delta e}{1 + e_0} = \Delta \epsilon_v = \mu \Delta \left( \frac{\gamma_{oct}}{\rho} \right) \dots\dots\dots(3)$$

Where, P : Effective mean stress  
 $\mu$  : Constant value

On the other hand, e-log P relation is expressed by the equation,

$$\Delta e = -\lambda \frac{\Delta \rho}{\rho} \dots\dots\dots(4)$$

Where, e : Void ratio  
 $-\lambda$  : Gradient of e-log P relation  
 $\Delta e$  : Volume change, given by the equation,

$$\Delta e = -\lambda \frac{\Delta \rho}{\rho} - \mu (1 + e_0) \Delta \left( \frac{\gamma_{oct}}{\rho} \right) \dots\dots\dots(5)$$

Then, integrating the equation (5) under  $e_0$  and  $P_0$  at normal consolidation line on  $\gamma_{oct} = 0$  plane, state boundary surface equation in the  $\gamma_{oct}$ -P-e plane is given by the following equation.

$$e - e_0 + \lambda \log \frac{\rho}{\rho_0} + \mu(1 + e_0) \frac{\gamma_{oct}}{\rho} = 0 \dots\dots\dots(6)$$

It is noted that the yield surface is given by projecting cross line of equation(6) and the elastic wall on (oct-P plane.

The elastic wall equation is defined by

$$\Delta e = -\kappa \frac{\Delta \rho}{\rho} \quad \text{or} \quad e - e_0 + \kappa \log \frac{\rho}{\rho_0} = 0 \dots\dots(7)$$

In this way, the yield surface equation is finally obtained as,

$$\frac{\gamma_{oct}}{\rho} + \frac{(\lambda - \kappa)}{(1 + e_0) \mu} \log \frac{\rho}{\rho_0} = 0 \dots\dots(8)$$

Comparing equation(8) and Roscoe's yield surface equation, the following relation can be obtained.

$$M = \frac{3}{\sqrt{2}} \frac{(\lambda - \kappa)}{(1 + e_0) \mu} \dots\dots(9)$$

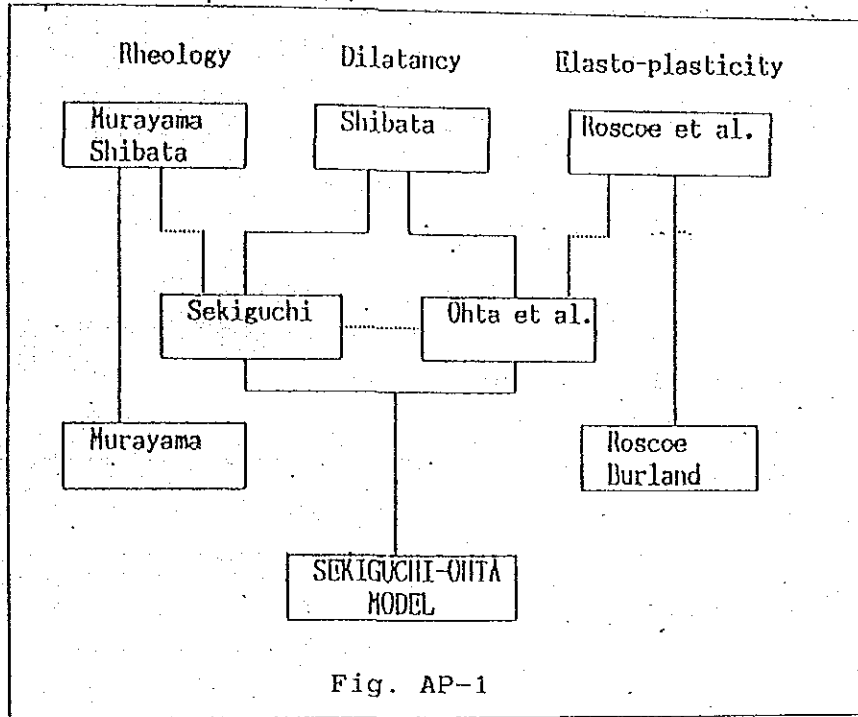
On this basis, it is judged that Ohta theory is the same as Roscoe's theory substantially.

Further, Sekiguchi and Ohta (1977) extended the Ohta model and introduced the inviscid and viscid constitutive relations for anisotropically and normally consolidated clay.

This model is called as "Sekiguchi Ohta Model".

## 2, Sekiguchi-Ohta Model

Sekiguchi and Ohta proposed a new constitutive law taking the effect of time and the stress-induced anisotropy into consideration. This model is called as "Sekiguchi-Ohta Model".



### (1) Volume creep equation

Sekiguchi and Ohta proposed the volumetric creep equation by the use of the new stress parameter,  $\eta^*$ , in the equation,

$$V = \frac{\lambda}{1 + e_0} \ln\left(\frac{P}{P_0}\right) + D \cdot \eta^* - \alpha \cdot \ln\left(\frac{V}{V_0}\right) \quad \dots\dots\dots(10)$$

- Where,  $\lambda$  ; Compression index
- $e_0$  : Initial void ratio
- $P_0$  : Initial effective stress
- $P$  : Effective stress
- $\eta^*$  : New stress parameter, given by

$$\eta^* = \sqrt{\frac{3}{2} (\eta_{ij} - \eta_{jo})(\eta_{ij} - \eta_{jo})} \quad \dots\dots\dots(11)$$

$D$  : Coefficient of dilatancy

(2) Scalar function

Sekiguchi et al.(1977) solved equation(11) and introduced a scalar function as the viscoplastic potential in the equation,

$$F \equiv \alpha \cdot l_n \{1 + (V_0 t / \alpha) \cdot \exp(f/\alpha)\} = v^p \quad \dots\dots\dots(12)$$

Where, f is a scalar function defined by,

$$f = \frac{\lambda - \kappa}{1 + e_0} l_n \left( \frac{p}{p_0} \right) + D \cdot \eta^* \quad \dots\dots\dots(13)$$

It is noted that  $V_p$  in the equation(12) plays as a so-called strain-hardening parameter.

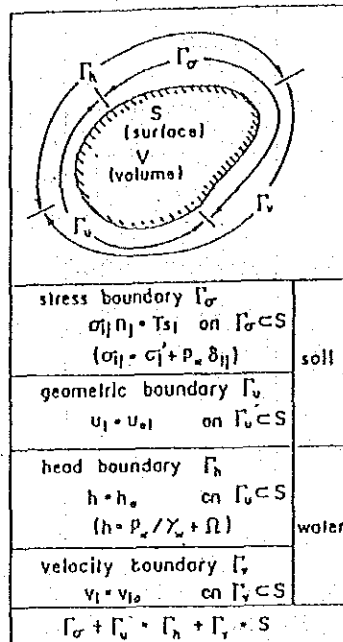
In this way, the strain rate effect of Ko-consolidated clay can be expressed using volumetric creep equation and scalar function. Figure AP-2 shows the summary of the elasto-viscoplastic model by Sekiguchi and Ohta.



volumetric strain of clays			continuum mechanics
consolidation	dilatancy		non-linear elasticity
$\dot{\epsilon}_v^e = \frac{\lambda}{1+e_0} \cdot \frac{\dot{p}'}{p'}$	$\dot{\epsilon}_v^e = 0$	elastic (recoverable)	elastic - limit (yield condition) $H \ln \frac{p'}{p'_0} \cdot D \eta' - \epsilon_v^p = 0$
$\dot{\epsilon}_v^p = \frac{\lambda - \mu}{1+e_0} \cdot \frac{\dot{p}'}{p'}$	$\dot{\epsilon}_v^p = D \eta'$	plastic (irreversible)	
$\epsilon_v^{vp} = \alpha \ln \left[ 1 + \frac{v_0 t}{\alpha} \cdot \exp \left( \frac{t}{\alpha} \right) \right] = f$ $f = \frac{\lambda - \mu}{1+e_0} \cdot \ln \frac{p'}{p'_0} + D \eta'$		viscous (time-dependent)	flow rule $\dot{\epsilon}_{ij}^p = E \cdot \frac{\partial f}{\partial \sigma_{ij}} \quad \text{or} \quad \dot{\epsilon}_{ij}^{vp} = H \cdot \frac{\partial f}{\partial \sigma_{ij}}$
AP-2 Summary of Elasto-plastic/Elasto-viscoplastic Constitutive Model Proposed by Sekiguchi and Ohta (1977)			

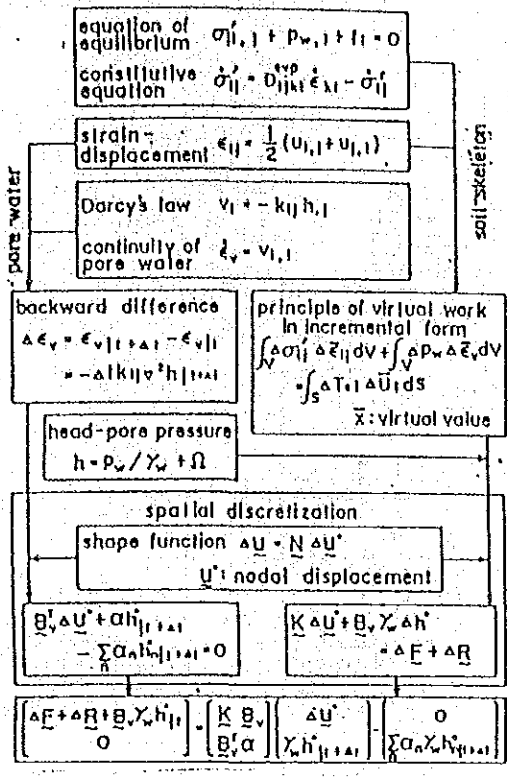
## Appendix 2 Modelling of Soil Mass

Most of the boundary value problems in soil engineering require two kinds of boundary condition to be applied on the soil skeleton and the pore water flow as shown in the following figure.

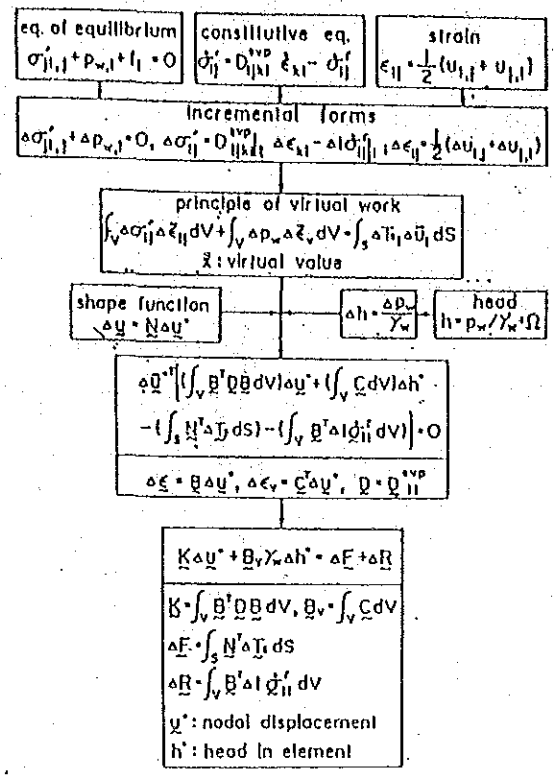


AP-3 Boundary Conditions of a Coupling Problem

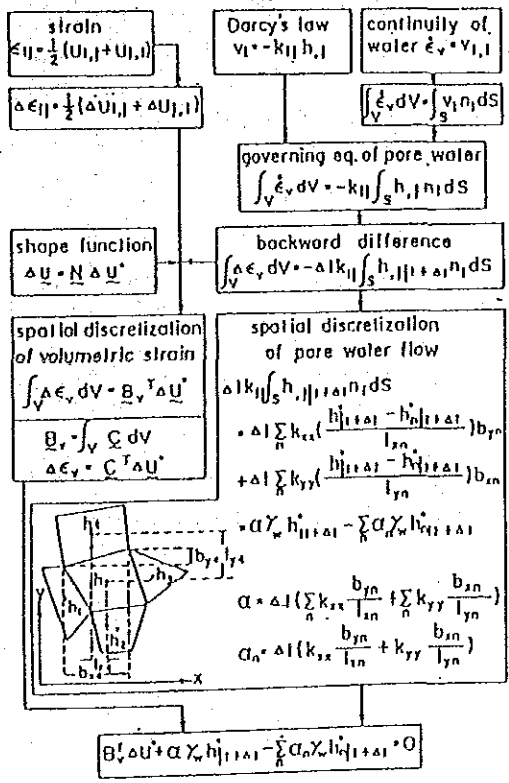
The governing equations of coupling problems of soil skeleton (regarded as the elasto-viscoplastic material) and pore water (regarded as the incompressible fluid) are summarized in Figs. AP-4, Fig. AP-5 and AP-6 indicate the discretization of soil skeleton and pore water respectively. Theoretical framework of the elasto-viscoplastic constitutive model proposed by Sekiguchi and Ohta is as follows.



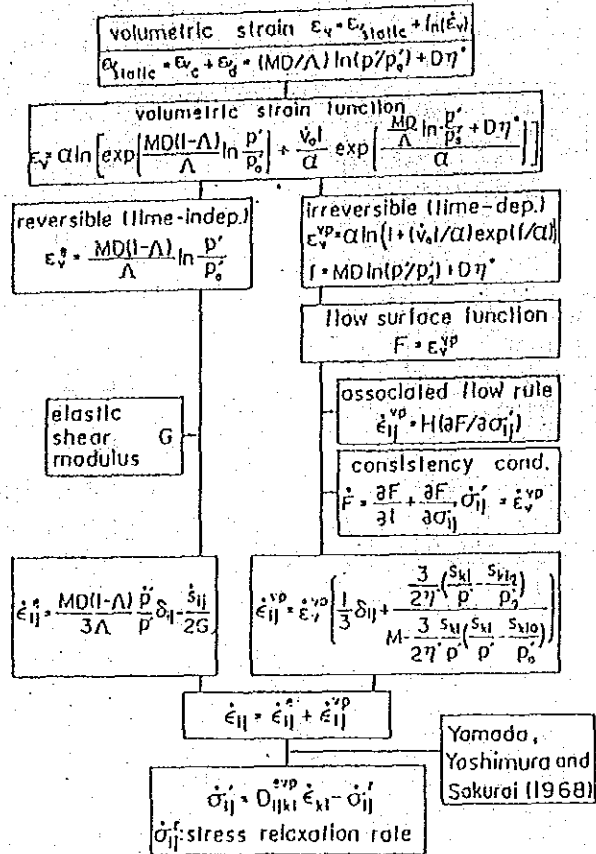
AP-4 Finite Element Formulation of DACSAR



AP-5 Discretization of Soil Skeleton



AP-6 Discretization of Pore Water Flow



AP-7 Theoretical Frame Work of the Elasto-Viscoplastic Constitutive Model Proposed by Sekiguchi and ohta

Rigidity matrix of the elasto-viscoplastic constitutive model used for the Finite Element Method is mathematically described in Fig. AP-8.

$$\begin{aligned} & \dot{\sigma}_{ij} = D_{ijkl}^{epv} \dot{\epsilon}_{kl} - \dot{\sigma}_{ij}^r \\ & \dot{\sigma}_{ij} = \frac{\Delta \sigma_{ij}}{\Delta t} = D_{ijkl}^{epv} (1 - \theta) \Delta \epsilon_{kl}^{epv} + \theta D_{ijkl}^{epv} \epsilon_{kl}^{epv} \\ & \dot{\epsilon}_{ij} = \frac{\Delta \epsilon_{ij}}{\Delta t} = \dot{\sigma}_{ij}^r (1 - \theta) + \dot{\sigma}_{ij}^e + \theta \dot{\sigma}_{ij}^r \\ & \text{plane strain } \dot{\epsilon}_{33} = 0 \quad \text{Eulerian } \theta = 0 \end{aligned}$$

$$\Delta \sigma^r = D_{ij}^{epv} \Delta \epsilon - \Delta \dot{\sigma}_{ij}^r$$

$$\Delta \sigma^r = \begin{pmatrix} \Delta \sigma_{xx}^r \\ \Delta \sigma_{yy}^r \\ \Delta \sigma_{zz}^r \\ \Delta \sigma_{xy}^r \\ \Delta \sigma_{yz}^r \\ \Delta \sigma_{zx}^r \end{pmatrix} \quad \Delta \epsilon = \begin{pmatrix} \Delta \epsilon_{xx} \\ \Delta \epsilon_{yy} \\ \Delta \epsilon_{zz} \\ \Delta \epsilon_{xy} \\ \Delta \epsilon_{yz} \\ \Delta \epsilon_{zx} \end{pmatrix} \quad \dot{\sigma}_{ij}^r = \frac{C_4}{C_2} \begin{pmatrix} A_{xx} \\ A_{yy} \\ A_{zz} \\ A_{xy} \\ A_{yz} \\ A_{zx} \end{pmatrix}$$

$$D_{ij}^{epv} = \begin{pmatrix} L+2G & L & 0 \\ L & L+2G & 0 \\ 0 & 0 & G \\ L & L & 0 \end{pmatrix} \frac{C_3}{C_2} \begin{pmatrix} A_{xx}^2 & A_{xx}A_{yy} & A_{xx}A_{zz} \\ A_{xx}A_{yy} & A_{yy}^2 & A_{xy}A_{yy} \\ A_{xx}A_{yy} & A_{yy}A_{xy} & A_{xy}^2 \\ A_{xx}A_{zz} & A_{yy}A_{zz} & A_{xy}A_{zz} \end{pmatrix}$$

$$L = \frac{3\nu}{1+\nu} \frac{\lambda}{MD(1-\lambda)} p^* \quad G = \frac{3(1-2\nu)}{2(1+\nu)} \frac{\lambda}{MD(1-\lambda)} p^*$$

$$A_{ij} = L(f_{kk} \delta_{ij} + 2G f_{ij}) \quad (i, j = x, y, z) \quad f_{kk} = f_{xx} + f_{yy} + f_{zz}$$

$$C_2 = [L(f_{kk}^2 + 2G(f_{xx}^2 + f_{yy}^2 + 2f_{xy}^2 + f_{zz}^2))] C_3 = f_{kk}$$

$$C_3 = 1 - \exp(-\epsilon^* \eta / \alpha) \quad C_4 = \dot{\nu} \exp[(1 - \epsilon^* \eta) / \alpha]$$

$$f_{ij} = \frac{D}{3p^*} \left[ M - \frac{3}{2\eta} (\eta_{kl} (\eta_{kl} - \eta_{kl0})) \right] \delta_{ij} + \frac{3D}{2\eta p^*} (\eta_{ij} - \eta_{ij0})$$

$$\eta_{ij} = \sigma_{ij}^r / p^* - \delta_{ij} \quad \eta_{ij0} = \sigma_{ij0}^r / p_0^* - \delta_{ij} \quad (M = MD \ln \frac{p^*}{p_0^*} + D \eta^*)$$

$$\eta_{kl} (\eta_{kl} - \eta_{kl0}) = \eta_{xx} (\eta_{xx} - \eta_{xx0}) + \eta_{yy} (\eta_{yy} - \eta_{yy0}) + 2\eta_{xy} (\eta_{xy} - \eta_{xy0})$$

$$+ \eta_{zz} (\eta_{zz} - \eta_{zz0})$$

$$\eta^* = \sqrt{(3/2)(\eta_{ij} - \eta_{ij0})(\eta_{ij} - \eta_{ij0})} \quad (i, j = x, y, z)$$

AP-8 Rigidity Matrix of the Elasto-Viscoplastic Constitutive Model proposed by Sekiguchi and Ohta

The discretization of continuum is carried out by the Finite Element Method using Sekiguchi - Ohta Model as mentioned in the precedings.

### Appendix 3 Estimation of $K_0$ Value

The following five methods are studied regarding presumptive equation to estimate coefficient of earth pressure at rest ( $K_0$ ) under pre-consolidated condition.

- ① Jaky's method (1944) :  $K_0 = 1 - \sin \phi'$
- ② Method of Brooker & Ireland (1965) :  $K_0 = 0.95 - \sin \phi'$
- ③ Frasier's method (1957) :  $K_0 = 0.9 \cdot (1 - \sin \phi')$
- ④ Kezdi's method (1962) :  $K_0 = \frac{(1 + 2 \sin \phi')}{(1 - \sin \phi')(1 + \sin \phi')}$
- ⑤ Aldan's method (1967) :  $K_0 = 0.19 + 0.233 \log I_n$

#### ① $K_0$ value for Bangkok Clay

The data on Bangkok Clay are quoted from the master thesis, "Determination of  $K_0$  Value by Hydraulic Fracture Method" by Wan Weng Tung, 1975, Asian Institute of Technology. Laboratory tests and insitu tests were performed on Bangkok Clay and Rengsit Clay in Nong Wgoo Hao and verification were carried out over the presumptive equations of the above five methods. The results are shown in Fig. AP-9 and Fig. AP-14. As a result, Alpan's equation is considered to be applicable compared with the others.

#### ② $K_0$ value of Kibushi clay

The data on Kibushi Clay are quoted from the doctoral thesis "Study on Lateral Flow of Soft Clay Foundation by Embankment" by Otohiko SUZUKI, August, 1986.

Uniform triaxial compression test, Ko-note triaxial compression test and plane shear test were performed on Kibushi Clay and the following data were obtained. Although the values obtained from Alpan's equation are somewhat bigger than the values from 2 ~ 4 's equations, there is no significant difference between them.

AP-9 Ko Value from Presumptive Equation

Method	Uniform triaxial Compression test	Ko-note triaxial Compression test	Plane shear test
①	0.523	0.597	0.590
②	0.518	0.542	0.540
③	0.470	0.537	0.531
④	0.467	0.540	0.533
⑤	0.545	0.545	0.545

AP-10 Comparison between Estimated Ko Value and measured Ko Value

Method	Ko-note Triaxial Compression Test	Ko Value of Plane Shear Test
①	$0.597 / 0.508 = 1.175$	$0.590 / 0.511 = 1.155$
②	$0.542 / 0.508 = 1.067$	$0.540 / 0.511 = 1.056$
③	$0.537 / 0.508 = 1.057$	$0.531 / 0.511 = 1.039$
④	$0.540 / 0.508 = 1.063$	$0.533 / 0.511 = 1.043$
⑤	$0.545 / 0.508 = 1.073$	$0.545 / 0.511 = 1.067$

Judging from the results shown in above, Alpan's equation seems seems applicable to Bangkok Clay, therefore, this presumptive equation is applied to the estimation of Ko value.

AP-11 Estimated  $K_0$  Values by Experiential Equation(1)

Bangkok Clay at Rangsit										
Depth (m)	$I_p$ (%)	$\phi$ (°)	$K_0$ Predicted					$K_0$ Measured		References
			ALPAN	BROOKER & IRELAND	FRASER	JAKY	KEZDI	Field	Laboratory	
1.2	43.6 ± 2.6	22.3 ± 0.5	0.57 ± 0.01	0.57 ± 0.01	0.56 ± 0.01	0.62 ± 0.01	0.56 ± 0.01		0.59	GULACHOL (1970)
1.75	43.6 ± 2.6	22.1 ± 0.5	0.57 ± 0.01	0.57 ± 0.01	0.57 ± 0.01	0.62 ± 0.01	0.56 ± 0.01		0.55	GULACHOL (1970)
2.5	45.8 ± 3.8	21.1 ± 0.5	0.58 ± 0.01	0.56 ± 0.01	0.56 ± 0.01	0.61 ± 0.01	0.56 ± 0.01		0.58	GULACHOL (1970)
4.0	48.1 ± 5.1	22.1 ± 0.5	0.58 ± 0.01	0.58 ± 0.01	0.56 ± 0.01	0.63 ± 0.01	0.57 ± 0.01	0.72 ± 0.05	0.56	GULACHOL (1970) WANG (1971)
7.0	50.7 ± 2.3	27.4	0.59 ± 0.01	0.57	0.56	0.62	0.56		0.60 ± 0.01	WANG (1971)
8.5	44.0 ± 7.5	25.0	0.56 ± 0.01	0.53	0.52	0.58	0.52	0.55 ± 0.009	0.59	WANG (1971)
9.0	39.1 ± 2.9	20 ± 2	0.56 ± 0.01	0.61 ± 0.03	0.59 ± 0.03	0.64 ± 0.03	0.61 ± 0.03		0.72	AHMAD (1971)

AP-12 Estimated  $K_0$  Values by Experiential Equation(2)

Bangkok Clay at Nong Ngoo Hoo										
Depth (m)	$I_p$ (%)	$\phi$ (°)	$K_0$ Predicted					$K_0$ Measured		References
			ALPAN	BROOKER & IRELAND	FRASER	JAKY	KEZDI	Laboratory		
1.1 ~ 1.3	65 ± 2	23	0.61 ± 0.01	0.56	0.55	0.61	0.56	0.70 ± 0.02		WANG (1974) CHANG (1974)
2.6 ~ 2.9	82 ± 4	25.6 ± 0.2	0.63 ± 0.01	0.52	0.51	0.57	0.51	0.65 ± 0.02		WANG (1974) CHANG (1974)
4.0	73	21.4	0.62	0.59	0.57	0.64	0.58	0.60		CHANG (1971)
5.7	75.3 ± 0.1	27.7 ± 0.1	0.63	0.49	0.48	0.54	0.48	0.63		CHAIYADHUMA (1974)
7.2	67.1 ± 0.1	28.1 ± 0.3	0.62	0.48	0.48	0.53	0.47	0.62		CHAIYADHUMA (1974)
10.0	30		0.53					0.65 ± 0.08		LIU (1974)

Notes:  $\phi$  shown in the table are obtained from  $CK_U$  tests, except that:

- \* --- CAD tests
- \*\* ---  $CU$  tests



AP-13  $K_0$  Values Obtained by Laboratory Tests  
(Nong Ngoo Hao)

Bangkok Clay at Nong Ngoo Hao				
Depth (m)	$K_0$	Size of Specimen	Method of Determination	Investigators
1.3	$0.70 \pm 0.02$	1.4 $\phi$ x 2.8	CHANG's Method	WANG (1974)
2.65	$0.65 \pm 0.02$	1.4 $\phi$ x 2.8	CHANG's Method	WANG (1974)
2.5	0.65 *	1.4 $\phi$ x 2.8	Controlled Stress Triaxial Test	HWANG (1975)
4.0	0.60 **	1.4 $\phi$ x 2.8	CHANG's Method	CHANG (1973)
5.5	0.65 +	1.4 $\phi$ x 2.8	Controlled Stress Triaxial Test	CHAUDRY (1975)
5.7	0.63 **	1.4 $\phi$ x 2.8	POULOS and DAVIS's Method	CHAIYADUNA (1974)
7.2	0.62 **	1.4 $\phi$ x 2.8	POULOS and DAVIS's Method	CHAIYADUNA (1974)
10.0	$0.65 \pm 0.08$	1.4 $\phi$ x 2.8	CHANG's Method	LIU (1974)

AP-14  $K_0$  Values Obtained by In-situ Tests  
and Laboratory Tests (Rangsit Clay)

Field Test Results			Laboratory Test Results		
Depth (m)	$K_0$	Method of Determination	Depth (m)	$K_0$	Method of Determination
4.0	$0.72 \pm 0.05$	BJERRUM and ANDERSEN	4.0	0.56	BISHOP and HENKEL
4.0	$0.67 \pm 0.04$	WILKES	4.5	$0.63 \pm 0.05$	Laboratory Hydraulic Frac.
6.0	$0.64 \pm 0.05$	BJERRUM and ANDERSEN	6.25	$0.56 \pm 0.06$	Laboratory Hydraulic Frac.
6.0	$0.61 \pm 0.03$	WILKES	7.0	$0.60 \pm 0.01$	BISHOP and HENKEL
8.0	$0.55 \pm 0.09$	BJERRUM and ANDERSEN	8.0	$0.52 \pm 0.03$	Laboratory Hydraulic Frac.
8.0	$0.53 \pm 0.03$	WILKES	8.5	0.59	BISHOP and HENKEL

1) Improved Slopes by Sand Compaction Piles and Gravel Compaction Piles

i) Diameter of Sand Compaction Pile

The diameter of the casing pipes applied to this construction method shall be selected as 0.40 m based on the general use in Japan.

Also, the diameters of piles produced by the use of the above pipes shall be selected as specified below, based on experience and practice in Japan:

Pile	Diameter
Sand Compaction Pile	0.70 m
Gravel Compaction Pile	0.50 m

ii) Distance between Each Compaction Pile

The relationship among the volume ratio of the improved material to the original clay material, the distance between each pile, and the diameter of pile can be presented by the following equation, under the condition of the right triangular arrangement by the piles:

$$L = \frac{0.2887 \times \pi}{Ass} \times D \quad \dots \dots \dots (4.4.1)$$

where, L : Distance between each compaction pile

D : Diameter of compaction pile

Ass: Volume ratio of the improved material to the original clay material

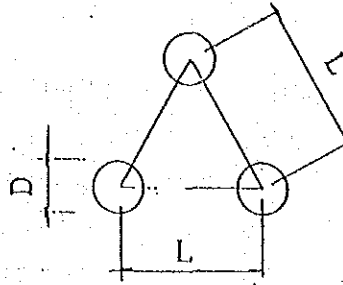


Fig.4.4.1 Arrangement of Compaction Piles

Since the volume ratio of sand compaction piles to the original clay material was decided as 10 %, the above equation (4.4.1) can be arranged as follows:

$$L = 3.011 \times D \quad \dots\dots\dots (4.4.2)$$

Therefore, the above relationship can be summarized as shown in Table 4.4.1.

Table 4.4.1 Arrangement of Compaction Piles

Pile	Diameter D (m)	Distance between each pile	Arrangement	Sectional projective distance l (m)
Sand compaction pile	0.70	2.00	Right triangle	1.73
Gravel compaction pile	0.50	1.50	-Ditto-	1.30

1) Improved Slopes by Soil Cement Columns

i) Diameter of Soil Cement Column

The diameter of the soil cement columns is to be 1.0 m based on experience and practice of soil cement columns constructed in Japan and economical conditions.

ii) Distance between each Soil Cement Column

The relationship among the volume ratio of the improved material to the original clay material, the distance between each column, and the diameter between columns can be presented by the equation (4.4.1) as mentioned above, under the condition of the right triangular arrangement of the columns.

Since the volume ratio of soil cement columns to the original clay material was decided as 30 %, the equation (4.4.1) can be arranged as follows:

$$L = \frac{0.2887 \times 3.14}{0.3} \times D$$

$$= 1.739 \times D \quad \dots\dots\dots (4.4.3)$$

Therefore, the distance between each Soil Cement Column can be decided as 1.75 m.

iii) Width of Improved Zone by Soil Cement Columns

As already mentioned, the arrangement of soil cement columns shall be settled as four (4) lines arrangement for the deep slip surface and also three (3) lines arrangement for the medium and shallow slip surfaces.

The distance (L<sub>1</sub>) between each column projected by two (2) lines cross-sectionally can be presented by the following equation under the condition of the right triangular arrangement of the columns, (L = 1.75 m):

$$L_1 = \frac{\sqrt{3}}{2} \times L \quad \dots\dots\dots (4.4.4)$$

where L<sub>1</sub> : Projective distance between each soil cement column along section of improved slope

L : Distance between each soil cement column

therefore,

$$L_1 = \frac{3}{2} \times L = \frac{3}{2} \times 1.75 = 1.51 \text{ (m)}$$

iv) Strength of Soil Cement Columns

The strength of soil cement columns shall be determined by taking into accounts the strengths and the range of strengths of the columns constructed in the field assumed or evaluated based on the strength data obtained by the laboratory tests.

From the past experiences, in general, the data obtained by the field tests in the actual construction stage indicate different values from the data obtained by the laboratory tests because of the variation of the site situations such as the heterogeneity of the improved material, the stirring degree of materials, the displacement of foundation materials and so on.

Fig. 4.4.2 shows the comparison between the strengths ( $q_{ul}$ ) obtained by laboratory tests using the ordinary portland cement and the strengths ( $q_{uf}$ ) obtained by field tests by core-samplings based on experience and practice in Japan.

From the Fig. 4.4.2, the values of  $q_{ul}/q_{uf}$  indicate the range of 1/2 to 1/5, and it is found that the strength by cement slurry indicate a larger value than the strength by fine cement.

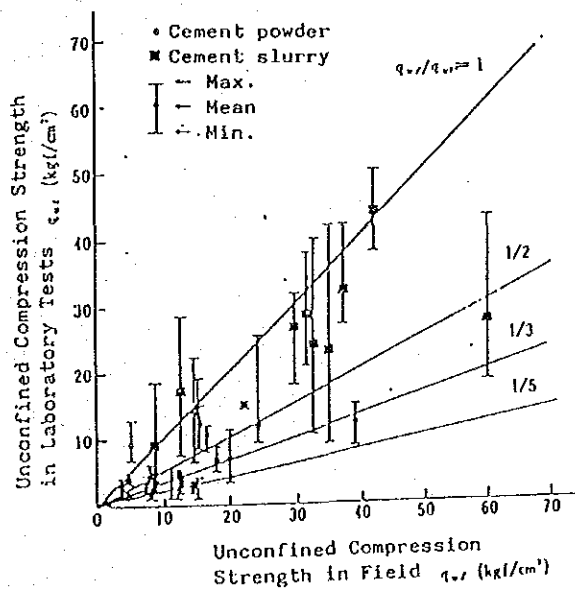


Fig.4.4.2 Comparison between Compression Strength of Columns Constructed in the Field and Those in the Laboratory (Quoted from "The Handbook for Design and Construction on Ground and Foundation for Structures", 1987)

Judging from the above situation, the value of  $q_{ul}/q_{uf} = 1/3$  shall be employed for the design strength.

$$\begin{aligned}\text{Therefore, } q_{uf} &= q_{ul} \times 3 \\ &= 2.9 \times 3 \\ &= 8.7 \text{ (kgf/cm}^2\text{)}\end{aligned}$$







## CHAPTER 5 DESIGN OF MONITORING SYSTEM

### 5-1 Objectives of Monitoring System

The purpose of the monitoring system for the proposed testing canal facility is to obtain geotechnical information by measuring and recording the behaviour of the soft soil foundation caused by the excavation work through the conditions before, during and after the construction.

Namely, the main purpose is to lead a determination method of design parameters by studying the back-analysis based on comparison between the testing results obtained by the in-situ and laboratory tests and the actual behaviour data of the soft soil foundation obtained from the project site.

At the construction stage, furthermore, these data obtained from the monitoring system would be very useful for safety control of the construction and for the review of the frequency of observation decided at the beginning stage of the monitoring.

Therefore, although the concept of real time construction control is not considered in this monitoring system, as to organizing data processing program in this monitoring system, it is desirable to make real time data sampling possible and to make processed data into a certain format transferable to other softwares for construction control.

### 5-2 Monitoring Items and Instruments

The monitoring items to be observed under the application of the monitoring system are mainly classified as follow:

- (1) : Displacement and deformation of the foundation in horizontal and vertical directions
- (2) : Excess pore water pressure in the foundation

The monitoring method is classified into two (2) types, that is, automatic recording method and manual reading method.

The Table 5.2.1 shows the monitoring items, the monitoring instruments and the monitoring methods.

Table 5.2.1 Monitoring Items, Instruments and Method

Monitoring Items and Their Method	Type of Instruments							Remarks
	Inclinometer	Differential Settlement Gauge	Extensometer	Displacement Piles	Piezometer	Water Stand Pipes		
Underground Excess Pore Water Pressure					○	○		
Displacement	Ground-surface			○				
	Vertical Displacement							
In Ground	Horizontal Displacement		○					
	Vertical Displacement							
Type of Monitoring	Horizontal Displacement							
	Vertical Displacement	○						
Method of Monitoring	Automatic or manual reading	Manual reading	Automatic reading	Manual measuring	Automatic reading	Manual reading		
	Set the inclinometer in a flexible pipes under the ground and then take measurement	Monitor the settled particles fixed in the boring holes	Monitor the expansion length from a stretched line set on the ground-surface	Measure vertical displacement by the level and measure horizontal displacement by using steel tape	Set the tip with filter into the ground and then take measurement	Measure the water level using the open atand pipes		

1) Selection of Monitoring Instruments

Monitoring instruments should conform to the conditions mentioned below, taking the characteristics of the project into consideration.

(1) Accuracy and capacity of instruments

All the instruments should have the accuracy and the capacity as shown in the specifications (Draft) specified in Table 5.8.1.

(2) Durability of instruments

Taking the site conditions at the project site into consideration, the instruments and cables should be sufficiently durable or have considerable countermeasures against the following points:

- a). Corrosion caused by salinity
- b). Damage to sensors or snapping of cables by heavy equipment during the excavation stage
- c). Generation of excess induced current by lightning
- d). Stability for insulation capacity of sensors themselves

5-3 Installation Plan of Monitoring Instruments

The testing Canal facility consists of four slopes as forementioned.

The installation plan of monitoring instruments shown in Fig. 5.3.1 is employed for this testing canal facility by taking into account the following matters:

- 1). The main purpose is to obtain the behaviour of the non-treatment slopes caused by excavation work.

Number of Monitoring Instruments

Installation Plan

Section Instrument		①	②	③	④	Remarks
		non-treat- ment 1:4	non treat- ment 1:6	Soil cement Column	Sand Com- paction pile	
Inclinometer	X	3 x 5	1 x 5	1 x 5	2 x 5	location X sensor
Settlement guage	O	3 x 5	1 x 5	1 x 5	2 x 5	location X sensor
Piezometer	□	2 x 3	2	—	2 x 3	location X sensor
Extensometer	┆	1 x 6	—	—	—	location X sensor
Displacement Pile	•	31	23	23	27	Piles

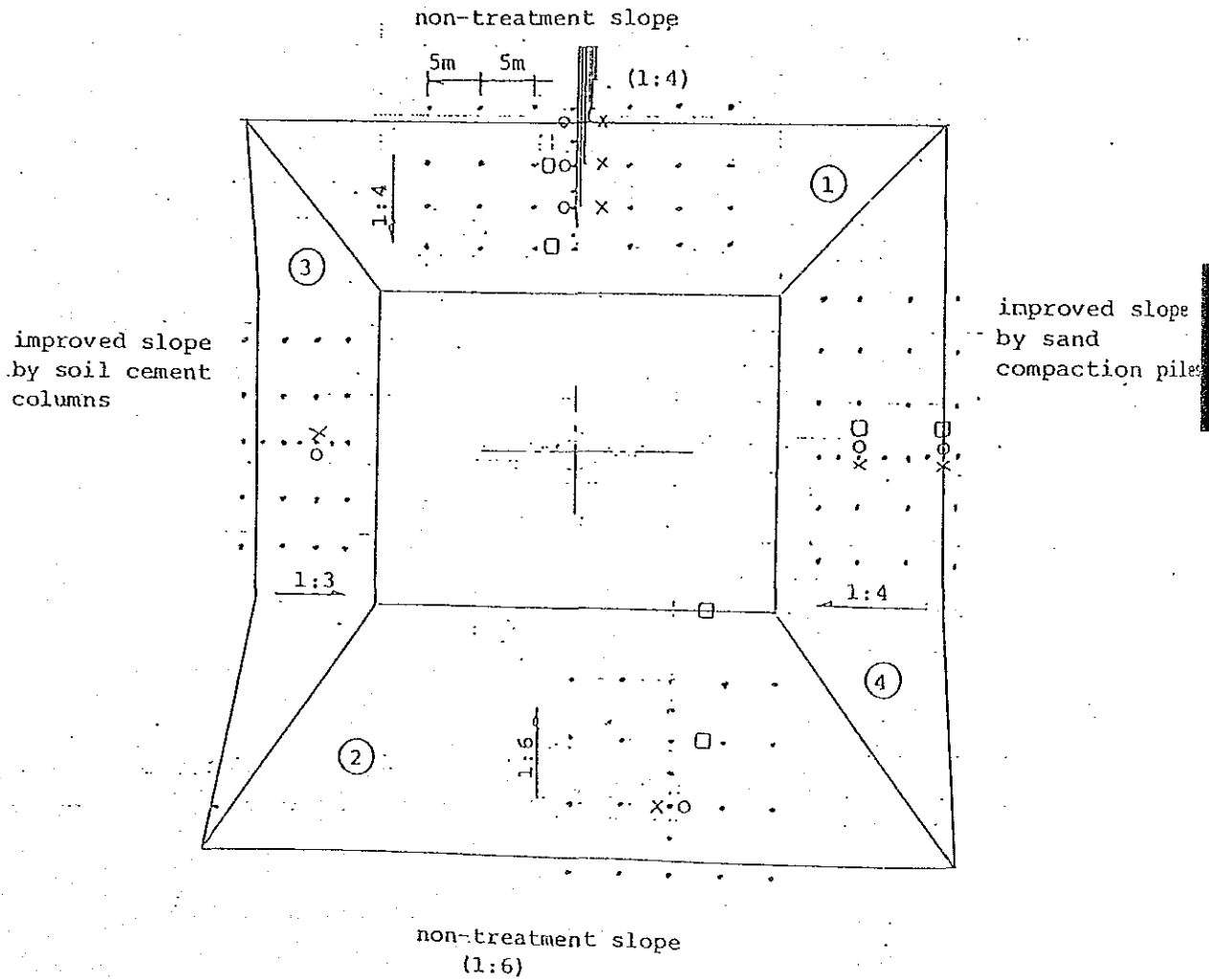


Fig.5.3.1 Arrangement Plan of Monitoring Instruments

Table 5.3.1 Number of Instrument

No.	Condition of Slope	Auto-Reading Instruments											
		Inclinometer				Extensometer				Piezometer			
		No. of Loca- tion	No. of Sensor	Boring Length m	Cable Length m	No. of Loca- tion	No. of Sensor	Wire Length m	Cable Length m	No. of Loca- tion	No. of Sensor	Boring Length m	Cable Length m
1	Non-treatment slope (1:4)	1	5	18	20	1	6	60	10	2	6	10	16
2	Non-treatment slope (1:6)	-	-	-	-	-	-	-	-	2	6	12	16
3	Improved slope by cement columns	-	-	-	-	-	-	-	-	-	-	-	-
4	Improved slope by sand compaction piles	1	5	18	20	-	-	-	-	2	6	8	16
Total		2	10	36	40	1	6	60	10	6	18	30	48

No.	Manual reading Instruments												REMARKS
	Inclinometer		Settlement gauge				Displacement piles			Water stand pipe			
	No. of Loca- tion	No. of Sensor	Boring Length m	No. of Loca- tion	No. of Sensor	Boring Length m	Cross section	Longi- tudinal section	Total	No. of Loca- tion	No. of Sensor	Boring Length m	
1	2	10	36	3	15	54	-	-	31	1	10	10	
2	1	5	18	1	5	18	-	-	23				
3	1	5	18	1	5	18	-	-	23				
4	1	5	18	2	10	36	-	-	27	1	10	10	
Total		5	25	90	7	35	126		104	2	20	20	